On Constellation Power Allocation over Gaussian Multiple Access Channel With Random Phase Offset

Prepared by Yi-An Wu
Advisory by Prof. Po-Ning Chen

Institute of Communications Engineering
National Chiao Tung University
Hsinchu, Taiwan 30010, R.O.C.

July 9, 2016

On Constellation Power Allocation over Gaussian Multiple Access Channel With Random Phase Offset

Student : Yi-An Wu Adivisor : Po-Ning Chen

Institute of Communications Engineering

National Chiao Tung University

Abstract

Recently, non-orthogonal multiple access (NOMA) technology has been widely discussed due to its better cell coverage and potentially higher user throughput than the traditional orthogonal multiple access (OMA) technology. In its implementation, user equipments (UEs) and the base station (BS) of NOMA are required to have an advanced interference cancellation capability in order to eliminate the signals generated by other users. In this thesis, we focus on the Constellation Power Allocation (CPA) transmission scheme and investigate its system performance over the uplink NOMA scenario. The channel model considered is the Gaussian Multiple Access Channel (GMAC) with additional random phase offset. Several alternative distance-based objective functions, other than the usual CC sum capacity objective function in the literature, for the algorithmic determination of the power allocation factor of the CPA scheme over a two-user GMAC with random phase offsets are proposed. Possible extension to the three-user GMAC with random phase offset is also addressed.

Contents

Chinese Abstract i

Abstract i

Contents ii

List of Figures iv

List of Tables ix

1 Introduction 1

2 System Model and Background 3

2.1 Application Scenarios for Non-Orthogonal Multiple Access (NOMA) 3

2.2 Uplink Non-Orthogonal Multiple Access (NOMA) 6

2.3 Multilevel Coding for NOMA 8

2.3.1 Multilevel Code Encoder 8

2.3.2 Multistage Decoder for Multilevel Codes 8

2.4 Joint Maximum-Likelihood (JML) Receiver 9

2.5 Successive Interference Cancellation (SIC) Receiver 11

3 Previous Work and Problem Formulation 12

3.1 Constellation Power Allocation (CPA) Scheme 13
3.2 Capacity Region and Constellation Constrained (CC) Sum Capacity for GMAC 14
3.2.1 Capacity Region for GMAC 14
3.2.2 Constellation Constrained (CC) Sum Capacity for GMAC 15
3.2.3 Constellation Constrained (CC) Sum Capacity for GMAC with Random Phase Effect 16
3.3 Power Allocation Based on CC Sum Capacity 17
3.4 Problem Formulation 17

4 Criterions for Power Allocation **19**
4.1 Motivations 19
4.2 Suboptimal Power Allocation for Three-User GMAC with Random Phase Offset 20
4.3 System Setting for Simulations 21

5 Simulation Results **24**
5.1 Two-user GMAC with Equal Average Power Constraint and Random Phase Offset 24
5.2 Two-user GMAC with Unequal Average Power Constraint and Random Phase Offset 57
5.3 Three-user GMAC with Equal Average Power Constraint and Random Phase Offset 70

6 Conclusion and Future Work **85**

Bibliography **87**

List of Figures

2.1 An application scenario of NOMA: Wireless backhaul for static small cells 4

2.2 An application scenario of NOMA: Multiple access for crowded wide area . 4

2.3 An application scenario of NOMA: Multiple access for crowded local area . 4

2.4 An application scenario of NOMA: Wireless backhaul for moving nodes . . 5

2.5 An uplink NOMA transmission scheme 6

2.6 An exemplified resource allotment with four resource elements and six users in an uplink NOMA 7

2.7 A multilevel code transmitter 8

2.8 Example of multistage decoding 10

2.9 Multistage decoding for multilevel codes 10

3.1 A two-user GMAC model 14

3.2 Capacity region for a two-user GMAC 15

4.1 Power allocation for the three-user GMAC with random phase offset 21

4.2 Transmitter setting for two-user multilevel-coding with the CPA scheme . . 22

4.3 JML receiver setting 22

4.4 SIC receiver setting 23

5.1 Capacity region and achievable rate pairs of the CPA scheme under two-user GMAC with random phase effect. Here, JML receiver is employed except that the capacity region is derived and drawn based on SIC receiver, and SNR = 3 dB. 28

5.2 Capacity region and achievable rate pairs of the CPA scheme under two-user GMAC with random phase offset. Here, SIC receiver is employed, and SNR = 3 dB. 32

5.3 Capacity region and achievable rate pairs of the CPA scheme under two-user GMAC with random phase offset. Here, JML receiver is employed except that the capacity region is derived and drawn based on SIC receiver, and SNR = 6 dB. 35

5.4 Capacity region and achievable rate pairs of the CPA scheme under two-user GMAC with random phase offset. Here, SIC receiver is employed, and SNR = 6 dB. 38

5.5 Capacity region and achievable rate pairs of the CPA scheme under two-user GMAC with random phase offset. Here, JML receiver is employed except that the capacity region is derived and drawn based on SIC receiver, and SNR = 10 dB. 41

5.6 Capacity region and achievable rate pairs of the CPA scheme under two-user GMAC with random phase offset. Here, SIC receiver is employed, and SNR = 10 dB. 44

5.7 CC sum capacity and achievable rates of BPSK+BPSK with equal average power constraint and random phase offset. Here, JML receiver is assumed. 45

5.8 CC sum capacity and achievable rates of BPSK+BPSK with equal average power constraint and random phase offset. Here, SIC receiver is assumed. 45

5.9 CC sum capacity and achievable rates of BPSK+QPSK with equal average power constraint and random phase offset. Here, JML receiver is assumed. 46

5.10 CC sum capacity and achievable rates of BPSK+QPSK with equal average power constraint and random phase offset. Here, SIC receiver is assumed. . 46

5.11 CC sum capacity and achievable rates of QPSK+QPSK with equal average power constraint and random phase offset. Here, JML receiver is assumed. 47

5.12 CC sum capacity and achievable rates of QPSK+QPSK with equal average power constraint and random phase offset. Here, SIC receiver is assumed. . 47

5.13 CC sum capacity and achievable rates of QPSK+8PSK with equal average power constraint and random phase offset. Here, JML receiver is assumed. 48

5.14 CC sum capacity and achievable rates of QPSK+8PSK with equal average power constraint and random phase offset. Here, SIC receiver is assumed. . 48

5.15 CC sum capacity and achievable rates of 8PSK+8PSK with equal average power constraint and random phase offset. Here, JML receiver is assumed. 49

5.16 CC sum capacity and achievable rates of 8PSK+8PSK with equal average power constraint and random phase offset. Here, SIC receiver is assumed. . 49

5.17 CC sum capacity and achievable rates of 8PSK+16QAM with equal average power constraint and random phase offset. Here, JML receiver is assumed. 50

5.18 CC sum capacity and achievable rates of 8PSK+16QAM with equal average power constraint and random phase offset. Here, SIC receiver is assumed. . 50

5.19 CC sum capacity and achievable rates of 16QAM+16QAM with equal average power constraint and random phase offset. Here, JML receiver is assumed. 51

5.20 CC sum capacity and achievable rates of 16QAM+16QAM with equal average power constraint and random phase offset. Here, SIC receiver is assumed. 51

5.21 Joint constellations of Case 1 and Case 2 for the odd and even channel uses under SNR = 0 dB 55

5.22 CC sum capacities of Case 1 and Case 2 under different SNRs 56

5.23 Capacity region and achievable rate pairs of the CPA scheme under two-user GMAC with random phase offset. Here, JML receiver is employed, UE1 SNR = 3 dB and UE2 SNR = 6 dB. 61

5.24 Capacity region and achievable rate pairs of the CPA scheme under two-user GMAC with random phase offset. Here, SIC receiver is employed, UE1 SNR = 3 dB and UE2 SNR = 6 dB. 63

5.25 Capacity region and achievable rate pairs of the CPA scheme under two-user GMAC with random phase offset. Here, JML receiver is employed, UE1 SNR = 3 dB and UE2 SNR = 10 dB. 65

5.26 Capacity region and achievable rate pairs of the CPA scheme under two-user GMAC with random phase offset. Here, SIC receiver is employed, UE1 SNR = 3 dB and UE2 SNR = 10 dB. 67

5.27 CC sum capacity and achievable rates of BPSK+BPSK+BPSK with equal average power constraint and random phase offset. Here, JML receiver is assumed. 79

5.28 CC sum capacity and achievable rates of BPSK+BPSK+BPSK with equal average power constraint and random phase offset. Here, SIC receiver is assumed. 79

5.29 CC sum capacity and achievable rates of BPSK+BPSK+QPSK with equal average power constraint and random phase offset. Here, JML receiver is assumed. 80

5.30 CC sum capacity and achievable rates of BPSK+BPSK+QPSK with equal average power constraint and random phase offset. Here, SIC receiver is assumed. 80

5.31 CC sum capacity and achievable rates of BPSK+QPSK+QPSK with equal average power constraint and random phase offset. Here, JML receiver is assumed. 81

5.32 CC sum capacity and achievable rates of BPSK+QPSK+QPSK with equal average power constraint and random phase offset. Here, SIC receiver is assumed. 81

5.33 CC sum capacity and achievable rates of QPSK+QPSK+QPSK with equal average power constraint and random phase offset. Here, JML receiver is assumed. 82

5.34 CC sum capacity and achievable rates of QPSK+QPSK+QPSK with equal average power constraint and random phase offset. Here, SIC receiver is assumed. 82

List of Tables

5.1 Parameter setting for two-user GMAC with equal average power constraint and random phase offset 25

5.2 α_{opt} and θ_{opt} selected based on different modulation combinations and different distance-based criterions 25

5.3 α_{opt} based on different modulation combinations and different SNRs . . . 26

5.4 Achievable rate pairs of the CPA scheme under two-user GMAC with random phase offset. Here, $(\alpha_{\text{opt}}, \theta_{\text{opt}}) = \text{argmax}_{\alpha\in(0,1]\,\&\,\theta\in\Theta}\{d_{\min}\}$, JML receiver is employed, and SNR = 3 dB. The receiver is also assumed to be able to rotate the two constellations accurately to match θ_{opt}. 27

5.5 Achievable rate pairs of the CPA scheme under two-user GMAC with random phase effect. Here, $\alpha_{\text{opt}} = \text{argmax}_{\alpha\in(0,1]}\,\text{avg}_{\theta\in\Theta}\{d_{\min}\}$, JML receiver is employed, and SNR = 3 dB. 27

5.6 Achievable rate pairs of the CPA scheme under two-user GMAC with random phase effect. Here, $\alpha_{\text{opt}} = \text{argmax}_{\alpha\in(0,1]}\,\min_{\theta\in\Theta}\{d_{\min}\}$, JML receiver is employed, and SNR = 3 dB. 27

5.7 Achievable rate pairs of the CPA scheme under two-user GMAC with random phase effect. Here, $\alpha_{\text{opt}} = \text{argmax}_{\alpha\in(0,1]}\{\text{CC sum capacity}\}$, JML receiver is employed, and SNR = 3 dB. 29

5.8 Achievable rate pairs of the CPA scheme under two-user GMAC with random phase offset. Here, $(\alpha_{\text{opt}}, \theta_{\text{opt}}) = \text{argmax}_{\alpha\in(0,1)\,\&\,\theta\in\Theta}\{d_{\min}\}$, SIC receiver is employed, and SNR = 3 dB. The receiver is also assumed to be able to rotate the two constellations accurately to match θ_{opt}. 30

5.9 Achievable rate pairs of the CPA scheme under two-user GMAC with random phase offset. Here, $\alpha_{\text{opt}} = \text{argmax}_{\alpha\in(0,1]}\,\text{avg}_{\theta\in\Theta}\{d_{\min}\}$, SIC receiver is employed, and SN = 3 dB. 30

5.10 Achievable rate pairs of the CPA scheme under two-user GMAC with random phase offset. Here, $\alpha_{\text{opt}} = \text{argmax}_{\alpha\in(0,1]}\,\min_{\theta\in\Theta}\{d_{\min}\}$, SIC receiver is employed, and SNR = 3 dB. 31

5.11 Achievable rate pairs of the CPA scheme under two-user GMAC with random phase offset. Here, $\alpha_{\text{opt}} = \text{argmax}_{\alpha\in(0,1]}\{\text{CC sum capacity of average phases}\}$, SIC receiver is employed, and SNR = 3 dB. 31

5.12 Achievable rate pairs of the CPA scheme under two-user GMAC with random phase offset. Here, $(\alpha_{\text{opt}}, \theta_{\text{opt}}) = \text{argmax}_{\alpha\in(0,1)\,\&\,\theta\in\Theta}\{d_{\min}\}$, JML receiver is employed, and SNR = 6 dB. The receiver is also assumed to be able to rotate the two constellations accurately to match θ_{opt}. 33

5.13 Achievable rate pairs of the CPA scheme under two-user GMAC with random phase offset. Here, $\alpha_{\text{opt}} = \text{argmax}_{\alpha\in(0,1]}\,\text{avg}_{\theta\in\Theta}\{d_{\min}\}$, JML receiver is employed, and SNR = 6 dB. 33

5.14 Achievable rate pairs of the CPA scheme under two-user GMAC with random phase offset. Here, $\alpha_{\text{opt}} = \text{argmax}_{\alpha\in(0,1]}\,\min_{\theta\in\Theta}\{d_{\min}\}$, JML receiver is employed, and SNR = 6 dB. 34

5.15 Achievable rate pairs of the CPA scheme under two-user GMAC with random phase offset. Here, $\alpha_{\text{opt}} = \text{argmax}_{\alpha\in(0,1]}\{\text{CC sum capacity of average phases}\}$, JML receiver is employed, and SNR = 6 dB. 34

5.16 Achievable rate pairs of the CPA scheme under two-user GMAC with random phase offset. Here, $(\alpha_{\text{opt}}, \theta_{\text{opt}}) = \text{argmax}_{\alpha\in(0,1)\,\&\,\theta\in\Theta}\{d_{\min}\}$, SIC receiver is employed, and SNR = 6 dB. The receiver is also assumed to be able to rotate the two constellations accurately to match θ_{opt}. 36

5.17 Achievable rate pairs of the CPA scheme under two-user GMAC with random phase offset. Here, $\alpha_{\text{opt}} = \text{argmax}_{\alpha\in(0,1]}\,\text{avg}_{\theta\in\Theta}\{d_{\min}\}$, SIC receiver is employed, and SNR = 6 dB. 36

5.18 Achievable rate pairs of the CPA scheme under two-user GMAC with random phase offset. Here, $\alpha_{\text{opt}} = \text{argmax}_{\alpha\in(0,1]}\,\min_{\theta\in\Theta}\{d_{\min}\}$, SIC receiver is employed, and SNR = 6 dB. 37

5.19 Achievable rate pairs of the CPA scheme under two-user GMAC with random phase offset. Here, $\alpha_{\text{opt}} = \text{argmax}_{\alpha\in(0,1]}\{\text{CC sum capacity of average phases}\}$, SIC receiver is employed, and SNR = 6 dB. 37

5.20 Achievable rate pairs of the CPA scheme under two-user GMAC with random phase offset. Here, $(\alpha_{\text{opt}}, \theta_{\text{opt}}) = \text{argmax}_{\alpha\in(0,1)\,\&\,\theta\in\Theta}\{d_{\min}\}$, JML receiver is employed, and SNR = 10 dB. The receiver is also assumed to be able to rotate the two constellations accurately to match θ_{opt}. 39

5.21 Achievable rate pairs of the CPA scheme under two-user GMAC with random phase offset. Here, $\alpha_{\text{opt}} = \text{argmax}_{\alpha\in(0,1]}\,\text{avg}_{\theta\in\Theta}\{d_{\min}\}$, JML receiver is employed, and SNR = 10 dB. 39

5.22 Achievable rate pairs of the CPA scheme under two-user GMAC with random phase offset. Here, $\alpha_{\text{opt}} = \text{argmax}_{\alpha\in(0,1]}\,\min_{\theta\in\Theta}\{d_{\min}\}$, JML receiver is employed, and SNR = 10 dB. 40

5.23 Achievable rate pairs of the CPA scheme under two-user GMAC with random phase offset. Here, $\alpha_{\text{opt}} = \text{argmax}_{\alpha\in(0,1]}\{\text{CC sum capacity of average phases}\}$, JML receiver is employed, and SNR = 10 dB. 40

5.24 Achievable rate pairs of the CPA scheme under two-user GMAC with random phase offset. Here, $(\alpha_{\text{opt}}, \theta_{\text{opt}}) = \text{argmax}_{\alpha\in(0,1)\,\&\,\theta\in\Theta}\{d_{\min}\}$, SIC receiver is employed, and SNR = 10 dB. The receiver is also assumed to be able to rotate the two constellations accurately to match θ_{opt}. 42

5.25 Achievable rate pairs of the CPA scheme under two-user GMAC with random phase offset. Here, $\alpha_{\text{opt}} = \text{argmax}_{\alpha\in(0,1]}\,\text{avg}_{\theta\in\Theta}\{d_{\min}\}$, SIC receiver is employed, and SNR = 10 dB. 42

5.26 Achievable rate pairs of the CPA scheme under two-user GMAC with random phase offset. Here, $\alpha_{\text{opt}} = \text{argmax}_{\alpha\in(0,1]}\,\min_{\theta\in\Theta}\{d_{\min}\}$, SIC receiver is employed, and SNR = 10 dB. 43

5.27 Achievable rate pairs of the CPA scheme under two-user GMAC with random phase offset. Here, $\alpha_{\text{opt}} = \text{argmax}_{\alpha\in(0,1]}\{\text{CC sum capacity of average phases}\}$, SIC receiver is employed, and SNR = 10 dB. 43

5.28 Parameter setting with or without adjustment of constellation rotation . . 54

5.29 α_{opt} and θ_{opt} selected based on different modulation combinations and different distance-based criterion. The SNRs of UE1 and UE2 are respectively 3 dB and 6 dB. 57

5.30 α_{opt} based on different modulation combinations and unequal SNRs 57

5.31 α_{opt} and θ_{opt} selected based on different modulation combinations and different distance-based criterion. The SNRs of UE1 and UE2 are respectively 3 dB and 10 dB. 58

5.32 α_{opt} based on different modulation combinations and unequal SNRs. The SNRs of UE1 and UE2 are respectively 3 dB and 10 dB. 58

5.33 Achievable rate pairs of the CPA scheme under two-user GMAC with random phase offset. Here, $(\alpha_{\text{opt}}, \theta_{\text{opt}}) = \text{argmax}_{\alpha\in(0,1)\,\&\,\theta\in\Theta}\{d_{\min}\}$, JML receiver is employed, UE1 SNR = 3 dB and UE2 SNR = 6 dB. The receiver is also assumed to be able to rotate the two constellations accurately to match θ_{opt}. 59

5.34 Achievable rate pairs of the CPA scheme under two-user GMAC with random phase offset. Here, $\alpha_{\text{opt}} = \text{argmax}_{\alpha\in(0,1]}\,\text{avg}_{\theta\in\Theta}\{d_{\min}\}$, JML receiver is employed, UE1 SNR = 3 dB and UE2 SNR = 6 dB. 59

5.35 Achievable rate pairs of the CPA scheme under two-user GMAC with random phase offset. Here, $\alpha_{\text{opt}} = \text{argmax}_{\alpha\in(0,1]}\,\min_{\theta\in\Theta}\{d_{\min}\}$, JML receiver is employed, UE1 SNR = 3 dB and UE2 SNR = 6 dB. 59

5.36 Achievable rate pairs of the CPA scheme under two-user GMAC with random phase offset. Here, $\alpha_{\text{opt}} = \text{argmax}_{\alpha\in(0,1]}\{\text{CC sum capacity of average phases}\}$, JML receiver is employed, UE1 SNR = 3 dB and UE2 SNR = 6 dB. 60

5.37 Achievable rate pairs of the CPA scheme under two-user GMAC with random phase offset. Here, $(\alpha_{\text{opt}}, \theta_{\text{opt}}) = \text{argmax}_{\alpha\in(0,1)\,\&\,\theta\in\Theta}\{d_{\min}\}$, SIC receiver is employed, UE1 SNR = 3 dB and UE2 SNR = 6 dB. The receiver is also assumed to be able to rotate the two constellations accurately to match θ_{opt}. 60

5.38 Achievable rate pairs of the CPA scheme under two-user GMAC with random phase offset. Here, $\alpha_{\text{opt}} = \text{argmax}_{\alpha\in(0,1]}\,\text{avg}_{\theta\in\Theta}\{d_{\min}\}$, SIC receiver is employed, UE1 SNR = 3 dB and UE2 SNR = 6 dB. 60

5.39 Achievable rate pairs of the CPA scheme under two-user GMAC with random phase offset. Here, $\alpha_{\text{opt}} = \text{argmax}_{\alpha\in(0,1]}\,\min_{\theta\in\Theta}\{d_{\min}\}$, SIC receiver is employed, UE1 SNR = 3 dB and UE2 SNR = 6 dB. 62

5.40 Achievable rate pairs of the CPA scheme under two-user GMAC with random phase offset. Here, $\alpha_{\text{opt}} = \text{argmax}_{\alpha\in(0,1]}\{\text{CC sum capacity of average phases}\}$, SIC receiver is employed, UE1 SNR = 3 dB and UE2 SNR = 6 dB. 62

5.41 Achievable rate pairs of the CPA scheme under two-user GMAC with random phase offset. Here, $(\alpha_{\text{opt}}, \theta_{\text{opt}}) = \text{argmax}_{\alpha\in(0,1)\,\&\,\theta\in\Theta}\{d_{\min}\}$, JML receiver is employed, UE1 SNR = 3 dB and UE2 SNR = 10 dB. The receiver is also assumed to be able to rotate the two constellations accurately to match θ_{opt}. 62

5.42 Achievable rate pairs of the CPA scheme under two-user GMAC with random phase offset. Here, $\alpha_{\text{opt}} = \text{argmax}_{\alpha\in(0,1]}\,\text{avg}_{\theta\in\Theta}\{d_{\min}\}$, JML receiver is employed, UE1 SNR = 3 dB and UE2 SNR = 10 dB. 64

5.43 Achievable rate pairs of the CPA scheme under two-user GMAC with random phase offset. Here, $\alpha_{\text{opt}} = \text{argmax}_{\alpha\in(0,1]}\,\min_{\theta\in\Theta}\{d_{\min}\}$, JML receiver is employed, UE1 SNR = 3 dB and UE2 SNR = 10 dB. 64

5.44 Achievable rate pairs of the CPA scheme under two-user GMAC with random phase offset. Here, $\alpha_{\text{opt}} = \text{argmax}_{\alpha\in(0,1]}\{\text{CC sum capacity of average phases}\}$, JML receiver is employed, UE1 SNR = 3 dB and UE2 SNR = 10 dB. . . . 64

5.45 Achievable rate pairs of the CPA scheme under two-user GMAC with random phase offset. Here, $(\alpha_{\text{opt}}, \theta_{\text{opt}}) = \text{argmax}_{\alpha\in(0,1)\,\&\,\theta\in\Theta}\{d_{\min}\}$, SIC receiver is employed, UE1 SNR = 3 dB and UE2 SNR = 10 dB. The receiver is also assumed to be able to rotate the two constellations accurately to match θ_{opt}. 66

5.46 Achievable rate pairs of the CPA scheme under two-user GMAC with random phase offset. Here, $\alpha_{\text{opt}} = \text{argmax}_{\alpha\in(0,1]}\,\text{avg}_{\theta\in\Theta}\{d_{\min}\}$, SIC receiver is employed, UE1 SNR = 3 dB and UE2 SNR = 10 dB. 66

5.47 Achievable rate pairs of the CPA scheme under two-user GMAC with random phase offset. Here, $\alpha_{\text{opt}} = \text{argmax}_{\alpha\in(0,1]}\,\min_{\theta\in\Theta}\{d_{\min}\}$, SIC receiver is employed, UE1 SNR = 3 dB and UE2 SNR = 10 dB. 66

5.48 Achievable rate pairs of the CPA scheme under two-user GMAC with random phase offset. Here, $\alpha_{\text{opt}} = \text{argmax}_{\alpha\in(0,1]}\{\text{CC sum capacity of average phases}\}$, SIC receiver is employed, UE1 SNR = 3 dB and UE2 SNR = 10 dB. 68

5.49 α_{opt} and $\theta_{\text{opt}} = (\theta_{\text{opt,UE2}}, \theta_{\text{opt,UE3}})$ selected based on different modulation combinations and different distance-based criterions 70

5.50 α_{opt} based on different modulation combinations and different SNRs 70

5.51 Achievable rate pairs of the CPA scheme for three-user GMAC with random phase offset. Here, $(\alpha_{\text{opt}}, \theta_{\text{opt}}) = \text{argmax}_{\alpha\in(0,1)\,\&\,\theta\in\Theta}\{d_{\min}\}$, JML receiver is employed, and SNR = 3 dB. The receiver is also assumed to be able to rotate the two constellations accurately to match θ_{opt}. 71

5.52 Achievable rate pairs of the CPA scheme for three-user GMAC with random phase offset. Here, $\alpha_{\text{opt}} = \text{argmax}_{\alpha\in(0,1]}\,\text{avg}_{\theta\in\Theta}\{d_{\min}\}$, JML receiver is employed, and SNR = 3 dB. 71

5.53 Achievable rate pairs of the CPA scheme for three-user GMAC with random phase offset. Here, $\alpha_{\text{opt}} = \text{argmax}_{\alpha\in(0,1]}\,\min_{\theta\in\Theta}\{d_{\min}\}$, JML receiver is employed, and SNR = 3 dB. 71

5.54 Achievable rate pairs of the CPA scheme for three-user GMAC with random phase offset. Here, $\alpha_{\text{opt}} = \text{argmax}_{\alpha\in(0,1]}\{\text{CC sum capacity of average phases}\}$, JML receiver is employed, and SNR = 3 dB. 72

5.55 Achievable rate pairs of the CPA scheme for three-user GMAC with random phase offset. Here, $(\alpha_{\text{opt}}, \theta_{\text{opt}}) = \text{argmax}_{\alpha\in(0,1)\,\&\,\theta\in\Theta}\{d_{\min}\}$, SIC receiver is employed, and SNR = 3 dB. 72

5.56 Achievable rate pairs of the CPA scheme for three-user GMAC with random phase offset. Here, $\alpha_{\text{opt}} = \text{argmax}_{\alpha\in(0,1]}\,\text{avg}_{\theta\in\Theta}\{d_{\min}\}$, SIC receiver is employed, and SNR = 3 dB. 72

5.57 Achievable rate pairs of the CPA scheme for three-user GMAC with random phase offset. Here, $\alpha_{\text{opt}} = \text{argmax}_{\alpha\in(0,1]}\,\min_{\theta\in\Theta}\{d_{\min}\}$, SIC receiver is employed, and SNR = 3 dB. 73

5.58 Achievable rate pairs of the CPA scheme for three-user GMAC with random phase offset. Here, $\alpha_{\text{opt}} = \text{argmax}_{\alpha\in(0,1]}\{\text{CC sum capacity of average phases}\}$, SIC receiver is employed, and SNR = 3 dB. 73

5.59 Achievable rate pairs of the CPA scheme for three-user GMAC with random phase offset. Here, $(\alpha_{\text{opt}}, \theta_{\text{opt}}) = \text{argmax}_{\alpha\in(0,1)\,\&\,\theta\in\Theta}\{d_{\min}\}$, JML receiver is employed, and SNR = 6 dB. The receiver is assumed to be able to rotate the two constellations accurately to match θ_{opt}. 73

5.60 Achievable rate pairs of the CPA scheme for three-user GMAC with random phase offset. Here, $\alpha_{\text{opt}} = \text{argmax}_{\alpha\in(0,1]}\,\text{avg}_{\theta\in\Theta}\{d_{\min}\}$, JML receiver is employed, and SNR = 6 dB. 74

5.61 Achievable rate pairs of the CPA scheme for three-user GMAC with random phase offset. Here, $\alpha_{\text{opt}} = \text{argmax}_{\alpha\in(0,1]}\,\min_{\theta\in\Theta}\{d_{\min}\}$, JML receiver is employed, and SNR = 6 dB. 74

5.62 Achievable rate pairs of the CPA scheme for three-user GMAC with random phase offset. Here, $\alpha_{\text{opt}} = \text{argmax}_{\alpha\in(0,1]}\{\text{CC sum capacity of average phases}\}$, JML receiver is employed, and SNR = 6 dB. 74

5.63 Achievable rate pairs of the CPA scheme for three-user GMAC with random phase offset. Here, $(\alpha_{\text{opt}}, \theta_{\text{opt}}) = \text{argmax}_{\alpha\in(0,1)\,\&\,\theta\in\Theta}\{d_{\min}\}$, SIC receiver is employed, and SNR = 6 dB. The receiver is assumed to be able to rotate the two constellations accurately to match θ_{opt}. 75

5.64 Achievable rate pairs of the CPA scheme for three-user GMAC with random phase offset. Here, $\alpha_{\text{opt}} = \text{argmax}_{\alpha\in(0,1]}\,\text{avg}_{\theta\in\Theta}\{d_{\min}\}$, SIC receiver is employed, and SNR = 6 dB. 75

5.65 Achievable rate pairs of the CPA scheme for three-user GMAC with random phase offset. Here, $\alpha_{\text{opt}} = \text{argmax}_{\alpha\in(0,1]}\,\min_{\theta\in\Theta}\{d_{\min}\}$, SIC receiver is employed, and SNR = 6 dB. 75

5.66 Achievable rate pairs of the CPA scheme for three-user GMAC with random phase offset. Here, $\alpha_{\text{opt}} = \text{argmax}_{\alpha\in(0,1]}\{\text{CC sum capacity of average phases}\}$, SIC receiver is employed, and SNR = 6 dB. 76

5.67 Achievable rate pairs of the CPA scheme for three-user GMAC with random phase offset. Here, $(\alpha_{\text{opt}}, \theta_{\text{opt}}) = \text{argmax}_{\alpha\in(0,1)\,\&\,\theta\in\Theta}\{d_{\min}\}$, JML receiver is employed, and SNR = 10 dB. The receiver is assumed to be able to rotate the two constellations accurately to match θ_{opt}. 76

5.68 Achievable rate pairs of the CPA scheme for three-user GMAC with random phase offset. Here, $\alpha_{\text{opt}} = \text{argmax}_{\alpha\in(0,1]}\,\text{avg}_{\theta\in\Theta}\{d_{\min}\}$, JML receiver is employed, and SNR = 10 dB. 76

5.69 Achievable rate pairs of the CPA scheme for three-user GMAC with random phase offset. Here, $\alpha_{\text{opt}} = \text{argmax}_{\alpha\in(0,1]}\,\min_{\theta\in\Theta}\{d_{\min}\}$, JML receiver is employed, and SNR = 6 dB. 77

5.70 Achievable rate pairs of the CPA scheme for three-user GMAC with random phase offset. Here, $\alpha_{\text{opt}} = \text{argmax}_{\alpha\in(0,1]}\{\text{CC sum capacity of average phases}\}$, JML receiver is employed, and SNR = 6 dB. 77

5.71 Achievable rate pairs of the CPA scheme for three-user GMAC with random phase offset. Here, $(\alpha_{\text{opt}}, \theta_{\text{opt}}) = \text{argmax}_{\alpha\in(0,1)\,\&\,\theta\in\Theta}\{d_{\min}\}$, SIC receiver is employed, and SNR = 10 dB. The receiver is assumed to be able to rotate the two constellations accurately to match θ_{opt}. 77

5.72 Achievable rate pairs of the CPA scheme for three-user GMAC with random phase offset. Here, $\alpha_{\text{opt}} = \text{argmax}_{\alpha\in(0,1]}\,\text{avg}_{\theta\in\Theta}\{d_{\min}\}$, SIC receiver is employed, and SNR = 10 dB. 78

5.73 Achievable rate pairs of the CPA scheme for three-user GMAC with random phase offset. Here, $\alpha_{\text{opt}} = \text{argmax}_{\alpha\in(0,1]}\,\min_{\theta\in\Theta}\{d_{\min}\}$, SIC receiver is employed, and SNR = 10 dB. 78

5.74 Achievable rate pairs of the CPA scheme for three-user GMAC with random phase offset. Here, $\alpha_{\text{opt}} = \text{argmax}_{\alpha \in (0,1]}\{\text{CC sum capacity of average phases}\}$, SIC receiver is employed, and SNR = 10 dB. 78

Chapter 1

Introduction

In wireless communication systems, multiple access (MA) [5] is one of the important technologies to improve the system capacity. It can be classified into two types: orthogonal multiple access (OMA) and non-orthogonal multiple access (NOMA). Examples of OMA include time division multiple access (TDMA), frequency division multiple access (FDMA), code division multiple access (CDMA), and orthogonal frequency division multiple access (OFDMA). Due to the simplicity in receiver design from orthogonality characteristic, OMA was a typical choice for system implementation.

However, the recent trend in mobile communications, particularly fourth generation (4G) Long-Term Evolution (LTE) [2] and the future fifth generation (5G) systems [17], anticipates an exponential growth of users and a significant spectrum resources scarcity. Hence, orthogonality becomes a restriction rather than an advantage in pushing further the increasing of transmission rates and spectral efficiency. At this background, NOMA was proposed and has been extensively studied [15].

The key idea of NOMA [3, 4, 8, 12] is that multiple users in the power domain are superposed at the symbol level. Thus, different from the OMA system, NOMA allows more than one users to transmit their data at the same time slot or at the same frequency band. Although such a system structure inevitably introduces intra-cell and inter-cell interference [11] and requires advanced receiver design to retrieve the user data, it has been

shown that NOMA yields a significant spectral efficiency gain over OMA. In comparison with conventional opportunistic user scheduling, which serves users subject to necessary knowledge of channel state information, NOMA strikes a good balance between system throughput and user fairness [13]. It also meets the demanding 5G requirements of ultra-low latency and massive connectivity [16]. As a consequence, NOMA is regarded as a promising candidate technology for cellular multiple access of future radio communication system.

In this thesis, we will focus on the Constellation Power Allocation (CPA) transmission scheme proposed in [7] and investigate its system performance over the uplink NOMA scenario [1]. The channel model considered is the Gaussian Multiple Access Channel (GMAC) with additional random phase offset.

The remaining parts of the thesis is organized as follows. Chapter 2 introduces the system model and background on NOMA. Also covered in Chapter 2 are the transmitter and receiver designs that we adopt in this thesis. Chapter 3 presents the CPA scheme and derives the CC sum capacity of the GMAC with random phase offsets. In Chapter 4, several alternative distance-based objective functions other than the CC sum capacity for the algorithmic determination of the power allocation factor of the CPA scheme transmitted over a two-user GMAC with random phase offsets is proposed. Possible extension to the three-user GMAC with random phase offset is also addressed. Chapter 5 gives and remarks on the simulation results, and Chapter 6 concludes the thesis.

Chapter 2

System Model and Background

Non-Orthogonal Multiple Access (NOMA) has been validated as an effective multiple access technique to improve the spectral efficiency and throughput for cell-edge users. In this chapter, we will introduce four application scenarios of NOMA. These four scenarios will be classified into two categories: (i) the base station (BS) can perfectly coordinate the transmission signals from user equipments (UEs), and (ii) the BS can only coordinate the transmission powers of UEs. Next, the basic conception of the uplink NOMA will be introduced. Typical transmitter and receiver designs for NOMA will be briefed at the last three sections.

2.1 Application Scenarios for Non-Orthogonal Multiple Access (NOMA)

Figure 2.1 depicts an application scenario of NOMA: Wireless backhaul for static small cells. Specifically, the wireless backhaul in Figure 2.1 comprises the wireless routes between small cells and mobile core network of the operator. These can be deployed in an urban area, where small cells are mounted on lampposts, or positioned on sides of buildings, or found in transport hubs. They provide mobile phone services and deliver

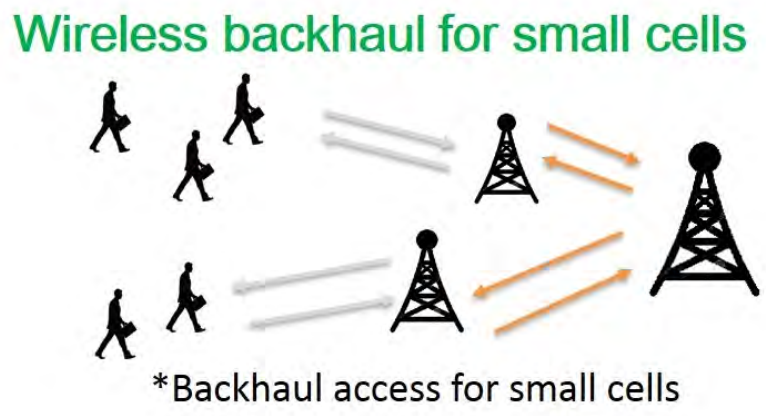

Figure 2.1: An application scenario of NOMA: Wireless backhaul for static small cells

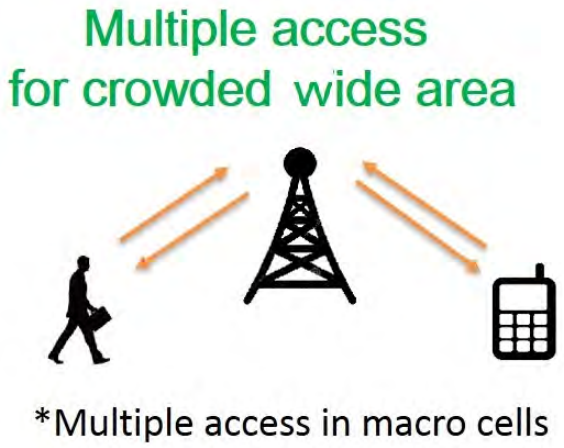

Figure 2.2: An application scenario of NOMA: Multiple access for crowded wide area

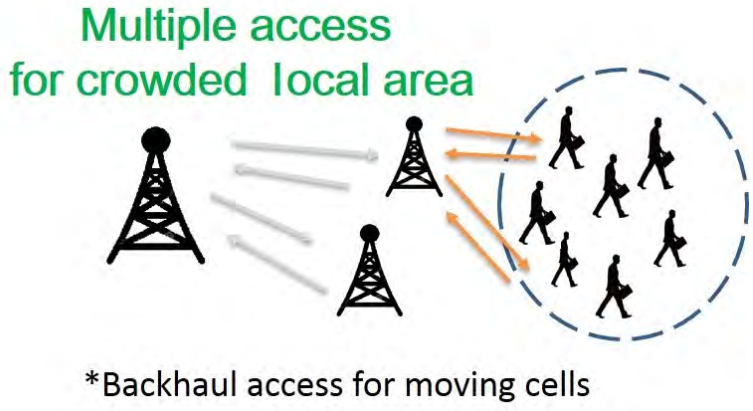

Figure 2.3: An application scenario of NOMA: Multiple access for crowded local area

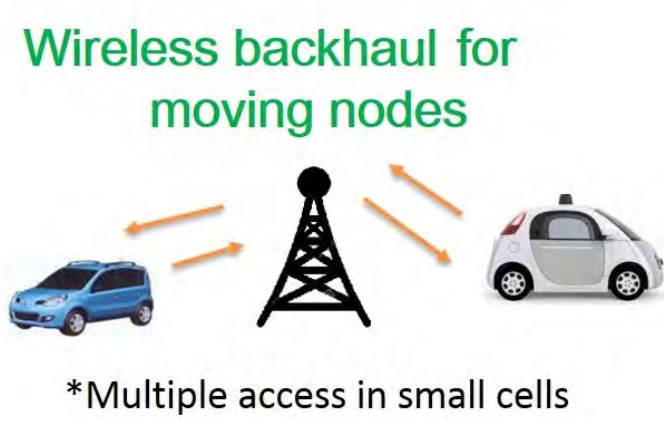

Figure 2.4: An application scenario of NOMA: Wireless backhaul for moving nodes

data at a very high transmission speed, and can solve cost-effectively the problem of growing data traffic demand in modern communication systems. Since in this scenario, both small cells and mobile core network are static and not moving, the channel state information (CSI) of the wireless links can be estimated accurately. Thus, the BS can coordinate both phase and amplitude of transmission signals in advance to achieve a better performance.

Figure 2.2 depicts a second scenario of NOMA: Multiple access for crowded wide area. It comprises the transmission links between macro cells and mobile devices, where mobile devices are served within the coverage of macro cells.

Figure 2.3 depicts a third scenario of NOMA: Multiple access for crowded local area. It comprises the transmission links between small cells and mobile devices, where mobile devices are served within the coverage of small cells. An example of this scenario is to mount small cells in train stations or schools in order to satisfy the network service demands from the local crowd.

Figure 2.4 depicts a fourth scenario of NOMA: Wireless backhaul for moving nodes. It is constituted of the transmission links between macro cells and moving nodes, for which unmanned flying vehicles is one of the applications in this scenario.

For the scenarios considered in Figures 2.2 –2.4, the position of a transmitter may change after each MIMO transmission and hence the receiver cannot estimate the CSI accurately. As a result, receivers can only coordinate the transmission powers of UEs, or

equivalently the amplitudes of transmission signals. The phases of transmission signals thus become random variables and will be assumed to be uniformly distributed over $[0, 2\pi)$. Equivalently, receivers encounter a random uniform rotation of the transmission constellations.

2.2 Uplink Non-Orthogonal Multiple Access (NOMA)

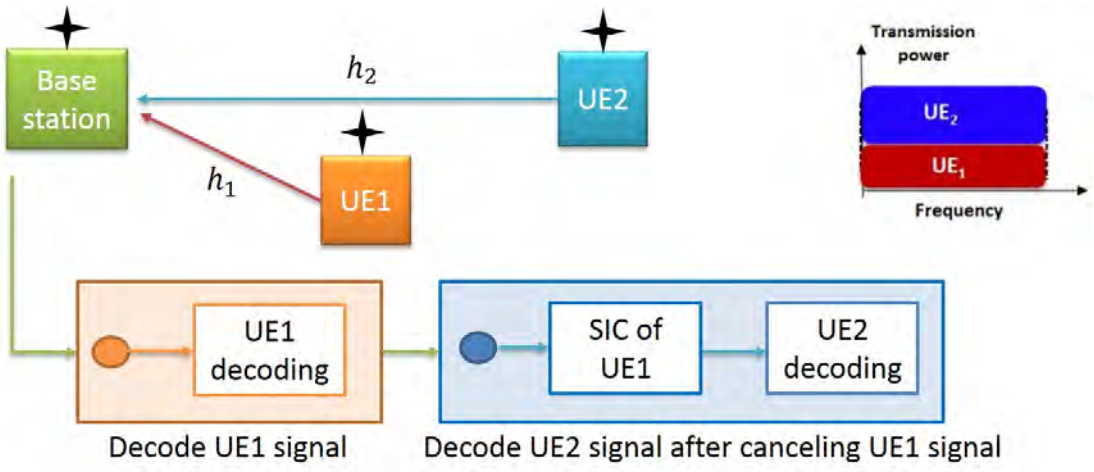

Figure 2.5: An uplink NOMA transmission scheme

In an uplink NOMA scheme, the BS serves multiple users of different power levels at the same time/frequency. In order to retrieve the signals from these users, techniques such as successive interference cancellation (SIC) are used within the BS.

In order to simplify the analysis, we consider the simplest uplink NOMA situation in Figure 2.5, where mobile devices and BSs are only equipped with a single antenna and only two users are served by the BS. The noise-free received signal s from the two UEs can be described by the following equation:

$$s = \sqrt{P_1} h_1 x_1 + \sqrt{P_2} h_2 x_2, \tag{2.1}$$

where x_1 and x_2 are the unit-power signals (satisfying $E[|x_1|^2] = E[|x_2|^2] = 1$) respectively transmitted by UE1 and UE2, P_1 and P_2 are their respective transmission powers, and h_1 and h_2 denote respectively the channel gains corresponding to UE1 and UE2. The noisy

received signal y at the BS is then given by

$$y = \sqrt{P_1}h_1x_1 + \sqrt{P_2}h_2x_2 + z, \tag{2.2}$$

where z is an additive white Gaussian noise (AWGN) with mean zero and variance σ^2. Assume that the power allocation applied to each user has an average power constraint that is in the form of

$$P_1 \leq 1; \tag{2.3}$$

$$P_2 \leq 1. \tag{2.4}$$

The model defined in (2.2) can be further exemplified as a resource allotment with four resource elements and six UEs as shown in Figure 2.6. A resource element could be a time slot or a frequency band in communication systems. A colored square in the figure indicates that the resource element is required and hence assigned to the user, while a white square is unassigned. A user may utilize two or more resource elements to transmit its data. The user signals occupied the same resource element thus superimpose when being received by the BS, and hence interfere with each other. In the scenario that the BS knows the CSI, the SIC technique can be employed to remove the interferences from other users successively and an acceptable system performance can be obtained.

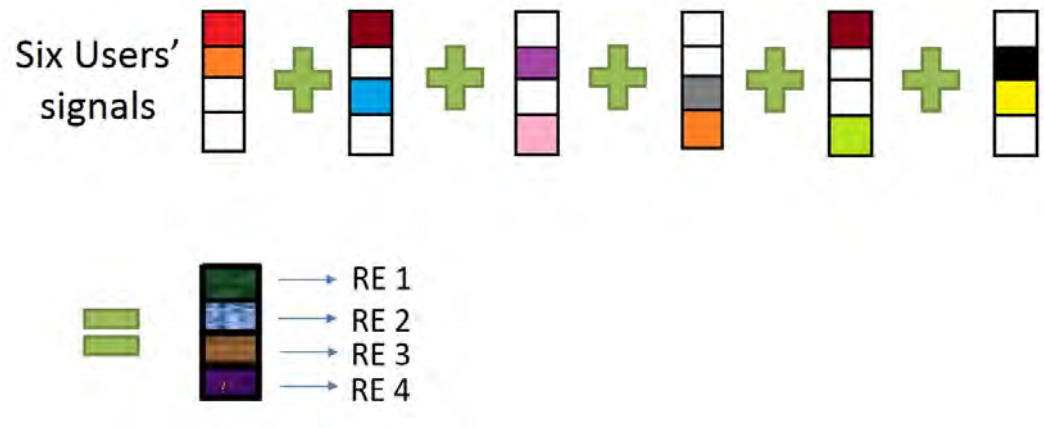

Figure 2.6: An exemplified resource allotment with four resource elements and six users in an uplink NOMA

2.3 Multilevel Coding for NOMA

In this section, the multilevel coding scheme will be introduced. How the multilevel coding scheme co-work with NOMA will be introduced in later sections.

2.3.1 Multilevel Code Encoder

The basic structure of a multilevel encoder is shown in Figure 2.7. It separates the information bits into l bit streams, each of which is encoded independently with possibly different code rate. The resulting coded bits are mapped in parallel to the constellation of modulation order 2^l. As an example with $l = 3$, Figure 2.8 indicates that the modulator maps the three code bits $b_i^0 b_i^1 b_i^2$ respectively from the three coded bit streams to an 8PAM symbol.

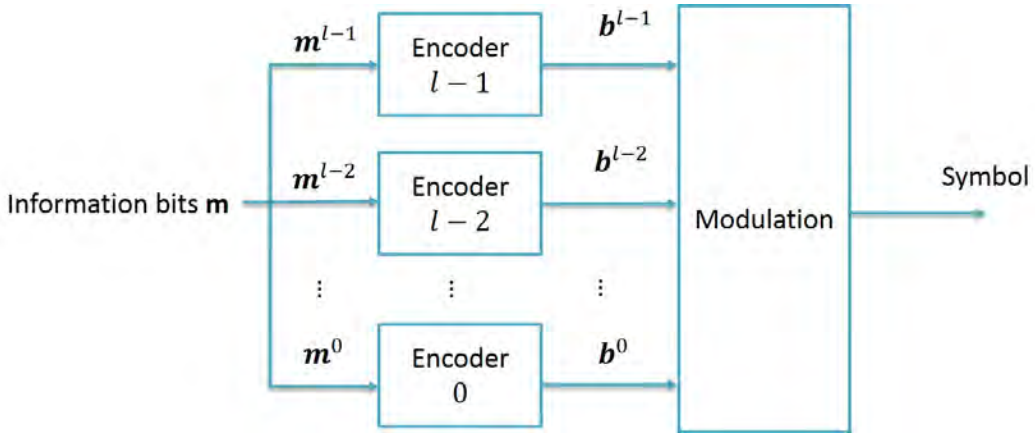

Figure 2.7: A multilevel code transmitter

2.3.2 Multistage Decoder for Multilevel Codes

The idea of multistage decoding is to jointly optimize decoding and demodulation, i.e., estimating the code bits in Euclidean space rather than only dealing with Hamming distance. The decoding procedure can be easier to understand by the example in Figure 2.8. At stage 0, each b_i^0 is demapped via a simplified constellation for the code bits at level 0 and the resulting code bits are decoded using the respective decoder 0. The resulting

information bit stream at level 0 are subsequently re-encoded at the receiver to decide the demapping constellation for the code bits at level 1. An example for $b_i^0 = 1$ is shown in Figure 2.8, where the constellation points correspond to $b_i^0 = 0$ are all eliminated. As such, we repeat the procedure for the decoding of the code bits at the next level. After the reconstruction of the information bit stream corresponding to b_i^1 via demapper and decoder at level 1, the resulting information bit stream is re-encoded to decide, jointly with b_i^0, the demapping constellation at level 2. An example for $b_i^1 b_i^0 = 10$ is shown in Figure 2.8, where again the constellation points correspond to $b_i^1 b_i^0 \neq 10$ are all eliminated. This completes the multistage decoding of a multilevel code.

We can put the above decoding procedure into a diagram shown in Figure 2.9. There are l successive decoders. At stage l, the decoding outputs of the previous stages are re-encoded and used to decide the constellation for the demapper at level l. In order to prevent error propagation from happening, cyclic redundancy check (CRC) are added to verify the integrity of the bit stream at each level. When CRC at stage l fails, the corresponding bit stream will not be used to eliminate the constellation points for the decoding of code bits at those level higher than l.

2.4 Joint Maximum-Likelihood (JML) Receiver

Starting from this section, two kinds of receiver component designs for multi-user signals received by the BS are introduced: Joint maximum-likelihood (JML) receiver and successive interference cancellation (SIC) receiver. The latter will be introduced in the next section.

Consider the simplest NOMA scenario in Figure 2.5, where the received signal is given by (2.2). For modulation of order $2^{K_1+K_2}$, suppose K_1 bits are allocated to the first UE and K_2 bits are assigned to the second UE, which for simplicity are denoted as $b_0 b_1 \dots b_{K_1-1}$ and $b_{K_1} b_{K_1+1} \dots b_{K_1+K_2-1}$, respectively. The BS calculates the log-likelihood

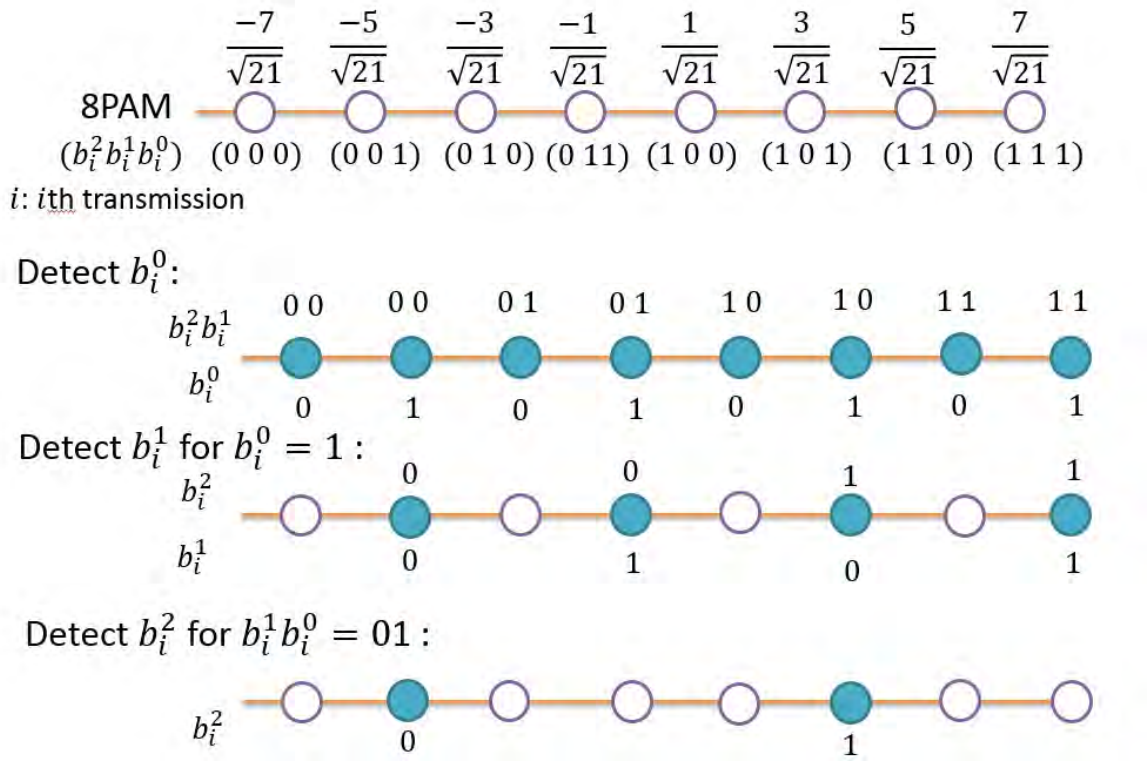

Figure 2.8: Example of multistage decoding

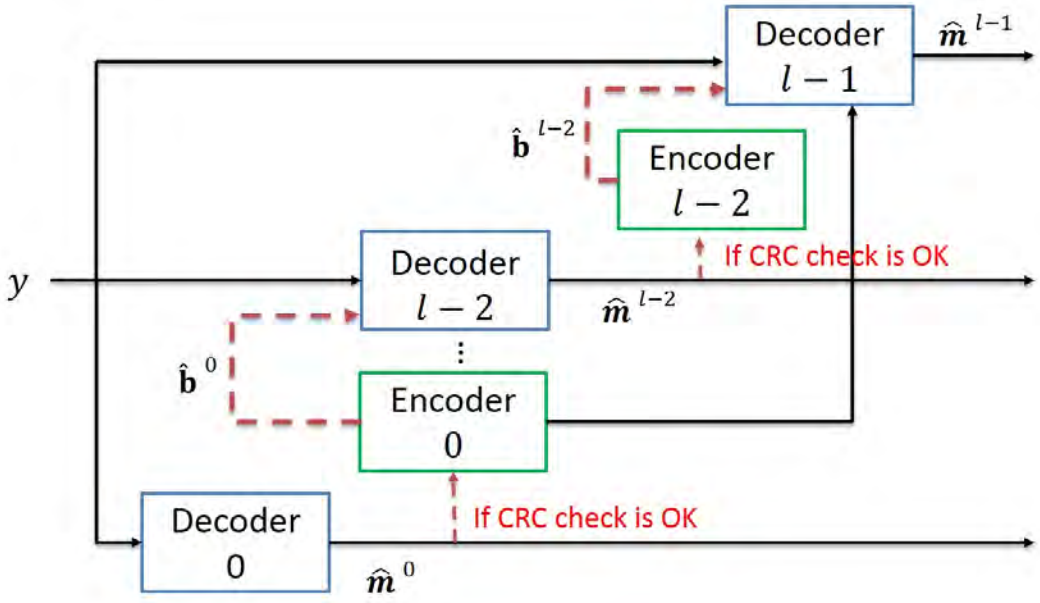

Figure 2.9: Multistage decoding for multilevel codes

ratios (LLRs) for bit b_k according to:

$$\mathrm{LLR}(b_k) = \log \frac{\max\limits_{s \in \mathcal{S}_k^{(1)}} \frac{1}{\sqrt{2\pi}\sigma} \exp\left(-\frac{1}{2\sigma^2} |y-s|^2\right)}{\max\limits_{s \in \mathcal{S}_k^{(0)}} \frac{1}{\sqrt{2\pi}\sigma} \exp\left(-\frac{1}{2\sigma^2} |y-s|^2\right)} \tag{2.5}$$

where $\mathcal{S}_k^{(b)}$ is the set of joint constellation points from (2.1) corresponding to $b_k = b$. These LLRs can be used for a soft-decision decoder to decode the information bits from the respective user.

2.5 Successive Interference Cancellation (SIC) Receiver

By using a similar notion to multilevel coding, interference cancellation can be done at bit level, which can be described in two steps as follows, where we suppose the first UE is the strong UE.

Step 1: Calculate LLRs corresponding to those code bits $b_0 b_1 \cdots b_{K_1-1}$ of the strong UE via (2.5), based on which the information bits of the strong UE are decoded. Verify CRC of the decoded information bits of the strong UE. If CRC check is succeeded, re-encode the decoded information bits of the strong UE and go to Step 2; else, fall back to use JML receiver to demodulate and decode the information bits of the weak UE.

Step 2: Calculate the LLRs corresponding to those coded bits of the weak UE according to:

$$\mathrm{LLR}(b_k) = \log \frac{\max\limits_{s \in \mathcal{S}_{\mathrm{weak},k}^{(1)}} \frac{1}{\sqrt{2\pi}\sigma} \exp\left(-\frac{1}{2\sigma^2} |y-s|^2\right)}{\max\limits_{s \in \mathcal{S}_{weak,k}^{(0)}} \frac{1}{\sqrt{2\pi}\sigma} \exp\left(-\frac{1}{2\sigma^2} |y-s|^2\right)}, \quad k = K_1, \ldots, K_1 + K_2 - 1 \tag{2.6}$$

where $\mathcal{S}_{\mathrm{weak},k}^{(b)}$ is the set of constellation points of the weak UE from (2.1) corresponding to $b_k = b$ and $b_0 b_1 \cdots b_{K_1-1}$ being obtained from Step 1. Perform decoding according to the LLRs for the weak UE.

Chapter 3

Previous Work and Problem Formulation

We present in this chapter the previous works over a two-user uplink NOMA transmission scenario. Problem formation will follow.

Specifically, we first introduce a novel transmission technique proposed in [7]. It is called *Constellation Power Allocation* (CPA) scheme and is the prototype transmission scheme studied in this thesis. In the CPA scheme, the transmission powers of the two users are varied subject to an average power constraint for each user. Then for the typical model of the Gaussian Multiple Access Channel (GMAC), the so-called Constellation Constrained (CC) capacity is addressed, which in the literature is often served as an objective function for the optimization of the power allocation among users of the CPA scheme. Based on these previous works, the problem that this thesis shoots for is addressed at the last section of this chapter.

3.1 Constellation Power Allocation (CPA) Scheme

Let $\tau \triangleq \{1, 2, \ldots, T\}$ be the set of indices of complex channel uses, where T is an even number. Denote by $\tau_{\text{odd}} \triangleq \{1, 3, \ldots, T-3, T-1\}$ and $\tau_{\text{even}} \triangleq \{2, 4, \ldots, T-2, T\}$ the sets of odd and even indices of channel uses, respectively. With these notations, the CPA scheme can be described as follows.

- If $t \in \tau_{\text{odd}}$
  - UE1 transmits $\sqrt{(2-\alpha)\,P_1}x_1$ for $x_1 \in \mathcal{S}_1$
  - UE2 transmits $\sqrt{\alpha P_2}x_2$ for $x_2 \in \mathcal{S}_2$
- Else if $t \in \tau_{\text{even}}$
  - UE1 transmits $\sqrt{\alpha P_1}x_1$ for $x_1 \in \mathcal{S}_1$
  - UE2 transmits $\sqrt{(2-\alpha)\,P_2}x_2$ for $x_2 \in \mathcal{S}_2$

Here, $\alpha \in [0, 1]$ is a real-valued parameter that controls the transmission powers of the two users.

As a consequence, at odd time instance $t \in \tau_{\text{odd}}$, the BS receives y_t that is of the form

$$y_t = \sqrt{(2-\alpha)\,P_1}x_1 + \sqrt{\alpha P_2}x_2 + z,$$

while when $t \in \tau_{\text{even}}$, the BS receives

$$y_t = \sqrt{\alpha P_1}x_1 + \sqrt{(2-\alpha)\,P_2}x_2 + z.$$

By this alternation, the transmission power for UE1 is equal to $(2-\alpha)P_1$ at exactly half of the time instances and αP_1 at another half of the time instances. Thus the overall average power for UE1 is given by

$$\frac{(2-\alpha)P_1 + \alpha P_1}{2} = P_1.$$

Likewise, the average power for UE2 remains P_2 by the same alternation.

Under such a design, UE1 and UE2 take turn to be the strong user and hence the SIC technique, for example, can be well applied for the demodulation of the information bit streams from UE1 and UE2.

3.2 Capacity Region and Constellation Constrained (CC) Sum Capacity for GMAC

3.2.1 Capacity Region for GMAC

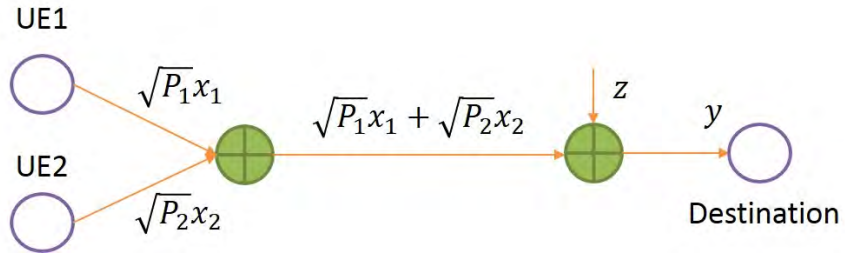

Figure 3.1: A two-user GMAC model

Consider a two-user GMAC channel model as shown in Figure 3.1. Denote by P_i the average power for UE-i, where $i = 1, 2$. Then it is well-known in the literature that the achievable rate pairs (R_1, R_2) satisfy three inequalities:

$$R_1 < \log\left(1 + \frac{P_1}{N_0}\right), \tag{3.1}$$

$$R_2 < \log\left(1 + \frac{P_2}{N_0}\right), \tag{3.2}$$

$$R_1 + R_2 < \log\left(1 + \frac{P_1 + P_2}{N_0}\right). \tag{3.3}$$

Inequalities (3.1) and (3.2) point out that the rate of any individual user cannot exceed the capacity of the point-to-point link with the other user being absent from the system. Inequality (3.3) says that the sum rate of the two users cannot exceed the capacity of the point-to-point channel by putting together both transmission powers.

The resulting capacity region is the pentagon as shown in Figure 3.2. It is known that point A can be achieved by using the SIC receiver. In short, the receiver first decodes the data of User 2 by treating the signal from User 1 as interference. After the reconstruction of the signal from User 2, subtract it from the aggregated received signal and based on the residue signal, decode the signal from User 1. Point B can be achieved by reversing

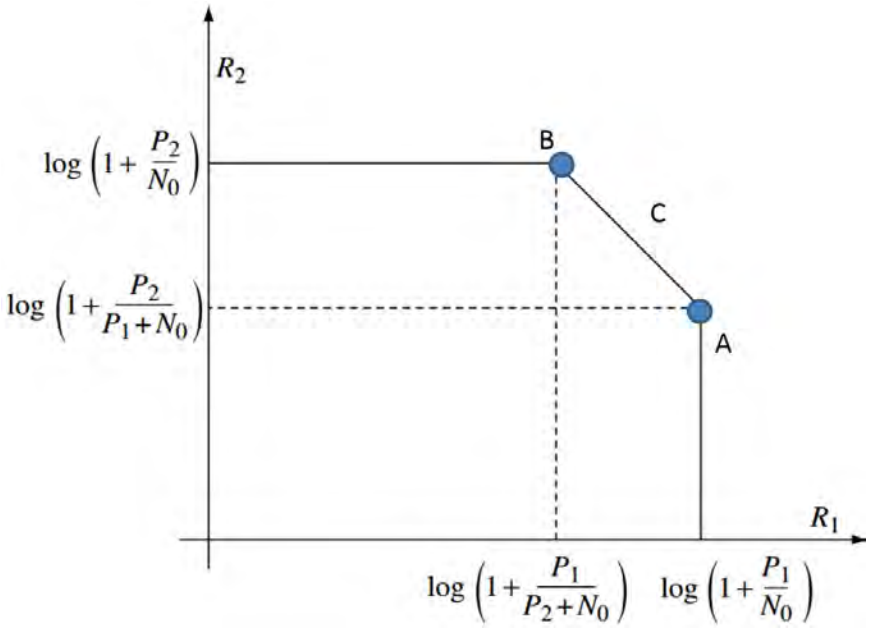

Figure 3.2: Capacity region for a two-user GMAC

the roles of User 1 and User 2. Segment C can be achieved by incorporating time-sharing technique.

3.2.2 Constellation Constrained (CC) Sum Capacity for GMAC

Consider again a two-user GMAC channel model as shown in Figure 3.1, where the transmission signals from the two users are now restricted to be selected from finite complex constellations $\mathcal{S}_1$ and $\mathcal{S}_2$, respectively. Then the BS receives the complex symbol y given by

$$y = \sqrt{P_1}x_1 + \sqrt{P_2}x_2 + z. \tag{3.4}$$

Based on this model, it is known that the so-called constellation constrained (CC) sum capacity is given by

$$I\left(\sqrt{P_1}x_1 + \sqrt{P_2}x_2; y\right) = \log_2(N_1N_2)$$
$$-\frac{1}{N_1N_2}\sum_{k_1=0}^{N_1-1}\sum_{k_2=0}^{N_2-1}\mathbb{E}\left[\log_2\frac{\sum_{i_1=0}^{N_1-1}\sum_{i_2=0}^{N_2-1}e^{-\frac{\left|z+\sqrt{P_1}(x_1(k_1)-x_1(i_1))+\sqrt{P_2}(x_2(k_2)-x_2(i_2))\right|^2}{\sigma^2}}}{e^{-|z|^2/\sigma^2}}\right],$$

where for $i = 1, 2$, $N_i = |\mathcal{S}_i|$ is the number of constellation points in $\mathcal{S}_i$ and $x_i(k)$ denotes the value corresponding to k-th constellation point in $\mathcal{S}_i$.

3.2.3 Constellation Constrained (CC) Sum Capacity for GMAC with Random Phase Effect

As stated in the previous chapter, the BS may not have a good control of the phases of signals from users. Thus in this section, we consider a slightly extended model of the two-user GMAC by introducing random phase offsets. The signal received by the BS is refined as

$$y = e^{i\theta_1}\sqrt{P_1}x_1 + e^{i\theta_2}\sqrt{P_2}x_2 + z, \tag{3.5}$$

where θ_1 and θ_2 are independent random variables that are uniformly distributed over $[0, 2\pi)$. The expectation value of the CC sum capacity for the CPA scheme transmitted over the two-user GMAC with random phase offset is given by

$$\mathbb{E}_{\theta_1,\theta_2}\left[\sum_{\alpha\in\Omega} I\left(\sqrt{(2-\alpha)P_1}x_1 + \sqrt{\alpha P_2}x_2; y\middle|\,\theta_1,\theta_2\right)\right] \tag{3.6}$$

$$= \mathbb{E}_{\theta_1,\theta_2}\left[\sum_{\alpha\in\Omega} I\left(\sqrt{P_L}x_1 + \sqrt{P_S}x_2; y\middle|\,\theta_1,\theta_2\right)\right] \tag{3.7}$$

where $\Omega \triangleq \{\alpha, 2-\alpha\}$, $P_L \triangleq (2-\alpha)\,P_1$, $P_S \triangleq \alpha P_2$, and the expectation value is taken over random phases θ_1 and θ_2. Here,

$$I\left(\sqrt{P_L}x_1 + \sqrt{P_S}x_2; y\middle|\,\theta_1,\theta_2\right) = \log_2(N_1N_2) - \frac{1}{N_1N_2}\sum_{k_1=0}^{N_1-1}\sum_{k_2=0}^{N_2-1}\mathbb{E}\left[\log_2\frac{\sum_{i_1=0}^{N_1-1}\sum_{i_2=0}^{N_2-1} e^{-\frac{\left|z+e^{i\theta_1}\sqrt{P_L}(x_1(k_1)-x_1(i_1))+e^{i\theta_2}\sqrt{P_S}(x_2(k_2)-x_2(i_2))\right|^2}{\sigma^2}}}{e^{-|z|^2/\sigma^2}}\right]. \tag{3.8}$$

In later chapters, for convenience, we will refer to (3.7) as *CC sum capacity of average phases* (or simply *CC sum capacity*), and (3.11) as *CC sum capacity with phase adjustment*.

3.3 Power Allocation Based on CC Sum Capacity

Recall that during the odd time instance uses of channels, the sum constellation $\mathcal{S}_{\text{sum,odd}}$ of UE1 and UE2, as a function of θ_1 and θ_2, is equal to

$$\mathcal{S}_{\text{sum,odd}} \triangleq \left\{ e^{i\theta_1}\sqrt{(2-\alpha)\,P_1}x_1 + e^{i\theta_2}\sqrt{\alpha P_2}x_2 \middle| \, \forall x_1 \in \mathcal{S}_1, \forall x_2 \in \mathcal{S}_2 \right\}. \tag{3.9}$$

Likewise, the sum constellation $\mathcal{S}_{\text{sum,even}}$ of UE1 and UE2, corresponding to the even time instance uses of channels, is given by

$$\mathcal{S}_{\text{sum,even}} \triangleq \left\{ e^{i\theta_1}\sqrt{\alpha P_1}x_1 + e^{i\theta_2}\sqrt{(2-\alpha)\,P_2}x_2 \middle| \, \forall x_1 \in \mathcal{S}_1, \forall x_2 \in \mathcal{S}_2 \right\}. \tag{3.10}$$

One of the focuses of this thesis is to determine α that maximizes the CC sum capacity of average phases, which can be formulated as

$$\alpha_{\text{opt}} = \underset{\alpha\in[0,1]}{\text{argmax}}\, \mathbb{E}_{\theta_1,\theta_2}\left[\sum_{\alpha\in\Omega} I\left(\sqrt{P_L}x_1 + \sqrt{P_S}x_2; y \middle| \, \theta_1, \theta_2 \right) \right]. \tag{3.11}$$

In a special occasion that the receiver can have an accurate estimate and exact adjustment of θ_1 and θ_2, we will perform

$$(\alpha_{\text{opt}}, \theta_{\text{opt}}) = \underset{\alpha\in[0,1]\,\&\,\theta\in[0,2\pi)}{\text{argmax}} \left\{ \sum_{\alpha\in\Omega} I\left(\sqrt{P_L}x_1 + \sqrt{P_S}x_2; y \middle| \, \theta_1 = 0, \theta_2 = \theta \right) \right\}. \tag{3.12}$$

3.4 Problem Formulation

In 1948, Claude E. Shannon has proven that if the transmission rate R is less than the so-called capacity C that is determined by the channel statistics, intelligent coding technique that achieves arbitrarily small error probability by extending the codeword length exists. Ever since the pioneer work of Shannon, capacity becomes a usual objective function for system optimization. However, in a practical system, codeword length must be finite and perfect codes that achieve the capacity may be too complicated to be feasible. Thus the power allocation factor α_{opt} obtained by maximizing the CC sum capacity might not be a best choice in a practical system. For this reason, in the next chapter, we will propose several alternative distance-based schemes to determine the power allocation

factor α for the CPA scheme transmitted over the GMAC with random phase offsets. Performance comparisons with those from α_{opt} that maximizes the CC sum capacity will follow.

Chapter 4

Criterions for Power Allocation

4.1 Motivations

In this section, an alternative distance-based objective function to determine the power allocation factor α for the CPA scheme transmitted over GMAC with random phase offset is proposed.

Since the error performance in a practical system design is mainly controlled by the minimum pairwise distance $d_{\min}$ among constellation points, it is justifiable to take the term as an objective function for the optimization of power allocation factor α. From the scenario in Figure 2.1, perfect coordination in both signal amplitudes and phases from users can be attained. Thus α can be chosen to be the one that achieves

$$\max_{\alpha\in[0,1]} \max_{\theta\in[0,2\pi)} \{d_{\min}\}.$$

Regarding the scenarios illustrated in Figures 2.2–2.4, the BS can only control the transmission powers of user signals; thus, the determination of the best power allocation factor α is changed to

$$\max_{\alpha\in[0,1]} \{\mathbb{E}_\theta[d_{\min}]\} = \max_{\alpha\in[0,1]} \text{avg}_\theta\{d_{\min}\}, \tag{4.1}$$

where in its realization, we will average all $d_{\min}$'s obtained over the θ values in $\Theta \triangleq$

$\{0°, 1°, 2°, \ldots, 359°\}$, i.e.,

$$\text{avg}_\theta\{d_{\min}\} \triangleq \frac{1}{|\Theta|}\sum_{\theta\in\Theta} d_{\min}.$$

Instead of considering the average $d_{\min}$ over all possible θ values in Θ, one may determine the best α value that maximizes the worst $d_{\min}$ over all $\theta \in \Theta$, which formulates as

$$\max_{\alpha\in[0,1]} \min_{\theta\in\Theta}\{d_{\min}\}.$$

This could be a better choice than the one from (4.1) when the system performance is dominated by that corresponding to the worst phase offset.

4.2 Suboptimal Power Allocation for Three-User GMAC with Random Phase Offset

For the CPA scheme with three users, it may not be numerically feasible to exhaustively examine all power allocation combinations among three users because it requires at least two parameters to express these combinations. Instead, we examine a sub-optimal power allocation policy with a single parameter α as shown in Figure 4.1.

As indicated in Figure 4.1, for the first 1/3 of the channel uses, the BS receives

$$y_t = \sqrt{\alpha P_1}x_1 + \sqrt{(2-\alpha)\,P_2}x_2 + \sqrt{P_3}x_3 + z.$$

For the second 1/3 of the channel uses, the BS receives instead

$$y_t = \sqrt{(2-\alpha)\,P_1}x_1 + \sqrt{P_2}x_2 + \sqrt{\alpha P_3}x_3 + z.$$

Fro the last 1/3 of the channel uses,

$$y_t = \sqrt{P_1}x_1 + \sqrt{\alpha P_2}x_2 + \sqrt{(2-\alpha)\,P_3}x_3 + z$$

are received by the BS. By this setting, the average power for UE1 is

$$\frac{\alpha P_1 + (2-\alpha)\,P_1 + P_1}{3} = P_1;$$

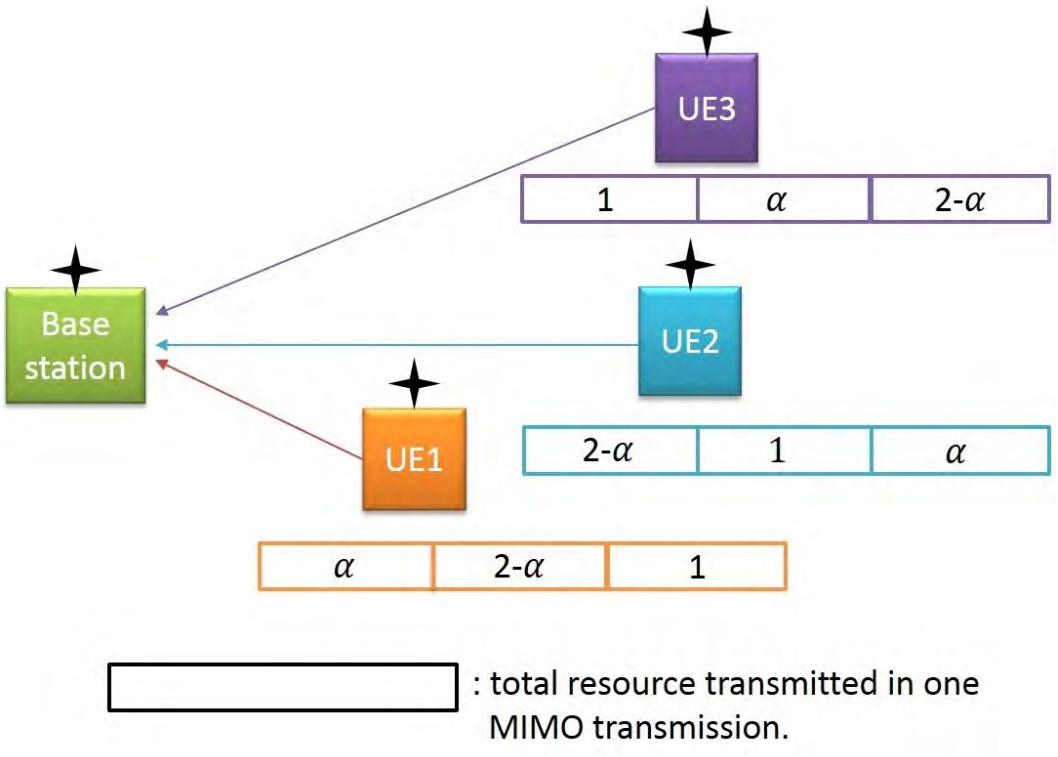

Figure 4.1: Power allocation for the three-user GMAC with random phase offset

thus in average, the transmission power of UE1 remains. Similar verification can be applied to UE2 and UE3.

We again emphasize that the one-parameter power allocation we propose for the three-user CPA scheme may not be optimal since we basically should have two parameters (such as αP_1, βP_1 and $(3-\alpha-\beta)P_1$) to identify all possible combinations. Our provision is simply to reduce the complexity of exhaustively searching for the best "sub-optimal" power allocation.

4.3 System Setting for Simulations

The system setting that we conduct for multilevel coding with the CPA scheme is illustrated in Figure 4.2. Since the modulation order of each user is 2^2, the multilevel coding technique then requires two encoders to be connected to one modulator.

Two receivers will be tested for the transmitter in Figure 4.2, which are JML and

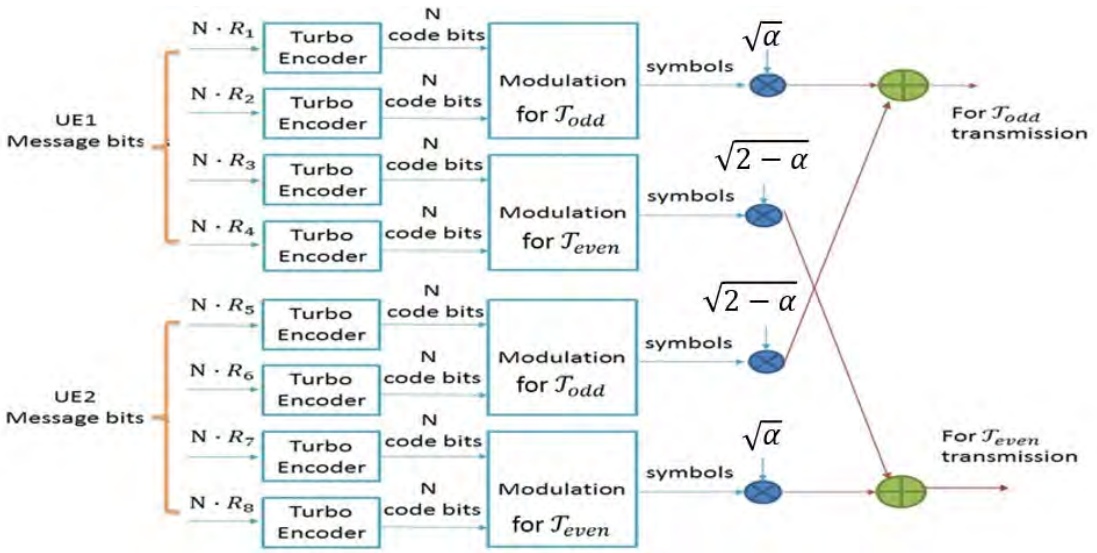

Figure 4.2: Transmitter setting for two-user multilevel-coding with the CPA scheme

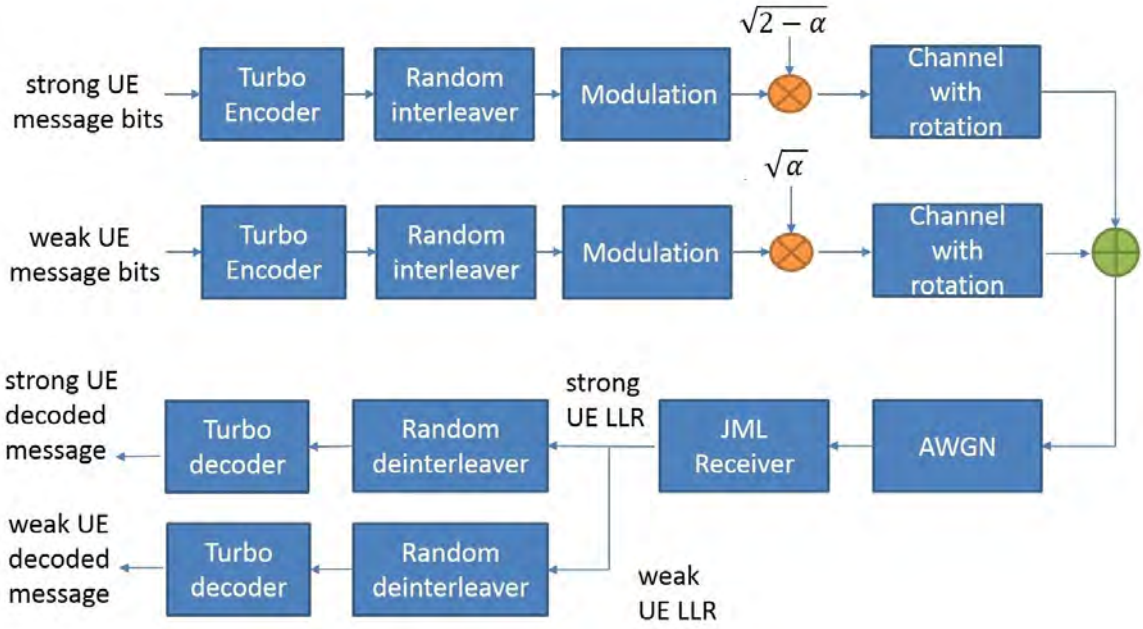

Figure 4.3: JML receiver setting

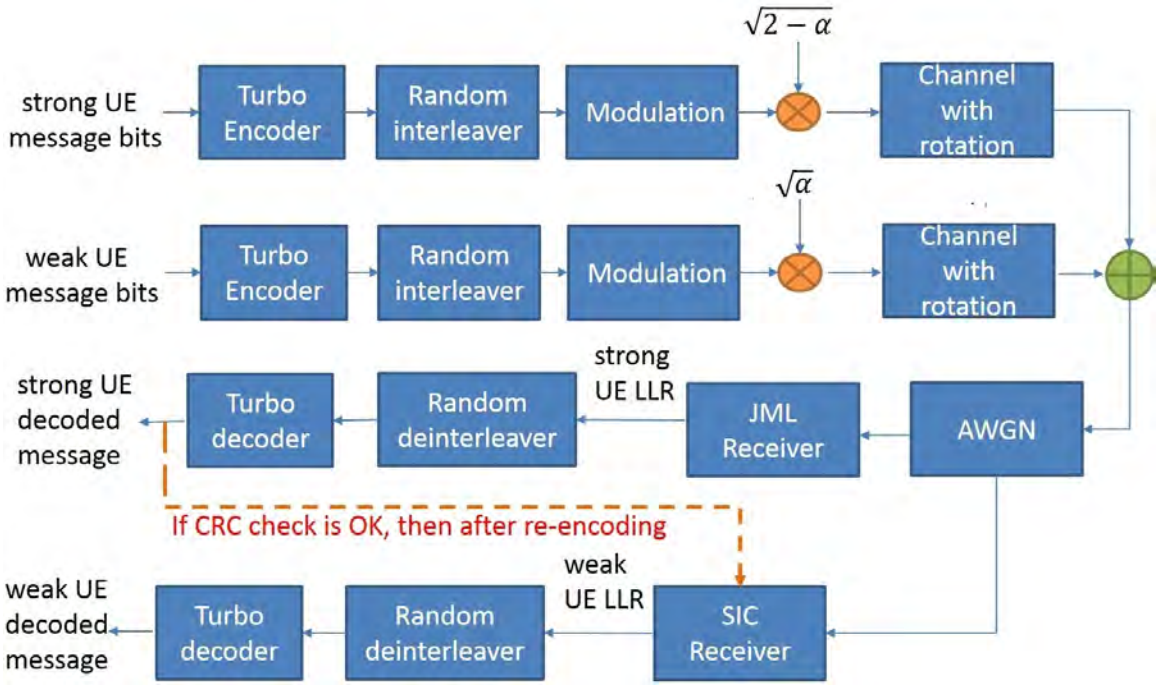

Figure 4.4: SIC receiver setting

SIC receivers. For simplicity, we let the modulation order be two (instead of four in Figure 4.2) in Figures 4.3 and 4.4; thus, each modulator is connected to just one turbo encoder. It can be observed that for the SIC receiver, the information from the strong UE is decoded first. If the CRC check succeeds for the decoded information stream from the strong UE, re-encoding of the decoded information stream will be conducted and only the constellation points corresponding to the re-encoded code bit streams from the strong UE will be used in the calculation of the LLRs for the decoding of information sequence from the weak UE.

Chapter 5

Simulation Results

5.1 Two-user GMAC with Equal Average Power Constraint and Random Phase Offset

In this section, we examine by simulations the performance of the CPA scheme transmitted over the two-user GMAC with equal average power constraint and random phase offset. We assume that the BS and the two UEs are equipped with only a single antenna, and the SNRs of the two UEs are both 3 dB, 6 dB and 10 dB. The channel code adopted is the turbo code. The number of REs per transmission is fixed to be $N = 4500$.

At the receiver end, turbo decoder is used. The performance index adopted in our simulations is the maximum transmission rate to achieve a block error rate (BLER) of 0.1. In other words, we will gradually decrease the turbo code rate from 0.995 down to 0.010 until BLER of 0.1 is reached. We summarize the parameters in Table 5.1.

In the simulations, we will examine the BLER-constrained maximum rate performance indices of different modulation combinations under power allocation factors α chosen by different distance-based criterions and by the CC sum capacity criterion. Such examinations will be performed for several SNRs.

Table 5.1: Parameter setting for two-user GMAC with equal average power constraint and random phase offset

Parameters	Values
Number of UEs	2
Antenna number per UE	1
Antenna number of BS	1
Channel coding	Turbo code
Target BLER	0.1
REs per data transmission	4500

Table 5.2: α_{opt} and θ_{opt} selected based on different modulation combinations and different distance-based criterions

Modulation (UE1+UE2)	$\underset{\alpha\in(0,1]\,\&\,\theta\in\Theta}{\text{argmax}}\{d_{\min}\}$		$\underset{\alpha\in(0,1]}{\text{argmax}}\,\underset{\theta\in\Theta}{\text{avg}}\{d_{\min}\}$	$\underset{\alpha\in(0,1]}{\text{argmax}}\,\underset{\theta\in\Theta}{\min}\{d_{\min}\}$
	α_{opt}	$(\theta_{\text{opt,odd}}, \theta_{\text{opt,even}})$	α_{opt}	α_{opt}
BPSK+BPSK	1.00	(61°, 61°)	1.00	0.40
BPSK+QPSK	0.40	(90°, 12°)	0.35	0.22
QPSK+QPSK	0.42	(15°, 15°)	0.32	0.29
QPSK+8PSK	0.47	(90°, 76°)	0.34	0.10
8PSK+8PSK	0.49	(43°, 43°)	0.15	0.14
8PSK+16QAM	0.12	(239°, 88°)	0.10	0.10
16QAM+16QAM	0.12	(5°, 172°)	0.08	0.07

Table 5.3: α_{opt} based on different modulation combinations and different SNRs

Modulation (UE1+UE2)	$\underset{\alpha\in(0,1]}{\text{argmax}}$\{CC sum capacity of average phases\}		
SNR of UE1 & UE2	3 dB	6 dB	10 dB
BPSK+BPSK	0.97	0.63	0.47
BPSK+QPSK	0.98	0.97	0.47
QPSK+QPSK	0.76	0.51	0.38
QPSK+8PSK	1.00	0.65	0.55
8PSK+8PSK	0.98	0.72	0.62
8PSK+16QAM	1.00	1.00	0.84
16QAM+16QAM	1.00	0.97	0.87

Tables 5.2 and 5.3 list the CPA parameters of α_{opt} (and θ_{opt} when being necessarily applied) for different modulation combinations transmitted over the two-user GMAC with equal average power constraint and random phase offset. For the case of

$$(\alpha_{\text{opt}}, \theta_{\text{opt}}) = \underset{\alpha\in(0,1] \text{ and } \theta\in[0,2\pi)}{\text{argmax}} \{d_{\min}\},$$

θ_{opt} is the difference between the two constellation rotation angles of UE1 and UE2. It can be equivalently regarded as fixing the rotation angle of UE1's constellation to be zero degree and setting the rotation angle of UE2's constellation to be θ_{opt}. Recall that in the previous chapter, we denote by $\theta_{\text{opt,odd}}$ and $\theta_{\text{opt,even}}$ the optimal rotation angles that maximize $d_{\min}$ for odd and even channel uses, respectively. Note that the distance-based criterion is nothing to do with SNRs; thus no such information is specified in Table 5.2.

Table 5.4: Achievable rate pairs of the CPA scheme under two-user GMAC with random phase offset. Here, $(\alpha_{\text{opt}}, \theta_{\text{opt}}) = \text{argmax}_{\alpha\in(0,1]\,\&\,\theta\in\Theta}\{d_{\min}\}$, JML receiver is employed, and SNR = 3 dB. The receiver is also assumed to be able to rotate the two constellations accurately to match θ_{opt}.

Modulation (UE1+UE2)	UE1 Rate	UE2 Rate
BPSK+BPSK	0.830	0.830
BPSK+QPSK	0.585	0.895
QPSK+QPSK	0.740	0.740
QPSK+8PSK	0.675	0.613
8PSK+8PSK	0.545	0.545

Table 5.5: Achievable rate pairs of the CPA scheme under two-user GMAC with random phase effect. Here, $\alpha_{\text{opt}} = \text{argmax}_{\alpha\in(0,1]}\,\text{avg}_{\theta\in\Theta}\{d_{\min}\}$, JML receiver is employed, and SNR = 3 dB.

Modulation (UE1+UE2)	UE1 Rate	UE2 Rate
BPSK+BPSK	0.685	0.685
BPSK+QPSK	0.565	0.905
QPSK+QPSK	0.770	0.770
QPSK+8PSK	0.715	0.663
8PSK+8PSK	0.768	0.768

Table 5.6: Achievable rate pairs of the CPA scheme under two-user GMAC with random phase effect. Here, $\alpha_{\text{opt}} = \text{argmax}_{\alpha\in(0,1]}\,\min_{\theta\in\Theta}\{d_{\min}\}$, JML receiver is employed, and SNR = 3 dB.

Modulation (UE1+UE2)	UE1 Rate	UE2 Rate
BPSK+BPSK	0.683	0.683
BPSK+QPSK	0.558	0.885
QPSK+QPSK	0.780	0.780
QPSK+8PSK	0.805	0.823
8PSK+8PSK	0.778	0.778

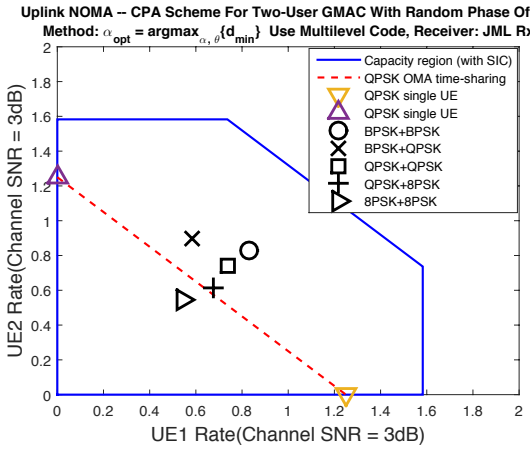

(a) $(\alpha_{\text{opt}}, \theta_{\text{opt}}) = \text{argmax}_{\alpha\in(0,1)\,\&\,\theta\in\Theta}\{d_{\min}\}$

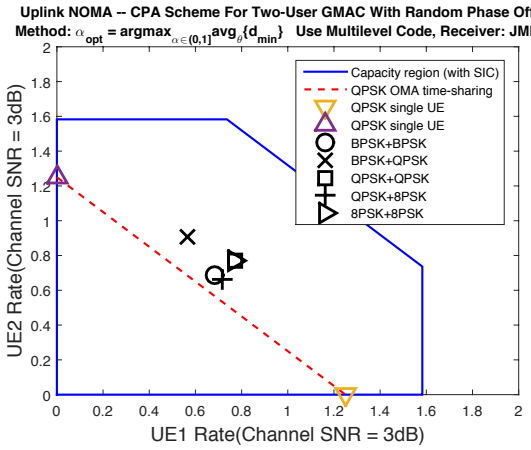

(b) $\alpha_{\text{opt}} = \text{argmax}_{\alpha\in(0,1]}\,\text{avg}_{\theta\in\Theta}\{d_{\min}\}$

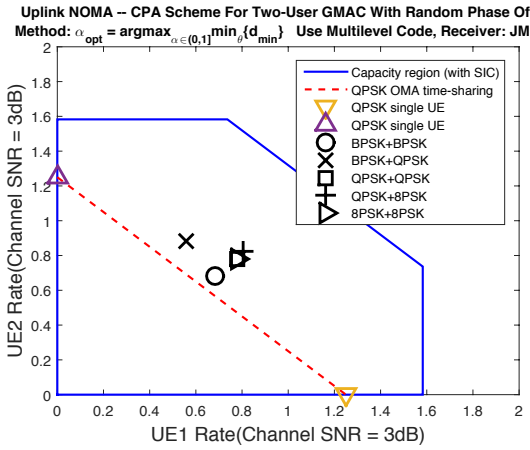

(c) $\alpha_{\text{opt}} = \text{argmax}_{\alpha\in(0,1]}\,\min_{\theta\in\Theta}\{d_{\min}\}$

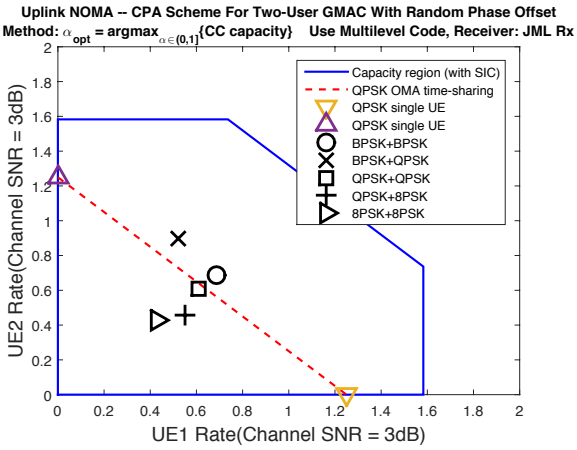

(d) $\alpha_{\text{opt}} = \text{argmax}_{\alpha\in(0,1]}\{\text{CC sum capacity}\}$

Figure 5.1: Capacity region and achievable rate pairs of the CPA scheme under two-user GMAC with random phase effect. Here, JML receiver is employed except that the capacity region is derived and drawn based on SIC receiver, and SNR = 3 dB.

Table 5.7: Achievable rate pairs of the CPA scheme under two-user GMAC with random phase effect. Here, $\alpha_{\text{opt}} = \text{argmax}_{\alpha\in(0,1]}\{\text{CC sum capacity}\}$, JML receiver is employed, and SNR = 3 dB.

Modulation (UE1+UE2)	UE1 Rate	UE2 Rate
BPSK+BPSK	0.688	0.688
BPSK+QPSK	0.520	0.895
QPSK+QPSK	0.610	0.610
QPSK+8PSK	0.550	0.458
8PSK+8PSK	0.430	0.430

Table 5.8: Achievable rate pairs of the CPA scheme under two-user GMAC with random phase offset. Here, $(\alpha_{\text{opt}}, \theta_{\text{opt}}) = \text{argmax}_{\alpha\in(0,1)\,\&\,\theta\in\Theta}\{d_{\min}\}$, SIC receiver is employed, and SNR = 3 dB. The receiver is also assumed to be able to rotate the two constellations accurately to match θ_{opt}.

Modulation (UE1+UE2)	UE1 Rate	UE2 Rate
BPSK+BPSK	0.843	0.843
BPSK+QPSK	0.695	0.975
QPSK+QPSK	0.920	0.920
QPSK+8PSK	0.810	0.795
8PSK+8PSK	0.738	0.710

Table 5.9: Achievable rate pairs of the CPA scheme under two-user GMAC with random phase offset. Here, $\alpha_{\text{opt}} = \text{argmax}_{\alpha\in(0,1]}\,\text{avg}_{\theta\in\Theta}\{d_{\min}\}$, SIC receiver is employed, and SN = 3 dB.

Modulation (UE1+UE2)	UE1 Rate	UE2 Rate
BPSK+BPSK	0.770	0.770
BPSK+QPSK	0.638	0.945
QPSK+QPSK	0.845	0.845
QPSK+8PSK	0.848	0.800
8PSK+8PSK	0.833	0.833

Table 5.10: Achievable rate pairs of the CPA scheme under two-user GMAC with random phase offset. Here, $\alpha_{\text{opt}} = \text{argmax}_{\alpha\in(0,1]} \min_{\theta\in\Theta}\{d_{\min}\}$, SIC receiver is employed, and SNR = 3 dB.

Modulation (UE1+UE2)	UE1 Rate	UE2 Rate
BPSK+BPSK	0.710	0.708
BPSK+QPSK	0.610	0.905
QPSK+QPSK	0.853	0.863
QPSK+8PSK	0.845	0.853
8PSK+8PSK	0.838	0.838

Table 5.11: Achievable rate pairs of the CPA scheme under two-user GMAC with random phase offset. Here, $\alpha_{\text{opt}} = \text{argmax}_{\alpha\in(0,1]}\{\text{CC sum capacity of average phases}\}$, SIC receiver is employed, and SNR = 3 dB.

Modulation (UE1+UE2)	UE1 Rate	UE2 Rate
BPSK+BPSK	0.770	0.770
BPSK+QPSK	0.688	1.093
QPSK+QPSK	0.798	0.795
QPSK+8PSK	0.895	0.895
8PSK+8PSK	0.713	0.723

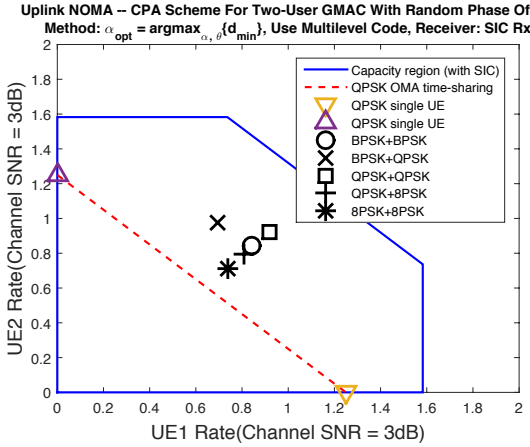

(a) $(\alpha_{\text{opt}}, \theta_{\text{opt}}) = \text{argmax}_{\alpha\in(0,1)\,\&\,\theta\in\Theta}\{d_{\min}\}$

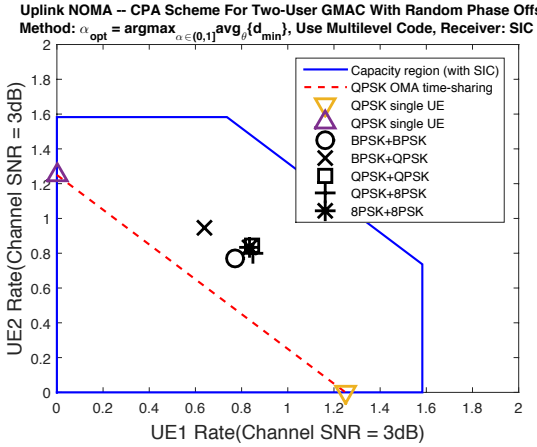

(b) $\alpha_{\text{opt}} = \text{argmax}_{\alpha\in(0,1]}\,\text{avg}_{\theta\in\Theta}\{d_{\min}\}$

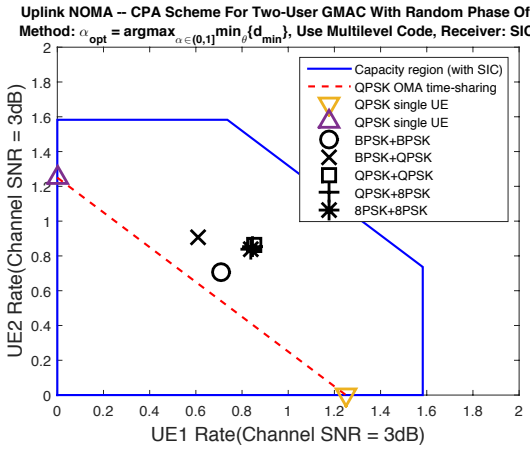

(c) $\alpha_{\text{opt}} = \text{argmax}_{\alpha\in(0,1]}\,\text{min}_{\theta\in\Theta}\{d_{\min}\}$

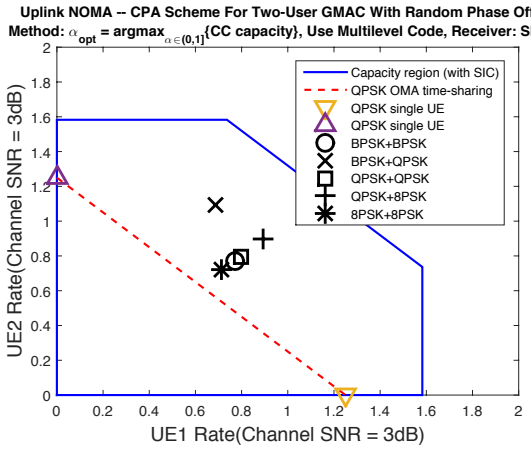

(d) $\alpha_{\text{opt}} = \text{argmax}_{\alpha\in(0,1]}\{\text{CC sum capacity}\}$

Figure 5.2: Capacity region and achievable rate pairs of the CPA scheme under two-user GMAC with random phase offset. Here, SIC receiver is employed, and SNR = 3 dB.

Table 5.12: Achievable rate pairs of the CPA scheme under two-user GMAC with random phase offset. Here, $(\alpha_{\text{opt}}, \theta_{\text{opt}}) = \text{argmax}_{\alpha\in(0,1)\,\&\,\theta\in\Theta}\{d_{\min}\}$, JML receiver is employed, and SNR = 6 dB. The receiver is also assumed to be able to rotate the two constellations accurately to match θ_{opt}.

Modulation (UE1+UE2)	UE1 Rate	UE2 Rate
BPSK+QPSK	0.785	1.370
QPSK+QPSK	1.115	1.110
QPSK+8PSK	0.880	0.965
8PSK+8PSK	0.743	0.743
8PSK+16QAM	1.010	1.098
16QAM+16QAM	1.065	1.070

Table 5.13: Achievable rate pairs of the CPA scheme under two-user GMAC with random phase offset. Here, $\alpha_{\text{opt}} = \text{argmax}_{\alpha\in(0,1]}\,\text{avg}_{\theta\in\Theta}\{d_{\min}\}$, JML receiver is employed, and SNR = 6 dB.

Modulation (UE1+UE2)	UE1 Rate	UE2 Rate
BPSK+QPSK	0.750	1.315
QPSK+QPSK	1.130	1.130
QPSK+8PSK	0.925	1.020
8PSK+8PSK	1.030	1.030
8PSK+16QAM	1.040	1.125
16QAM+16QAM	1.135	1.135

Table 5.14: Achievable rate pairs of the CPA scheme under two-user GMAC with random phase offset. Here, $\alpha_{\text{opt}} = \text{argmax}_{\alpha\in(0,1]} \min_{\theta\in\Theta}\{d_{\min}\}$, JML receiver is employed, and SNR = 6 dB.

Modulation (UE1+UE2)	UE1 Rate	UE2 Rate
BPSK+QPSK	0.730	1.228
QPSK+QPSK	1.135	1.140
QPSK+8PSK	0.995	1.128
8PSK+8PSK	1.038	1.038
8PSK+16QAM	1.040	1.125
16QAM+16QAM	1.150	1.150

Table 5.15: Achievable rate pairs of the CPA scheme under two-user GMAC with random phase offset. Here, $\alpha_{\text{opt}} = \text{argmax}_{\alpha\in(0,1]}\{\text{CC sum capacity of average phases}\}$, JML receiver is employed, and SNR = 6 dB.

Modulation (UE1+UE2)	UE1 Rate	UE2 Rate
BPSK+QPSK	0.635	1.300
QPSK+QPSK	1.018	1.018
QPSK+8PSK	0.805	0.808
8PSK+8PSK	0.643	0.643
8PSK+16QAM	0.490	0.498
16QAM+16QAM	0.395	0.395

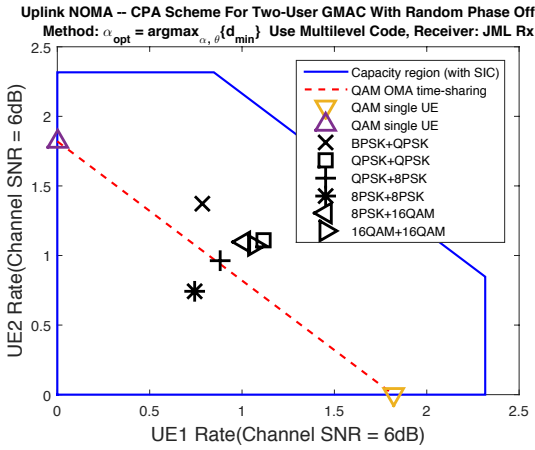

(a) $(\alpha_{\text{opt}}, \theta_{\text{opt}}) = \text{argmax}_{\alpha\in(0,1)\,\&\,\theta\in\Theta}\{d_{\min}\}$

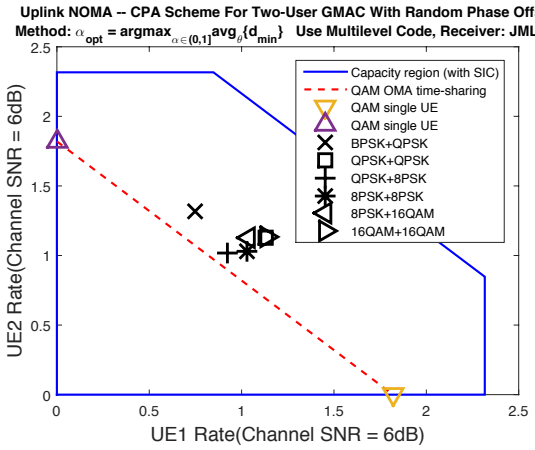

(b) $\alpha_{\text{opt}} = \text{argmax}_{\alpha\in(0,1]}\,\text{avg}_{\theta\in\Theta}\{d_{\min}\}$

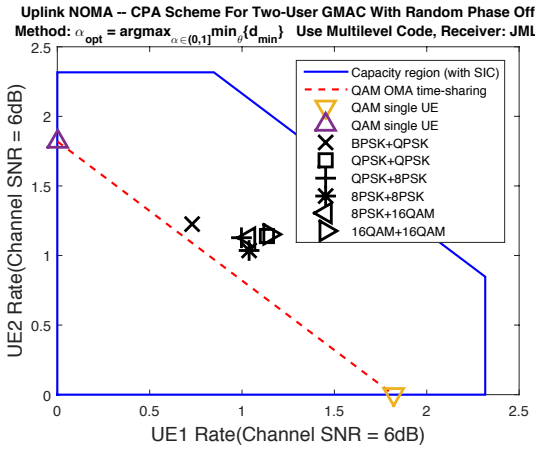

(c) $\alpha_{\text{opt}} = \text{argmax}_{\alpha\in(0,1]}\,\min_{\theta\in\Theta}\{d_{\min}\}$

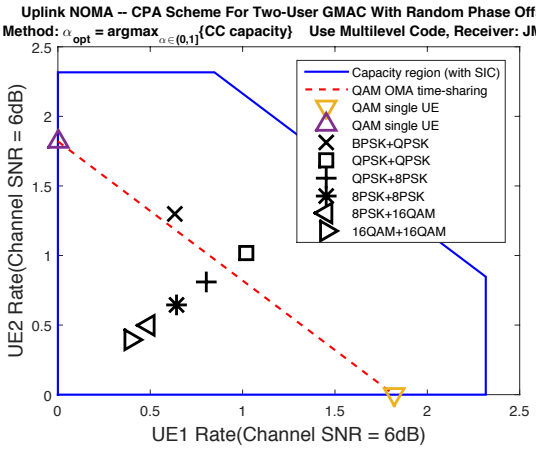

(d) $\alpha_{\text{opt}} = \text{argmax}_{\alpha\in(0,1]}\{\text{CC sum capacity}\}$

Figure 5.3: Capacity region and achievable rate pairs of the CPA scheme under two-user GMAC with random phase offset. Here, JML receiver is employed except that the capacity region is derived and drawn based on SIC receiver, and SNR = 6 dB.

Table 5.16: Achievable rate pairs of the CPA scheme under two-user GMAC with random phase offset. Here, $(\alpha_{\text{opt}}, \theta_{\text{opt}}) = \text{argmax}_{\alpha\in(0,1)\,\&\,\theta\in\Theta}\{d_{\min}\}$, SIC receiver is employed, and SNR = 6 dB. The receiver is also assumed to be able to rotate the two constellations accurately to match θ_{opt}.

Modulation (UE1+UE2)	UE1 Rate	UE2 Rate
BPSK+QPSK	0.848	1.405
QPSK+QPSK	1.283	1.265
QPSK+8PSK	1.143	1.213
8PSK+8PSK	1.095	1.070
8PSK+16QAM	1.103	1.178
16QAM+16QAM	1.158	1.145

Table 5.17: Achievable rate pairs of the CPA scheme under two-user GMAC with random phase offset. Here, $\alpha_{\text{opt}} = \text{argmax}_{\alpha\in(0,1]}\,\text{avg}_{\theta\in\Theta}\{d_{\min}\}$, SIC receiver is employed, and SNR = 6 dB.

Modulation (UE1+UE2)	UE1 Rate	UE2 Rate
BPSK+QPSK	0.853	1.333
QPSK+QPSK	1.233	1.238
QPSK+8PSK	1.180	1.213
8PSK+8PSK	1.133	1.130
8PSK+16QAM	1.125	1.190
16QAM+16QAM	1.200	1.200

Table 5.18: Achievable rate pairs of the CPA scheme under two-user GMAC with random phase offset. Here, $\alpha_{\text{opt}} = \text{argmax}_{\alpha\in(0,1]} \min_{\theta\in\Theta}\{d_{\min}\}$, SIC receiver is employed, and SNR = 6 dB.

Modulation (UE1+UE2)	UE1 Rate	UE2 Rate
BPSK+QPSK	0.785	1.233
QPSK+QPSK	1.228	1.228
QPSK+8PSK	1.070	1.150
8PSK+8PSK	1.133	1.133
8PSK+16QAM	1.125	1.190
16QAM+16QAM	1.210	1.208

Table 5.19: Achievable rate pairs of the CPA scheme under two-user GMAC with random phase offset. Here, $\alpha_{\text{opt}} = \text{argmax}_{\alpha\in(0,1]}\{\text{CC sum capacity of average phases}\}$, SIC receiver is employed, and SNR = 6 dB.

Modulation (UE1+UE2)	UE1 Rate	UE2 Rate
BPSK+QPSK	0.805	1.540
QPSK+QPSK	1.193	1.193
QPSK+8PSK	1.173	1.098
8PSK+8PSK	1.205	1.093
8PSK+16QAM	0.875	0.630
16QAM+16QAM	0.850	0.850

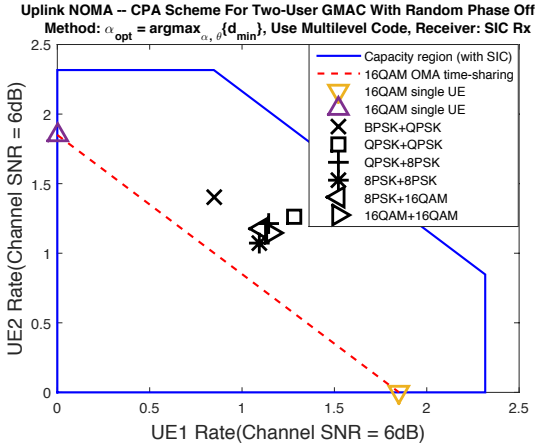

(a) $(\alpha_{\text{opt}}, \theta_{\text{opt}}) = \text{argmax}_{\alpha\in(0,1)\,\&\,\theta\in\Theta}\{d_{\min}\}$

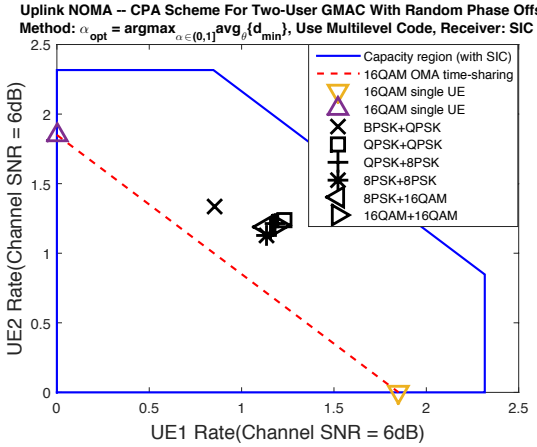

(b) $\alpha_{\text{opt}} = \text{argmax}_{\alpha\in(0,1]}\,\text{avg}_{\theta\in\Theta}\{d_{\min}\}$

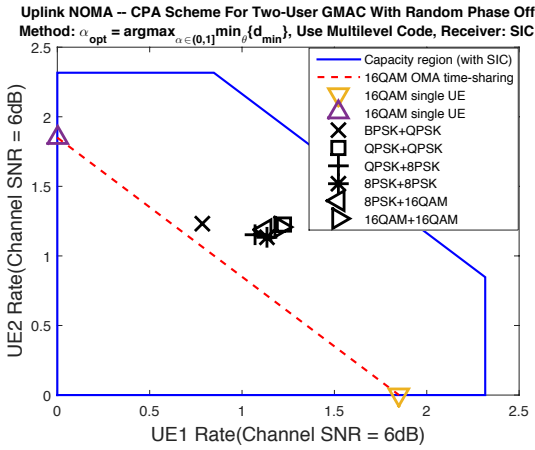

(c) $\alpha_{\text{opt}} = \text{argmax}_{\alpha\in(0,1]}\,\min_{\theta\in\Theta}\{d_{\min}\}$

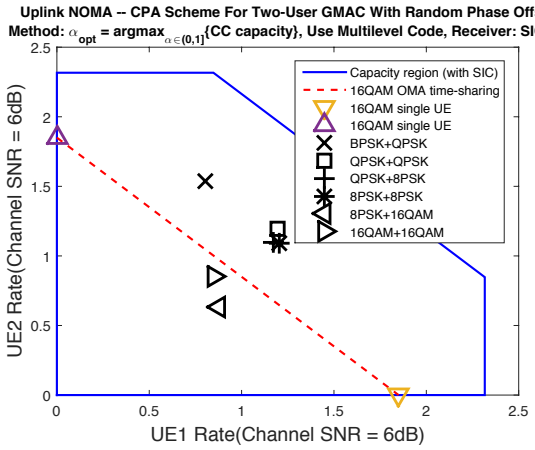

(d) $\alpha_{\text{opt}} = \text{argmax}_{\alpha\in(0,1]}\{\text{CC sum capacity}\}$

Figure 5.4: Capacity region and achievable rate pairs of the CPA scheme under two-user GMAC with random phase offset. Here, SIC receiver is employed, and SNR = 6 dB.

Table 5.20: Achievable rate pairs of the CPA scheme under two-user GMAC with random phase offset. Here, $(\alpha_{\text{opt}}, \theta_{\text{opt}}) = \text{argmax}_{\alpha\in(0,1)\,\&\,\theta\in\Theta}\{d_{\min}\}$, JML receiver is employed, and SNR = 10 dB. The receiver is also assumed to be able to rotate the two constellations accurately to match θ_{opt}.

Modulation (UE1+UE2)	UE1 Rate	UE2 Rate
QPSK+QPSK	1.700	1.693
QPSK+8PSK	1.213	1.683
8PSK+8PSK	1.133	1.133
8PSK+16QAM	1.415	1.443
16QAM+16QAM	1.458	1.455

Table 5.21: Achievable rate pairs of the CPA scheme under two-user GMAC with random phase offset. Here, $\alpha_{\text{opt}} = \text{argmax}_{\alpha\in(0,1]}\,\text{avg}_{\theta\in\Theta}\{d_{\min}\}$, JML receiver is employed, and SNR = 10 dB.

Modulation (UE1+UE2)	UE1 Rate	UE2 Rate
QPSK+QPSK	1.673	1.670
QPSK+8PSK	1.280	1.710
8PSK+8PSK	1.423	1.423
8PSK+16QAM	1.455	1.455
16QAM+16QAM	1.540	1.540

Table 5.22: Achievable rate pairs of the CPA scheme under two-user GMAC with random phase offset. Here, $\alpha_{\text{opt}} = \text{argmax}_{\alpha\in(0,1]} \min_{\theta\in\Theta}\{d_{\min}\}$, JML receiver is employed, and SNR = 10 dB.

Modulation (UE1+UE2)	UE1 Rate	UE2 Rate
QPSK+QPSK	1.670	1.673
QPSK+8PSK	1.235	1.583
8PSK+8PSK	1.428	1.428
8PSK+16QAM	1.455	1.455
16QAM+16QAM	1.585	1.585

Table 5.23: Achievable rate pairs of the CPA scheme under two-user GMAC with random phase offset. Here, $\alpha_{\text{opt}} = \text{argmax}_{\alpha\in(0,1]}\{\text{CC sum capacity of average phases}\}$, JML receiver is employed, and SNR = 10 dB.

Modulation (UE1+UE2)	UE1 Rate	UE2 Rate
QPSK+QPSK	1.648	1.638
QPSK+8PSK	1.165	1.543
8PSK+8PSK	1.028	1.028
8PSK+16QAM	0.580	0.580
16QAM+16QAM	0.573	0.573

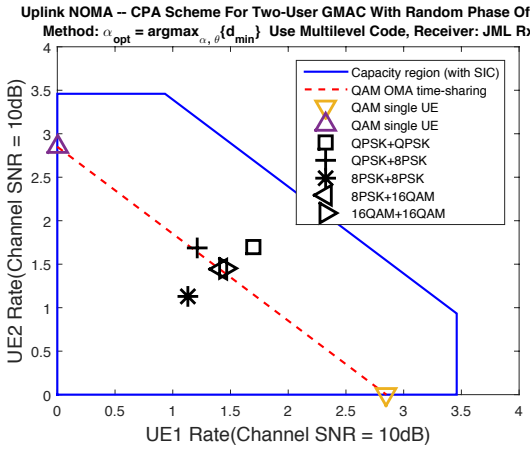

(a) $(\alpha_{\text{opt}}, \theta_{\text{opt}}) = \text{argmax}_{\alpha\in(0,1)\,\&\,\theta\in\Theta}\{d_{\min}\}$

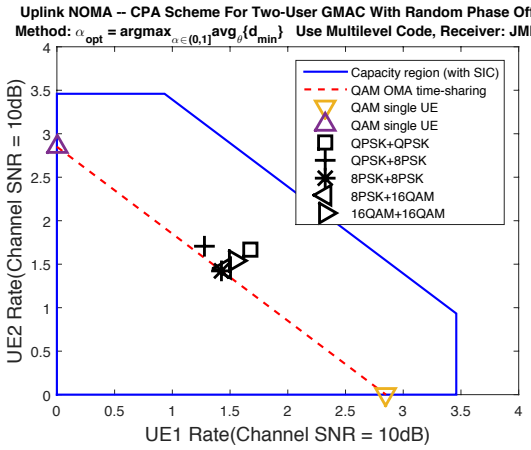

(b) $\alpha_{\text{opt}} = \text{argmax}_{\alpha\in(0,1]}\,\text{avg}_{\theta\in\Theta}\{d_{\min}\}$

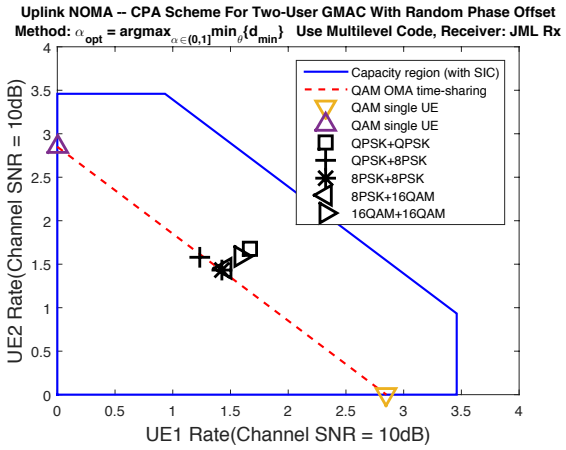

(c) $\alpha_{\text{opt}} = \text{argmax}_{\alpha\in(0,1]}\,\min_{\theta\in\Theta}\{d_{\min}\}$

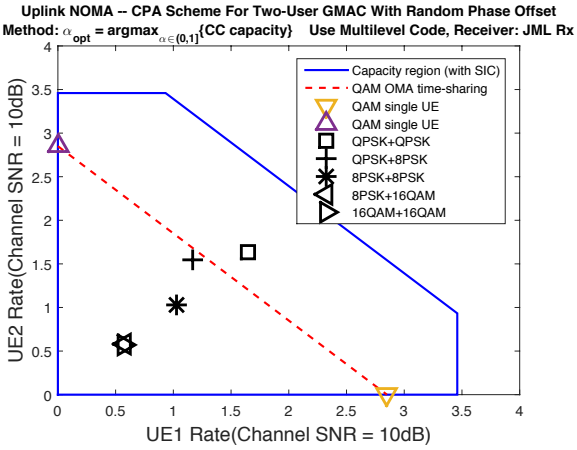

(d) $\alpha_{\text{opt}} = \text{argmax}_{\alpha\in(0,1]}\{\text{CC sum capacity}\}$

Figure 5.5: Capacity region and achievable rate pairs of the CPA scheme under two-user GMAC with random phase offset. Here, JML receiver is employed except that the capacity region is derived and drawn based on SIC receiver, and SNR = 10 dB.

Table 5.24: Achievable rate pairs of the CPA scheme under two-user GMAC with random phase offset. Here, $(\alpha_{\text{opt}}, \theta_{\text{opt}}) = \text{argmax}_{\alpha\in(0,1)\,\&\,\theta\in\Theta}\{d_{\min}\}$, SIC receiver is employed, and SNR = 10 dB. The receiver is also assumed to be able to rotate the two constellations accurately to match θ_{opt}.

Modulation (UE1+UE2)	UE1 Rate	UE2 Rate
QPSK+QPSK	1.778	1.770
QPSK+8PSK	1.555	1.868
8PSK+8PSK	1.793	1.790
8PSK+16QAM	1.103	1.878
16QAM+16QAM	1.663	1.655

Table 5.25: Achievable rate pairs of the CPA scheme under two-user GMAC with random phase offset. Here, $\alpha_{\text{opt}} = \text{argmax}_{\alpha\in(0,1]}\,\text{avg}_{\theta\in\Theta}\{d_{\min}\}$, SIC receiver is employed, and SNR = 10 dB.

Modulation (UE1+UE2)	UE1 Rate	UE2 Rate
QPSK+QPSK	1.705	1.705
QPSK+8PSK	1.615	1.785
8PSK+8PSK	1.623	1.625
8PSK+16QAM	1.540	1.725
16QAM+16QAM	1.695	1.695

Table 5.26: Achievable rate pairs of the CPA scheme under two-user GMAC with random phase offset. Here, $\alpha_{\text{opt}} = \text{argmax}_{\alpha\in(0,1]} \min_{\theta\in\Theta}\{d_{\min}\}$, SIC receiver is employed, and SNR = 10 dB.

Modulation (UE1+UE2)	UE1 Rate	UE2 Rate
QPSK+QPSK	1.708	1.703
QPSK+8PSK	1.373	1.593
8PSK+8PSK	1.620	1.618
8PSK+16QAM	1.540	1.725
16QAM+16QAM	1.705	1.708

Table 5.27: Achievable rate pairs of the CPA scheme under two-user GMAC with random phase offset. Here, $\alpha_{\text{opt}} = \text{argmax}_{\alpha\in(0,1]}\{\text{CC sum capacity of average phases}\}$, SIC receiver is employed, and SNR = 10 dB.

Modulation (UE1+UE2)	UE1 Rate	UE2 Rate
QPSK+QPSK	1.750	1.750
QPSK+8PSK	1.573	1.900
8PSK+8PSK	1.683	1.683
8PSK+16QAM	1.570	1.910
16QAM+16QAM	1.250	1.250

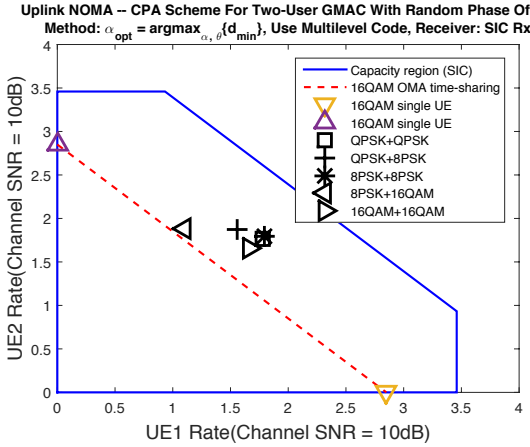

(a) $(\alpha_{\text{opt}}, \theta_{\text{opt}}) = \text{argmax}_{\alpha\in(0,1)\,\&\,\theta\in\Theta}\{d_{\min}\}$

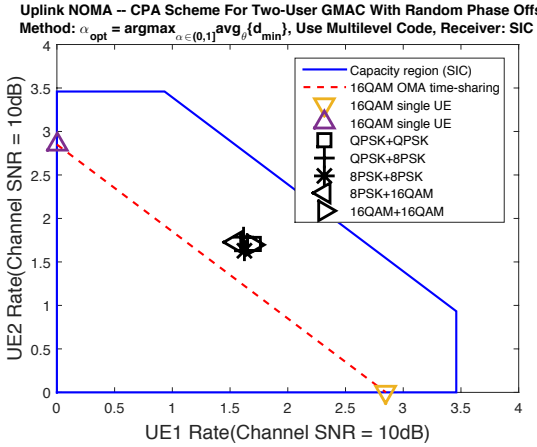

(b) $\alpha_{\text{opt}} = \text{argmax}_{\alpha\in(0,1]}\,\text{avg}_{\theta\in\Theta}\{d_{\min}\}$

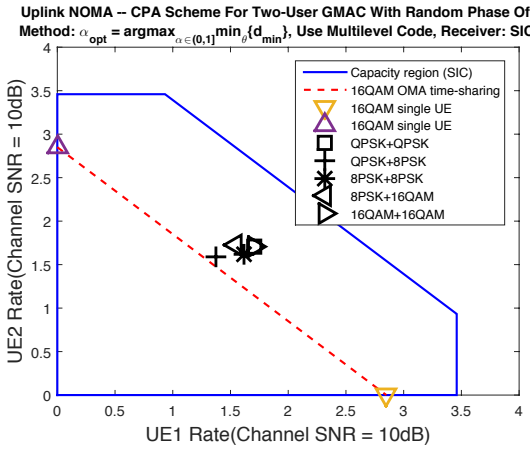

(c) $\alpha_{\text{opt}} = \text{argmax}_{\alpha\in(0,1]}\,\text{min}_{\theta\in\Theta}\{d_{\min}\}$

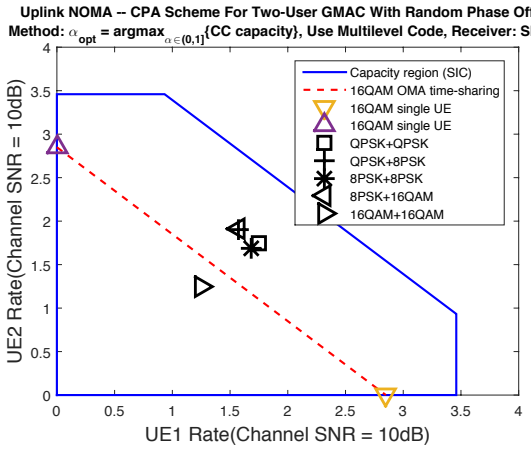

(d) $\alpha_{\text{opt}} = \text{argmax}_{\alpha\in(0,1]}\{\text{CC sum capacity}\}$

Figure 5.6: Capacity region and achievable rate pairs of the CPA scheme under two-user GMAC with random phase offset. Here, SIC receiver is employed, and SNR = 10 dB.

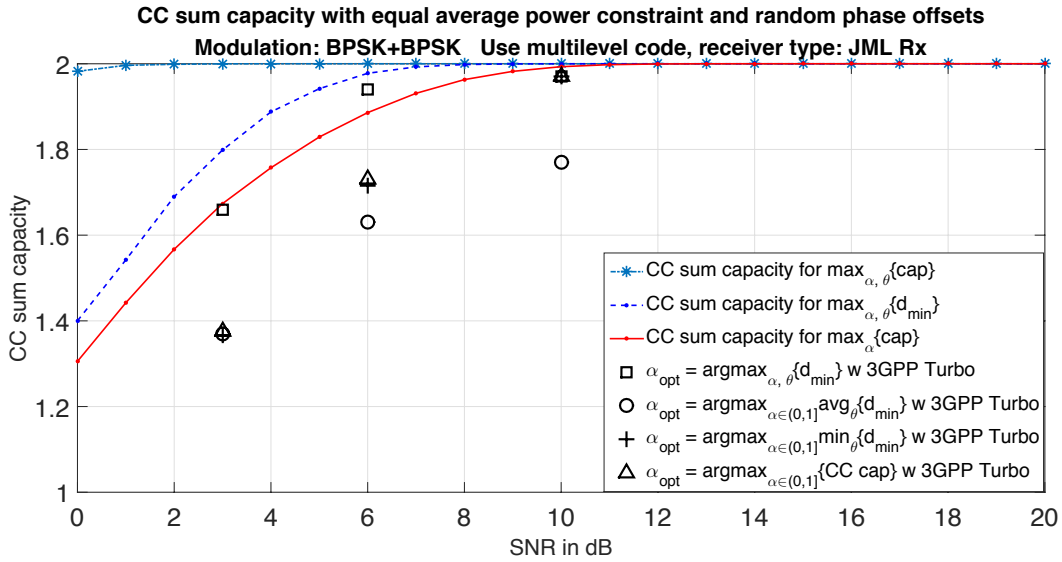

Figure 5.7: CC sum capacity and achievable rates of BPSK+BPSK with equal average power constraint and random phase offset. Here, JML receiver is assumed.

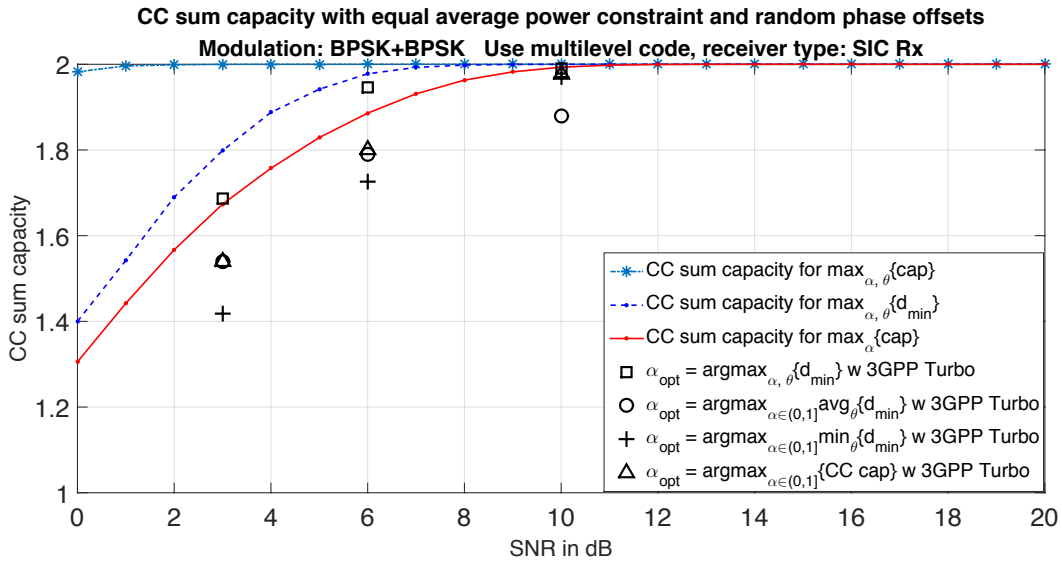

Figure 5.8: CC sum capacity and achievable rates of BPSK+BPSK with equal average power constraint and random phase offset. Here, SIC receiver is assumed.

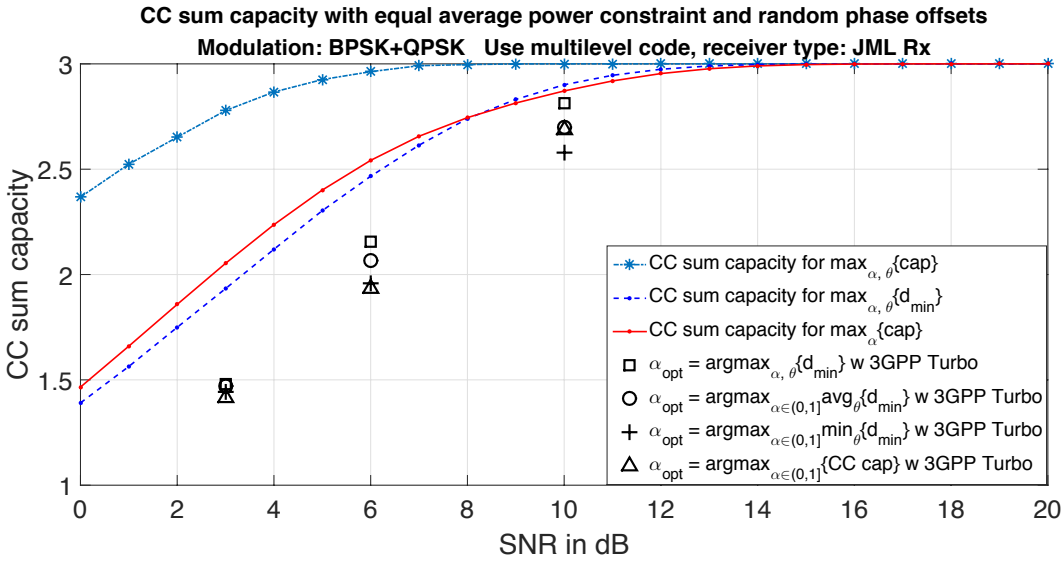

Figure 5.9: CC sum capacity and achievable rates of BPSK+QPSK with equal average power constraint and random phase offset. Here, JML receiver is assumed.

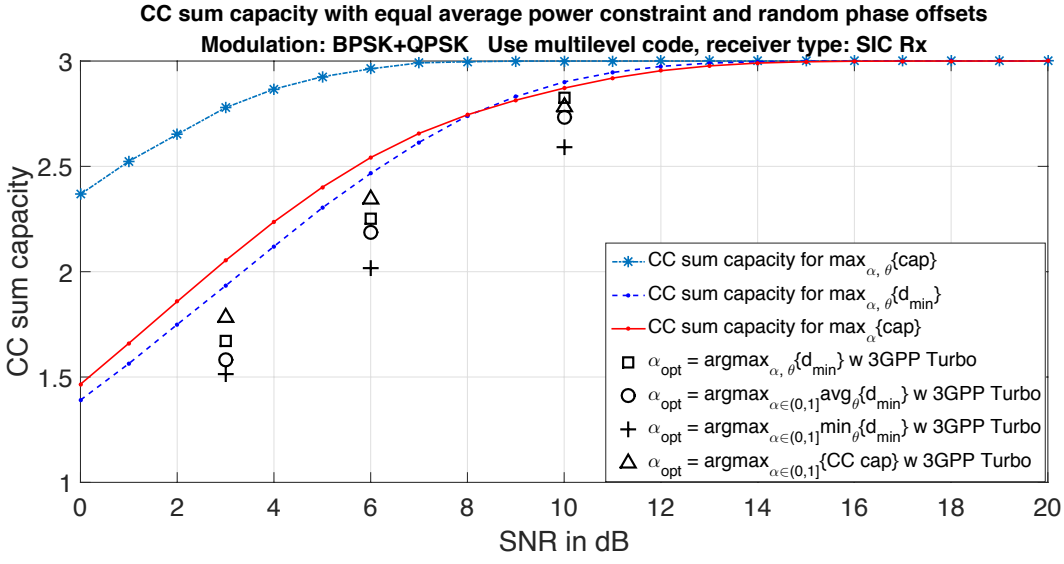

Figure 5.10: CC sum capacity and achievable rates of BPSK+QPSK with equal average power constraint and random phase offset. Here, SIC receiver is assumed.

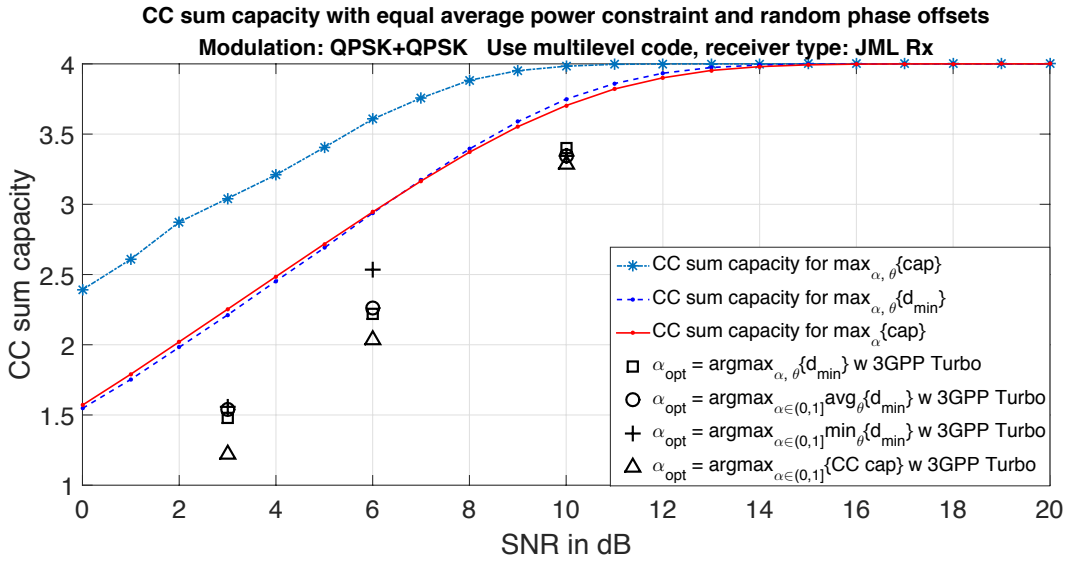

Figure 5.11: CC sum capacity and achievable rates of QPSK+QPSK with equal average power constraint and random phase offset. Here, JML receiver is assumed.

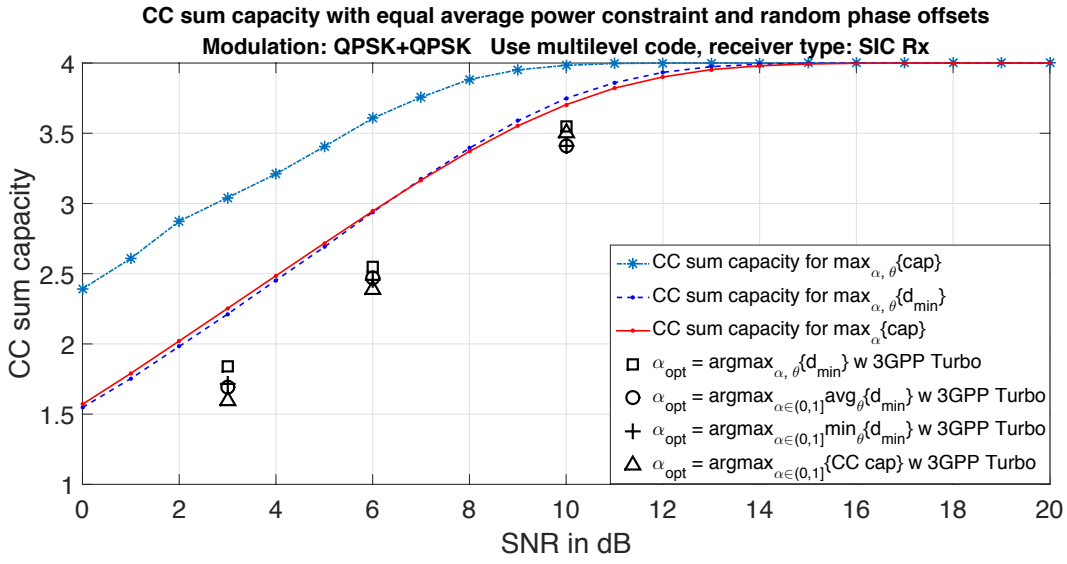

Figure 5.12: CC sum capacity and achievable rates of QPSK+QPSK with equal average power constraint and random phase offset. Here, SIC receiver is assumed.

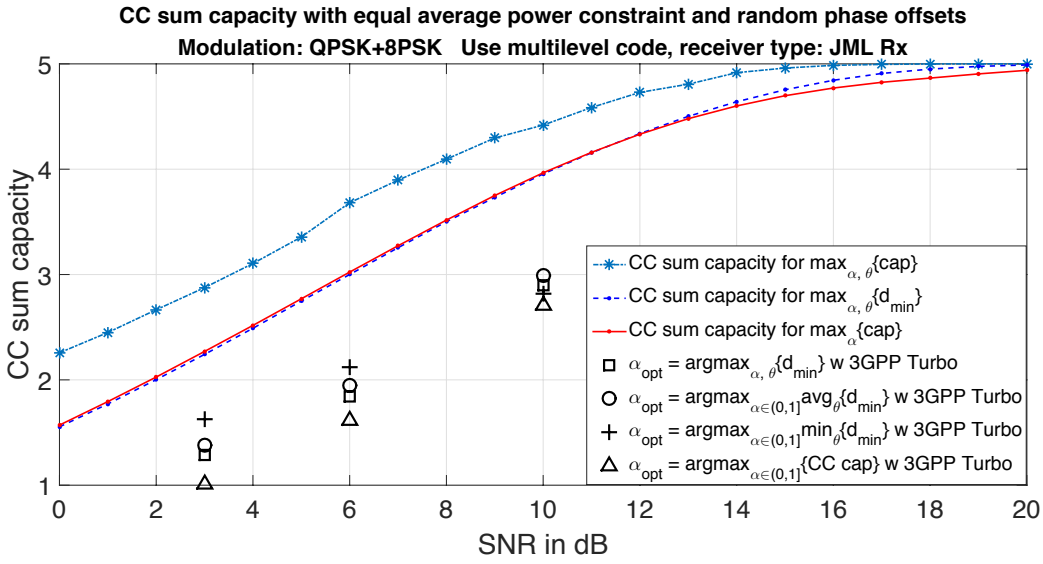

Figure 5.13: CC sum capacity and achievable rates of QPSK+8PSK with equal average power constraint and random phase offset. Here, JML receiver is assumed.

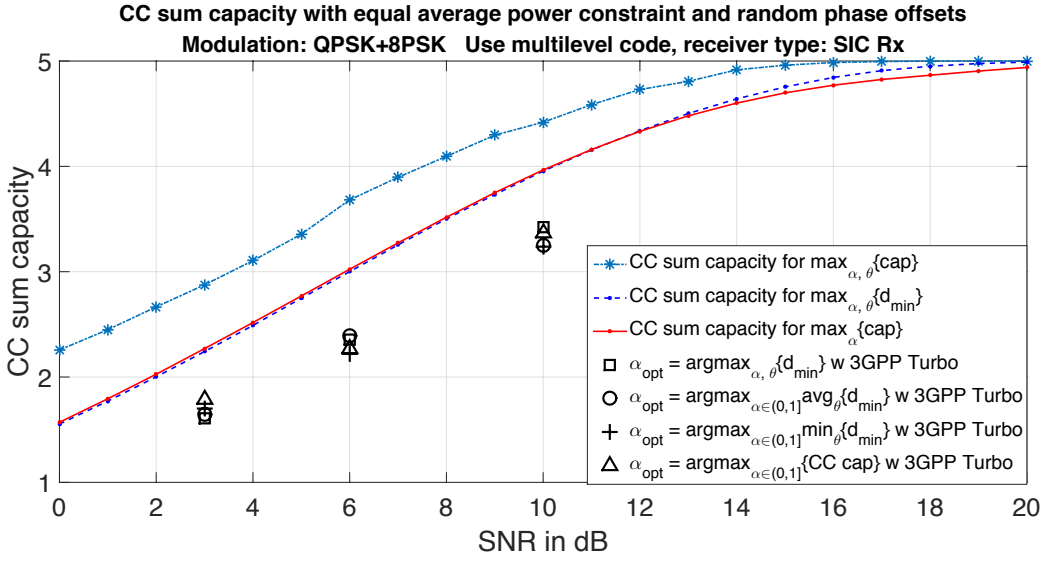

Figure 5.14: CC sum capacity and achievable rates of QPSK+8PSK with equal average power constraint and random phase offset. Here, SIC receiver is assumed.

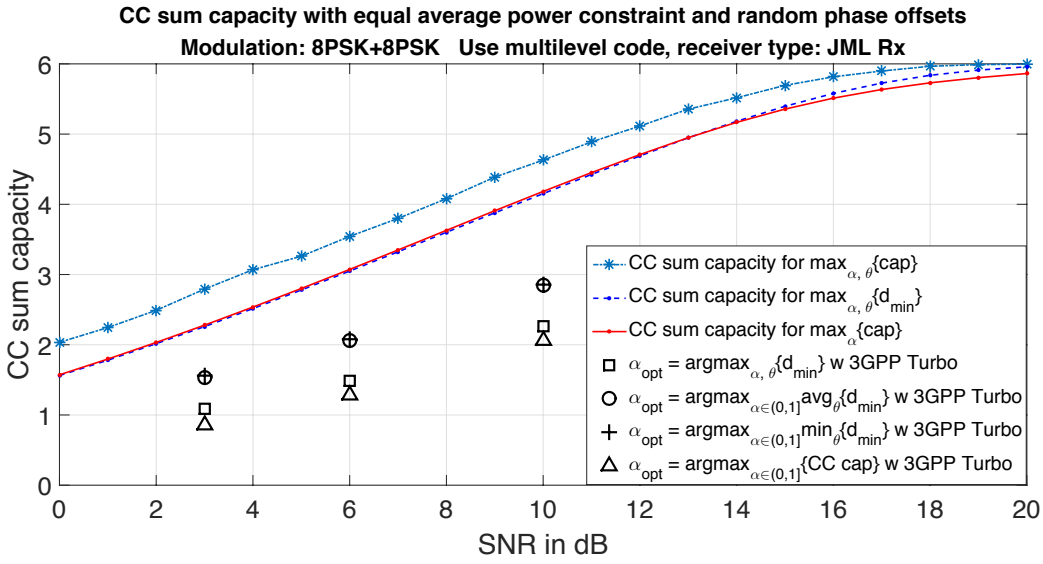

Figure 5.15: CC sum capacity and achievable rates of 8PSK+8PSK with equal average power constraint and random phase offset. Here, JML receiver is assumed.

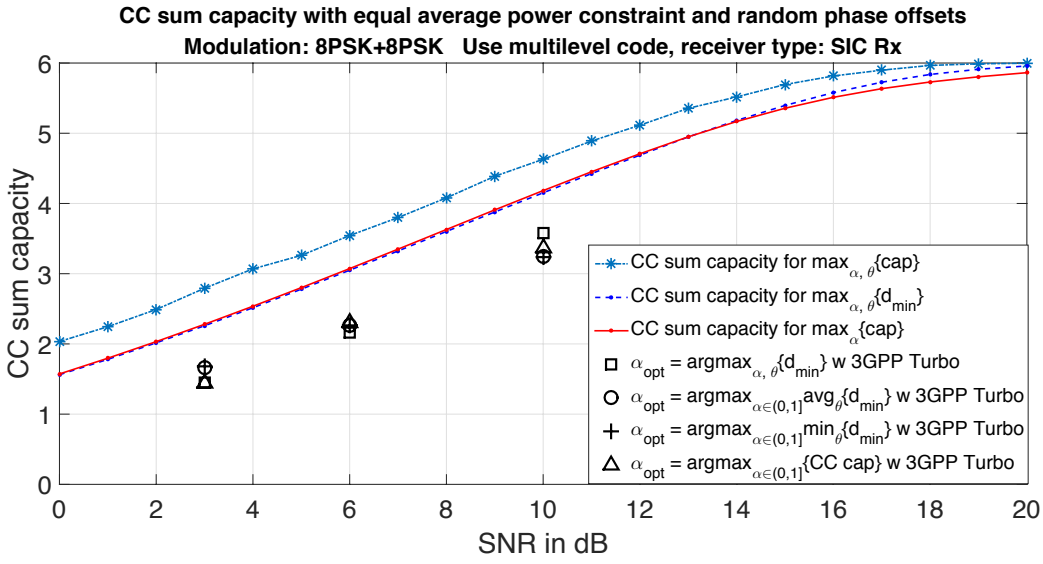

Figure 5.16: CC sum capacity and achievable rates of 8PSK+8PSK with equal average power constraint and random phase offset. Here, SIC receiver is assumed.

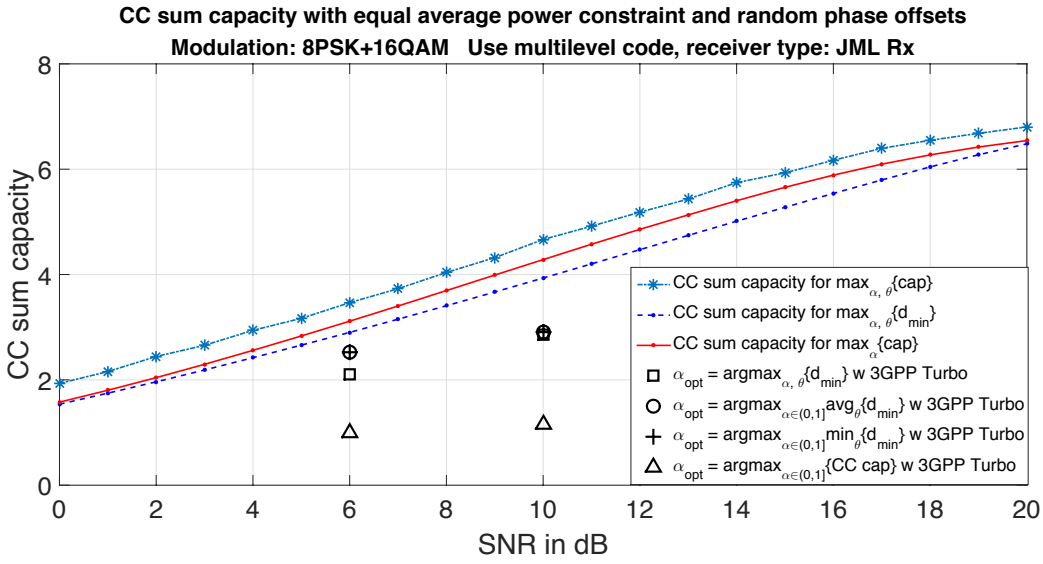

Figure 5.17: CC sum capacity and achievable rates of 8PSK+16QAM with equal average power constraint and random phase offset. Here, JML receiver is assumed.

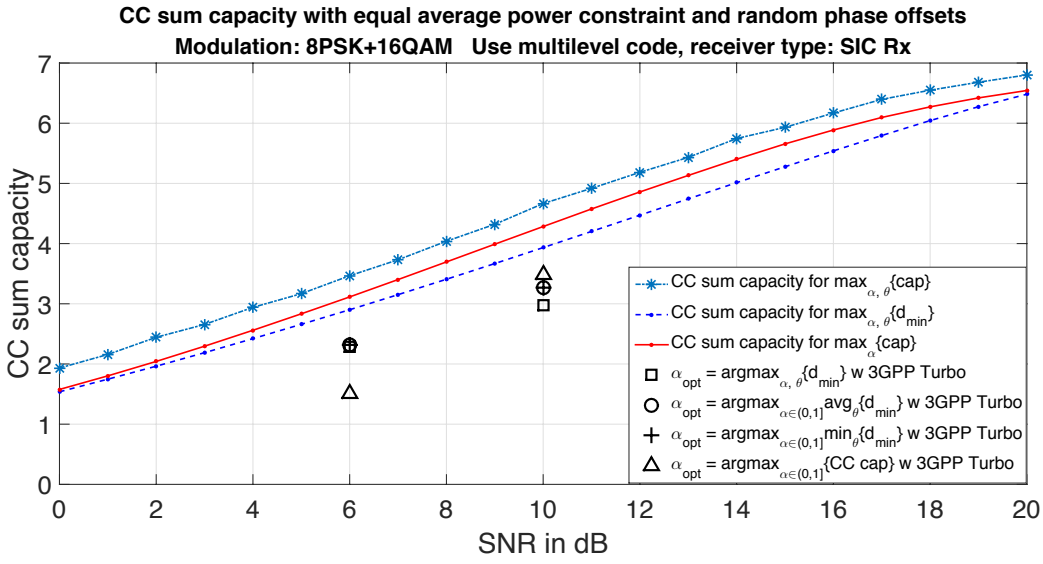

Figure 5.18: CC sum capacity and achievable rates of 8PSK+16QAM with equal average power constraint and random phase offset. Here, SIC receiver is assumed.

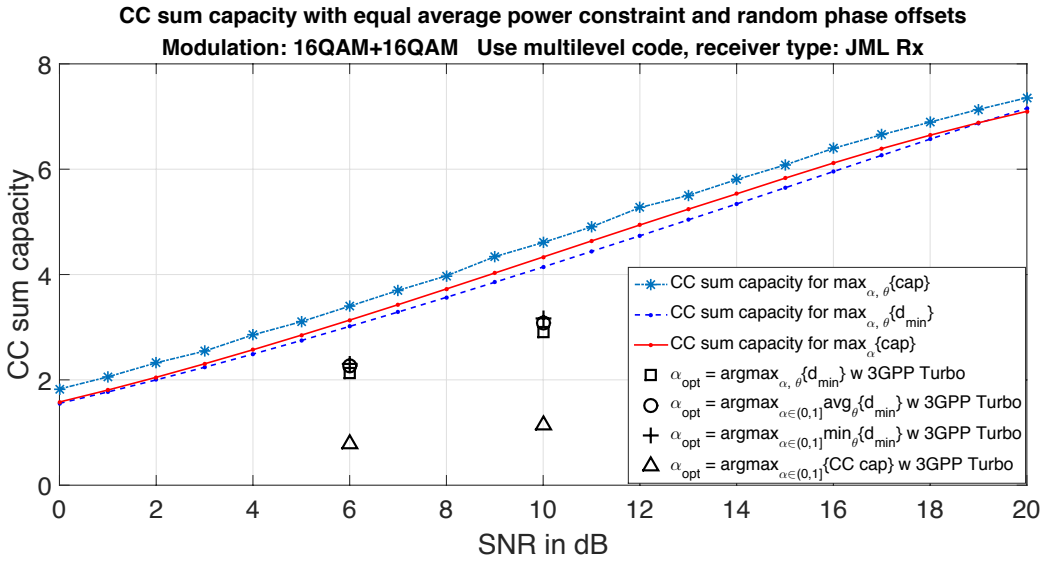

Figure 5.19: CC sum capacity and achievable rates of 16QAM+16QAM with equal average power constraint and random phase offset. Here, JML receiver is assumed.

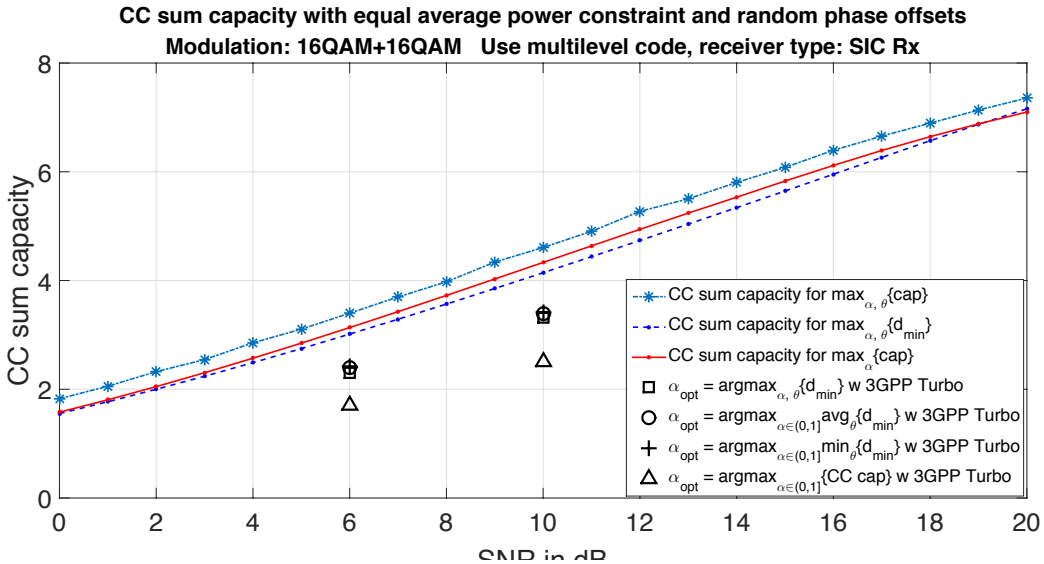

Figure 5.20: CC sum capacity and achievable rates of 16QAM+16QAM with equal average power constraint and random phase offset. Here, SIC receiver is assumed.

Tables 5.4, 5.5, 5.6 and 5.7 list the maximum achievable rates subject to BLER ≤ 0.1, where JML receiver is employed and signals received from both UEs give SNR = 3 dB. In Figure 5.1, we mark the rate pairs in these tables. The capacity region for SIC receiver and the time-sharing curve based on QPSK modulation and OMA are also plotted in blue solid line and red dotted line, respectively.

Subsequently, the following results are summarized:

(i) Tables 5.8, 5.9, 5.10 and 5.11 and Figure 5.2 for SIC receiver and SNR = 3 dB;

(ii) Tables 5.12, 5.13, 5.14 and5.15 and Figure 5.3 for JML receiver and SNR = 6 dB;

(iii) Table 5.16, 5.17, 5.18 and5.19 and Figure 5.4 for SIC receiver and SNR = 6 dB;

(iv) Tables 5.20, 5.21, 5.22 and 5.23 and Figure 5.5 for JML receiver and SNR = 10 dB;

(v) Tables 5.24, 5.25, 5.26 and5.27 and Figure 5.6 for SIC receiver and SNR = 10 dB.

In order to realize how far our maximum achievable rates are from the CC sum capacity, the following figures are also plotted.

(i) Figure 5.7 for BPSK+BPSK and JML receiver;

(ii) Figure 5.8 for BPSK+BPSK case and SIC receiver;

(iii) Figure 5.9 for BPSK+QPSK and JML receiver;

(iv) Figure 5.10 for BPSK+QPSK and SIC receiver;

(v) Figure 5.11 for QPSK+QPSK and JML receiver;

(vi) Figure 5.12 for QPSK+QPSK and SIC receiver;

(vii) Figure 5.13 for QPSK+8PSK and JML receiver;

($viii$) Figure 5.14 for QPSK+8PSK and SIC receiver;

(ix) Figure 5.15 for 8PSK+8PSK and JML receiver;

(x) Figure 5.16 for 8PSK+8PSK and SIC receiver;

(xi) Figure 5.17 for 8PSK+16QAM and JML receiver;

(xii) Figure 5.18 for 8PSK+16QAM and SIC receiver;

(*xiii*) Figure 5.19 for 16QAM+16QAM and JML receiver;

(*xiv*) Figure 5.20 for 16QAM+16QAM and SIC receiver.

In these figures, the light blue star-marked dotted line portraits the *CC sum capacity with phase adjustment* for parameters chosen by

$$(\alpha_{\text{opt}}, \theta_{\text{opt}}) = \underset{\alpha\in(0,1]\,\&\,\theta\in[0,2\pi)}{\text{argmax}} \{\text{CC sum capacity in (3.12)}\}.$$

The purple dotted line depicts the *CC sum capacity of with phase adjustment* for parameters chosen by

$$(\alpha_{\text{opt}}, \theta_{\text{opt}}) = \underset{\alpha\in(0,1]\,\&\,\theta\in[0,2\pi)}{\text{argmax}} \{d_{\min}\}.$$

The red solid line is the value of the *CC sum capacity of average phases* for parameters chosen by

$$\alpha_{\text{opt}} = \underset{\alpha\in(0,1]}{\text{argmax}}\{\text{CC sum capacity in (3.7)}\}.$$

The case of α chosen to be the one that achieves $\max_{\alpha\in(0,1]} \max_{\theta\in[0,2\pi)}\{d_{\min}\}$ is upper-bounded by the dotted line. And the other three cases of α chosen to be the one that achieves $\underset{\alpha\in(0,1]}{\text{argmax}}\, \underset{\theta\in\Theta}{\text{avg}}\{d_{\min}\}$, $\underset{\alpha\in(0,1]}{\text{argmax}}\, \underset{\theta\in\Theta}{\min}\{d_{\min}\}$ and $\max_{\alpha\in(0,1]}\{\text{CC sum capacity}\}$ are upper-bounded by the solid line.

Several observations can be made based on these tables and figures. First, the transmission powers of the two UEs are alternately varied in odd and even channels uses. This is the reason why the BS can still distinguish their individual information from the superimposed signal even if their SNRs are the same. It also makes feasible the use of the SIC receiver.

Second, the maximum achievable rates corresponding to the SIC receiver is surprisingly better than that those corresponding to the JML receiver. For the SIC receiver, the information of the strong UE is decoded first, and then re-encoded and subtracted from the combined signal. From the practical design point of view, the CPA design is particularly suitable for the SIC receiver.

Third, from Figures 5.1–5.6, we observe that most of the practically obtained rate pairs surpass the time-sharing line. This, once again, confirms the superiority of the

CPA/NOMA scheme over the conventional OMA scheme. However, the resulting rates are still distant away from the ideal capacity region.

Fourth, using α_{opt} from $\text{argmax}_{\alpha\in(0,1]}\{\text{CC sum capacity of average phases}\}$ results in a worse maximum achievable sum rate than adopting the one that achieves either

$$\max_{\alpha\in(0,1]} \operatorname*{avg}_{\theta\in\Theta}\{d_{\min}\} \quad \text{or} \quad \max_{\alpha\in(0,1]} \min_{\theta\in\Theta}\{d_{\min}\}$$

in most simulations. This points out that for a practical communication system, the performance is mainly determined by the error rate and hence $d_{\min}$ is a more crucial factor than the ideal sum capacity.

Table 5.28: Parameter setting with or without adjustment of constellation rotation

	Case 1: $= \text{argmax}_{\alpha\in(0,1]\,\&\,\theta\in[0,2\pi)}\{d_{\min}\}$	Case 2: $\neq \text{argmax}_{\alpha\in(0,1]\,\&\,\theta\in[0,2\pi)}\{d_{\min}\}$
Modulation	BPSK+QPSK	
α	0.40	1.00
$(\theta_{\text{odd}}, \theta_{\text{even}})$	(90°, 12°)	(0°, 0°)

We close this section by presenting an experiment to remark on the essentiality of manipulating the rotation of constellation in the CPA scheme when GMAC channel has additional random phase offset. This can somehow explain why in some figures among Figures 5.7–5.20, the purple dotted line has a sightly smaller CC sum capacity than the red solid line at low SNR but it then exceeds the red solid line at high SNR.

The parameter setting of this example is shown in Table 5.28, where Case 1 is exactly the case corresponding to the purple dotted line in Figures 5.9 and 5.10. Case 2 simply assumes $\alpha = 1$ and $\theta = 0$. The joint constellations in the odd and even channel uses for both cases are depicted in Figure 5.21. It can be observed that the joint constellation corresponding to Case 2 has two constellation points overlapping at the origin, resulting in $d_{\min} = 0$ but except for the two overlapping points, other pairwise distances for Case 2 are seemingly much larger than those for Case 1. By this observation, we can infer that Case 1 will perform better than Case 2 at high SNR due to its larger $d_{\min}$; however, it may have a worse performance at low SNR due to having a larger number of pairwise

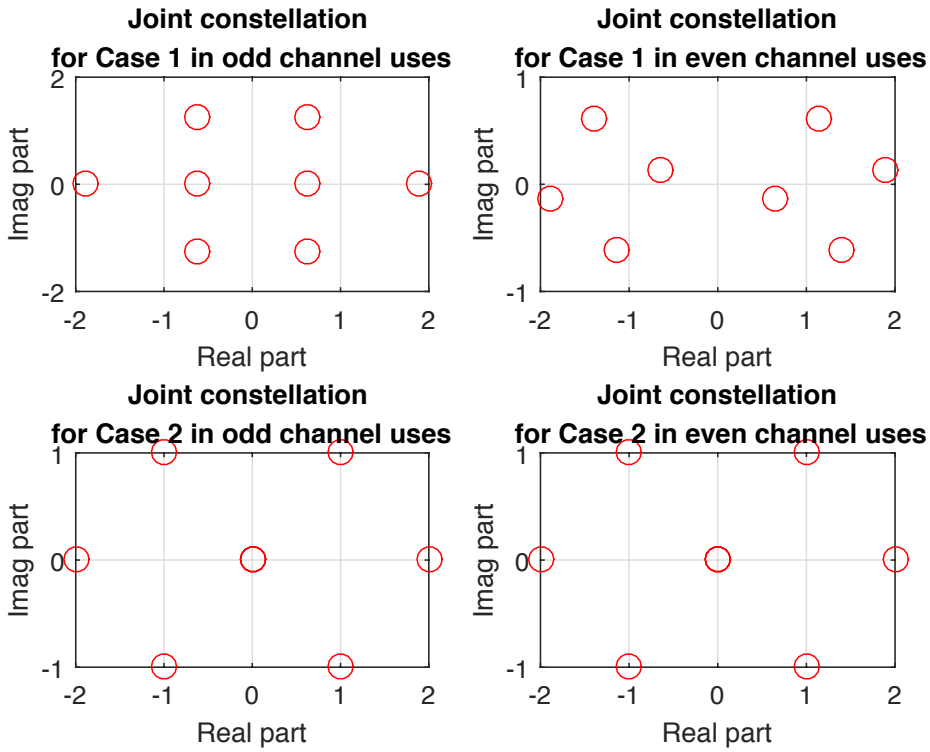

Figure 5.21: Joint constellations of Case 1 and Case 2 for the odd and even channel uses under SNR = 0 dB

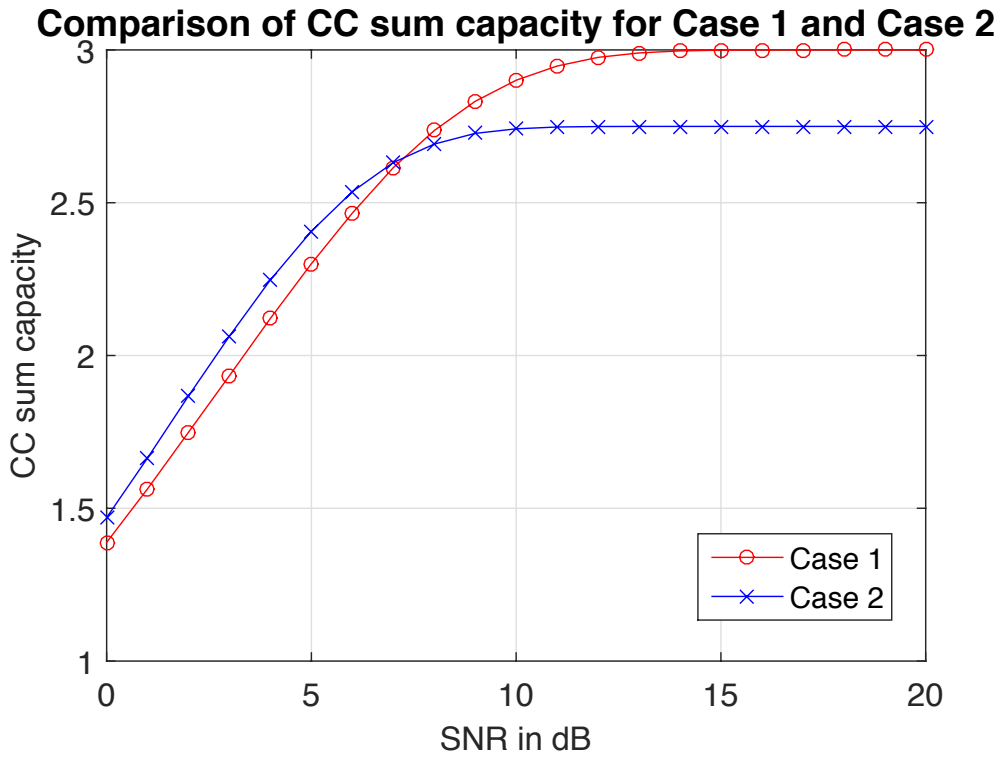

Figure 5.22: CC sum capacities of Case 1 and Case 2 under different SNRs

distances that is equal to $d_{\min}$. This matches exactly what has been shown in Figure 5.22, where the CC sum capacities of both cases are illustrated.

5.2 Two-user GMAC with Unequal Average Power Constraint and Random Phase Offset

Table 5.29: α_{opt} and θ_{opt} selected based on different modulation combinations and different distance-based criterion. The SNRs of UE1 and UE2 are respectively 3 dB and 6 dB.

Modulation (UE1+UE2)	$\underset{\alpha\in(0,1]\,\&\,\theta\in\Theta}{\text{argmax}}\{d_{\min}\}$		$\underset{\alpha\in(0,1]}{\text{argmax}}\,\underset{\theta\in\Theta}{\text{avg}}\{d_{\min}\}$	$\underset{\alpha\in(0,1]}{\text{argmax}}\,\underset{\theta\in\Theta}{\min}\{d_{\min}\}$
	α_{opt}	$(\theta_{\text{opt,odd}}, \theta_{\text{opt,even}})$	α_{opt}	α_{opt}
BPSK+BPSK	1.00	(46°, 46°)	1.00	0.23
BPSK+QPSK	0.43	(1°, 120°)	0.4	0.3
QPSK+QPSK	0.67	(6°, 30°)	0.58	0.16
QPSK+8PSK	0.23	(315°, 31°)	0.20	0.18
8PSK+8PSK	0.28	(34°, 313°)	0.28	0.07

Table 5.30: α_{opt} based on different modulation combinations and unequal SNRs

Modulation (UE1+UE2)	$\underset{\alpha\in(0,1]}{\text{argmax}}\{\text{CC sum capacity of average phases}\}$
SNRs of UE1 & UE2	UE1 SNR = 3 dB and UE2 SNR = 6 dB
BPSK+BPSK	0.99
BPSK+QPSK	0.79
QPSK+QPSK	0.98
QPSK+8PSK	1.00
8PSK+8PSK	0.98

Table 5.31: α_{opt} and θ_{opt} selected based on different modulation combinations and different distance-based criterion. The SNRs of UE1 and UE2 are respectively 3 dB and 10 dB.

Modulation (UE1+UE2)	$\underset{\alpha\in(0,1]\,\&\,\theta\in\Theta}{\text{argmax}}\{d_{\min}\}$		$\underset{\alpha\in(0,1]}{\text{argmax}}\,\underset{\theta\in\Theta}{\text{avg}}\{d_{\min}\}$	$\underset{\alpha\in(0,1]}{\text{argmax}}\,\underset{\theta\in\Theta}{\min}\{d_{\min}\}$
	α_{opt}	$(\theta_{\text{opt,odd}}, \theta_{\text{opt,even}})$	α_{opt}	α_{opt}
BPSK+BPSK	1.00	(1°, 1°)	1.00	1.00
BPSK+QPSK	1.00	(1°, 1°)	1.00	1.00
QPSK+QPSK	1.00	(1°, 1°)	1.00	1.00
QPSK+8PSK	0.48	(45°, 347°)	0.45	0.45
8PSK+8PSK	0.60	(62°, 77°)	0.60	0.45

Table 5.32: α_{opt} based on different modulation combinations and unequal SNRs. The SNRs of UE1 and UE2 are respectively 3 dB and 10 dB.

Modulation (UE1+UE2)	$\underset{\alpha\in(0,1]}{\text{argmax}}\{\text{CC sum capacity of average phases}\}$
SNRs of UE1 & UE2	UE1 SNR = 3 dB and UE2 SNR = 10 dB
BPSK+BPSK	0.97
BPSK+QPSK	0.98
QPSK+QPSK	1.00
QPSK+8PSK	1.00
8PSK+8PSK	0.98

Table 5.33: Achievable rate pairs of the CPA scheme under two-user GMAC with random phase offset. Here, $(\alpha_{\text{opt}}, \theta_{\text{opt}}) = \text{argmax}_{\alpha\in(0,1)\,\&\,\theta\in\Theta}\{d_{\min}\}$, JML receiver is employed, UE1 SNR = 3 dB and UE2 SNR = 6 dB. The receiver is also assumed to be able to rotate the two constellations accurately to match θ_{opt}.

Modulation (UE1+UE2)	UE1 Rate	UE2 Rate
BPSK+BPSK	0.820	0.920
BPSK+QPSK	0.600	1.353
QPSK+QPSK	0.660	1.060
QPSK+8PSK	0.680	1.095
8PSK+8PSK	0.543	1.038

Table 5.34: Achievable rate pairs of the CPA scheme under two-user GMAC with random phase offset. Here, $\alpha_{\text{opt}} = \text{argmax}_{\alpha\in(0,1]}\,\text{avg}_{\theta\in\Theta}\{d_{\min}\}$, JML receiver is employed, UE1 SNR = 3 dB and UE2 SNR = 6 dB.

Modulation (UE1+UE2)	UE1 Rate	UE2 Rate
BPSK+BPSK	0.750	0.850
BPSK+QPSK	0.588	1.310
QPSK+QPSK	0.640	1.050
QPSK+8PSK	0.690	1.118
8PSK+8PSK	0.543	1.038

Table 5.35: Achievable rate pairs of the CPA scheme under two-user GMAC with random phase offset. Here, $\alpha_{\text{opt}} = \text{argmax}_{\alpha\in(0,1]}\,\min_{\theta\in\Theta}\{d_{\min}\}$, JML receiver is employed, UE1 SNR = 3 dB and UE2 SNR = 6 dB.

Modulation (UE1+UE2)	UE1 Rate	UE2 Rate
BPSK+BPSK	0.630	0.768
BPSK+QPSK	0.598	1.285
QPSK+QPSK	0.795	1.070
QPSK+8PSK	0.715	1.135
8PSK+8PSK	0.783	1.113

Table 5.36: Achievable rate pairs of the CPA scheme under two-user GMAC with random phase offset. Here, $\alpha_{\text{opt}} = \text{argmax}_{\alpha\in(0,1]}\{\text{CC sum capacity of average phases}\}$, JML receiver is employed, UE1 SNR = 3 dB and UE2 SNR = 6 dB.

Modulation (UE1+UE2)	UE1 Rate	UE2 Rate
BPSK+BPSK	0.750	0.853
BPSK+QPSK	0.493	1.275
QPSK+QPSK	0.560	1.020
QPSK+8PSK	0.430	0.860
8PSK+8PSK	0.335	0.835

Table 5.37: Achievable rate pairs of the CPA scheme under two-user GMAC with random phase offset. Here, $(\alpha_{\text{opt}}, \theta_{\text{opt}}) = \text{argmax}_{\alpha\in(0,1)\,\&\,\theta\in\Theta}\{d_{\min}\}$, SIC receiver is employed, UE1 SNR = 3 dB and UE2 SNR = 6 dB. The receiver is also assumed to be able to rotate the two constellations accurately to match θ_{opt}.

Modulation (UE1+UE2)	UE1 Rate	UE2 Rate
BPSK+BPSK	0.838	0.920
BPSK+QPSK	0.645	1.458
QPSK+QPSK	0.838	1.083
QPSK+8PSK	0.758	1.273
8PSK+8PSK	0.658	1.230

Table 5.38: Achievable rate pairs of the CPA scheme under two-user GMAC with random phase offset. Here, $\alpha_{\text{opt}} = \text{argmax}_{\alpha\in(0,1]}\,\text{avg}_{\theta\in\Theta}\{d_{\min}\}$, SIC receiver is employed, UE1 SNR = 3 dB and UE2 SNR = 6 dB.

Modulation (UE1+UE2)	UE1 Rate	UE2 Rate
BPSK+BPSK	0.803	0.850
BPSK+QPSK	0.635	1.410
QPSK+QPSK	0.813	1.268
QPSK+8PSK	0.763	1.258
8PSK+8PSK	0.658	1.238

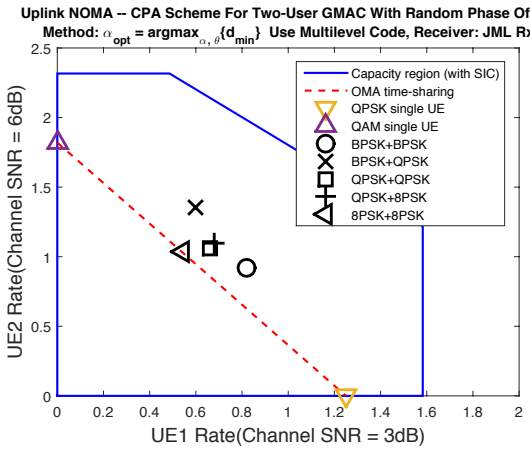

(a) $(\alpha_{\text{opt}}, \theta_{\text{opt}}) = \text{argmax}_{\alpha\in(0,1)\,\&\,\theta\in\Theta}\{d_{\min}\}$

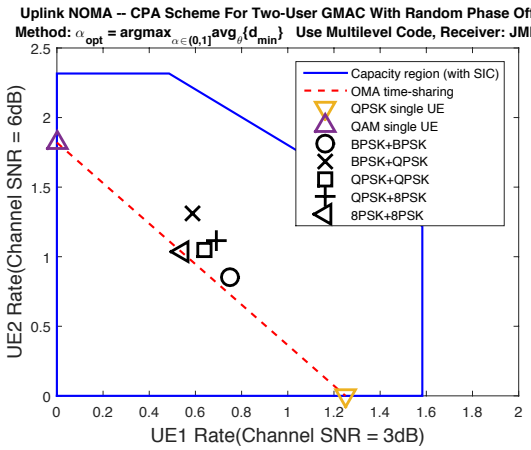

(b) $\alpha_{\text{opt}} = \text{argmax}_{\alpha\in(0,1]}\,\text{avg}_{\theta\in\Theta}\{d_{\min}\}$

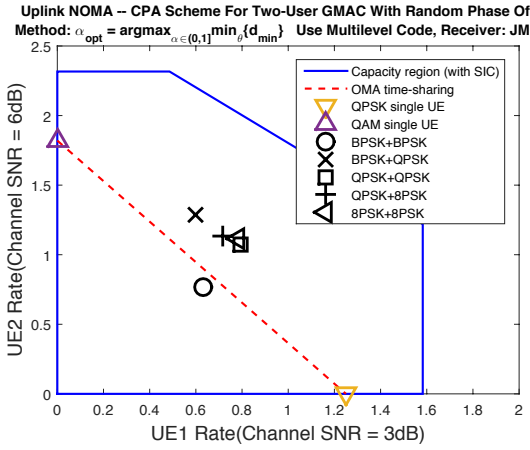

(c) $\alpha_{\text{opt}} = \text{argmax}_{\alpha\in(0,1]}\,\min_{\theta\in\Theta}\{d_{\min}\}$

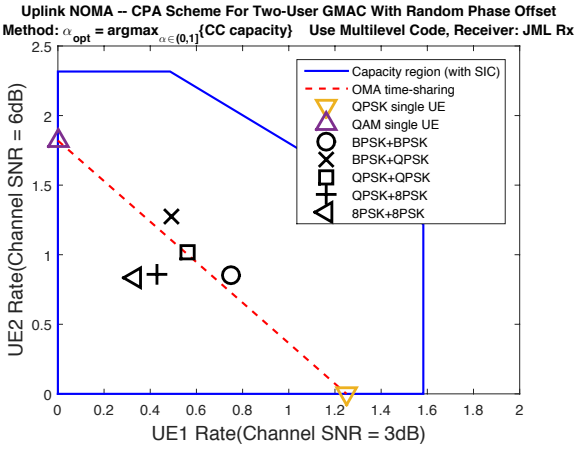

(d) $\alpha_{\text{opt}} = \text{argmax}_{\alpha\in(0,1]}\{\text{CC sum capacity}\}$

Figure 5.23: Capacity region and achievable rate pairs of the CPA scheme under two-user GMAC with random phase offset. Here, JML receiver is employed, UE1 SNR = 3 dB and UE2 SNR = 6 dB.

Table 5.39: Achievable rate pairs of the CPA scheme under two-user GMAC with random phase offset. Here, $\alpha_{\text{opt}} = \text{argmax}_{\alpha\in(0,1]} \min_{\theta\in\Theta}\{d_{\min}\}$, SIC receiver is employed, UE1 SNR = 3 dB and UE2 SNR = 6 dB.

Modulation (UE1+UE2)	UE1 Rate	UE2 Rate
BPSK+BPSK	0.630	0.790
BPSK+QPSK	0.630	1.345
QPSK+QPSK	0.810	1.150
QPSK+8PSK	0.785	1.218
8PSK+8PSK	0.820	1.158

Table 5.40: Achievable rate pairs of the CPA scheme under two-user GMAC with random phase offset. Here, $\alpha_{\text{opt}} = \text{argmax}_{\alpha\in(0,1]}\{\text{CC sum capacity of average phases}\}$, SIC receiver is employed, UE1 SNR = 3 dB and UE2 SNR = 6 dB.

Modulation (UE1+UE2)	UE1 Rate	UE2 Rate
BPSK+BPSK	0.803	0.853
BPSK+QPSK	0.638	1.318
QPSK+QPSK	0.798	1.028
QPSK+8PSK	0.765	0.928
8PSK+8PSK	0.678	0.898

Table 5.41: Achievable rate pairs of the CPA scheme under two-user GMAC with random phase offset. Here, $(\alpha_{\text{opt}}, \theta_{\text{opt}}) = \text{argmax}_{\alpha\in(0,1)\,\&\,\theta\in\Theta}\{d_{\min}\}$, JML receiver is employed, UE1 SNR = 3 dB and UE2 SNR = 10 dB. The receiver is also assumed to be able to rotate the two constellations accurately to match θ_{opt}.

Modulation (UE1+UE2)	UE1 Rate	UE2 Rate
BPSK+BPSK	0.845	0.970
BPSK+QPSK	0.783	1.885
QPSK+QPSK	1.120	1.760
QPSK+8PSK	0.480	1.610
8PSK+8PSK	0.375	1.575

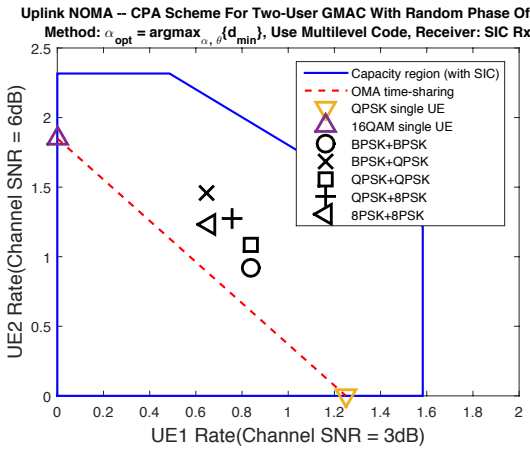

(a) $(\alpha_{\text{opt}}, \theta_{\text{opt}}) = \text{argmax}_{\alpha\in(0,1)\,\&\,\theta\in\Theta}\{d_{\min}\}$

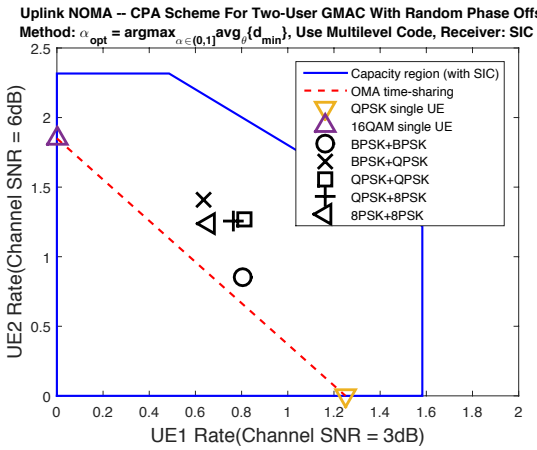

(b) $\alpha_{\text{opt}} = \text{argmax}_{\alpha\in(0,1]}\,\text{avg}_{\theta\in\Theta}\{d_{\min}\}$

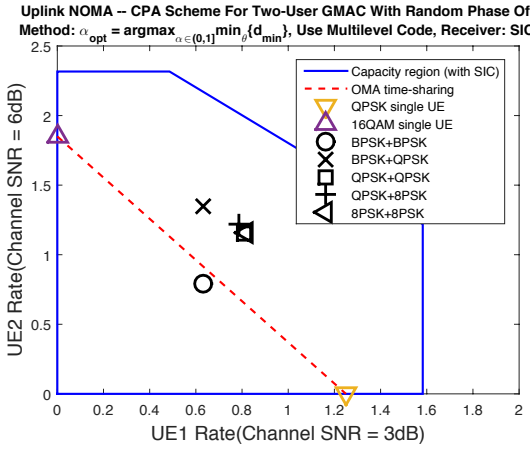

(c) $\alpha_{\text{opt}} = \text{argmax}_{\alpha\in(0,1]}\,\text{min}_{\theta\in\Theta}\{d_{\min}\}$

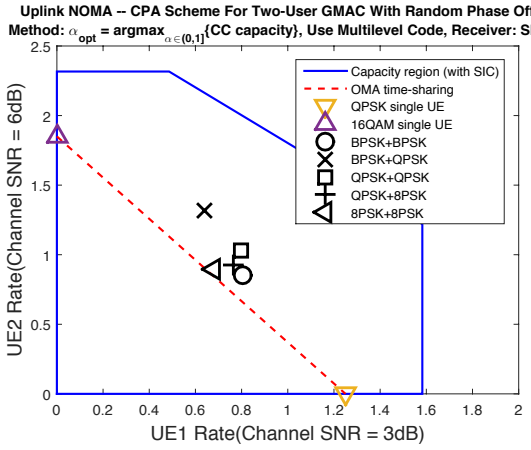

(d) $\alpha_{\text{opt}} = \text{argmax}_{\alpha\in(0,1]}\{\text{CC sum capacity}\}$

Figure 5.24: Capacity region and achievable rate pairs of the CPA scheme under two-user GMAC with random phase offset. Here, SIC receiver is employed, UE1 SNR = 3 dB and UE2 SNR = 6 dB.

Table 5.42: Achievable rate pairs of the CPA scheme under two-user GMAC with random phase offset. Here, $\alpha_{\text{opt}} = \text{argmax}_{\alpha\in(0,1]} \text{avg}_{\theta\in\Theta}\{d_{\min}\}$, JML receiver is employed, UE1 SNR = 3 dB and UE2 SNR = 10 dB.

Modulation (UE1+UE2)	UE1 Rate	UE2 Rate
BPSK+BPSK	0.855	0.990
BPSK+QPSK	0.715	1.800
QPSK+QPSK	1.020	1.730
QPSK+8PSK	0.485	1.618
8PSK+8PSK	0.378	1.575

Table 5.43: Achievable rate pairs of the CPA scheme under two-user GMAC with random phase offset. Here, $\alpha_{\text{opt}} = \text{argmax}_{\alpha\in(0,1]} \min_{\theta\in\Theta}\{d_{\min}\}$, JML receiver is employed, UE1 SNR = 3 dB and UE2 SNR = 10 dB.

Modulation (UE1+UE2)	UE1 Rate	UE2 Rate
BPSK+BPSK	0.855	0.990
BPSK+QPSK	0.715	1.800
QPSK+QPSK	1.020	1.730
QPSK+8PSK	0.485	1.618
8PSK+8PSK	0.393	1.573

Table 5.44: Achievable rate pairs of the CPA scheme under two-user GMAC with random phase offset. Here, $\alpha_{\text{opt}} = \text{argmax}_{\alpha\in(0,1]}\{\text{CC sum capacity of average phases}\}$, JML receiver is employed, UE1 SNR = 3 dB and UE2 SNR = 10 dB.

Modulation (UE1+UE2)	UE1 Rate	UE2 Rate
BPSK+BPSK	0.855	0.988
BPSK+QPSK	0.715	1.795
QPSK+QPSK	1.020	1.730
QPSK+8PSK	0.460	1.685
8PSK+8PSK	0.355	1.640

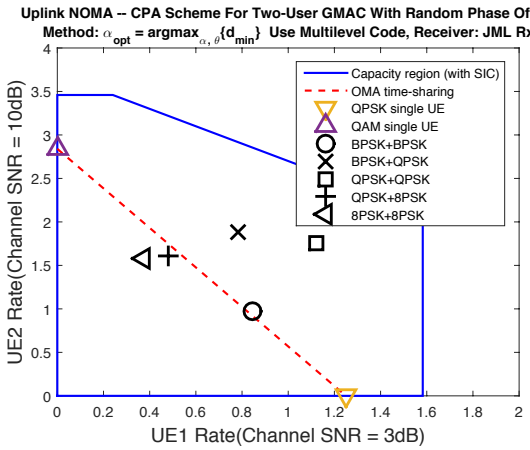

(a) $(\alpha_{\text{opt}}, \theta_{\text{opt}}) = \text{argmax}_{\alpha\in(0,1)\,\&\,\theta\in\Theta}\{d_{\min}\}$

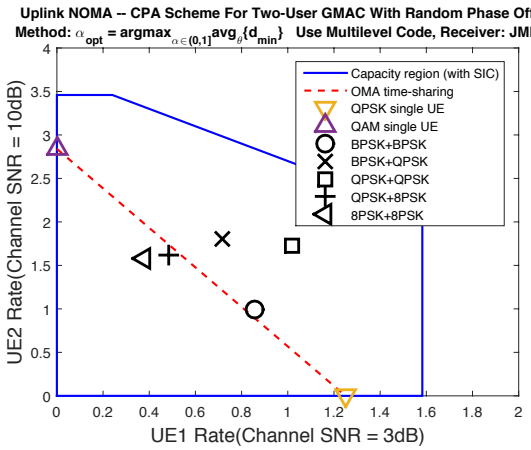

(b) $\alpha_{\text{opt}} = \text{argmax}_{\alpha\in(0,1]}\,\text{avg}_{\theta\in\Theta}\{d_{\min}\}$

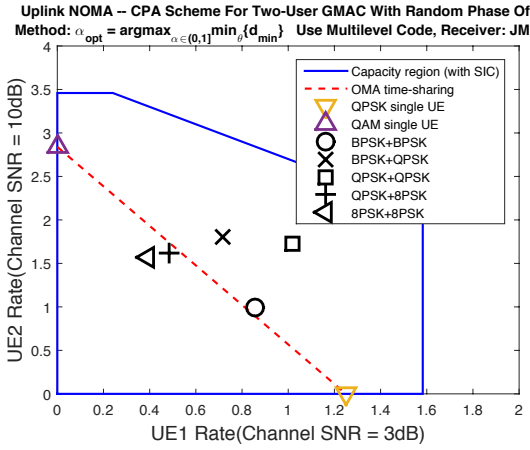

(c) $\alpha_{\text{opt}} = \text{argmax}_{\alpha\in(0,1]}\,\min_{\theta\in\Theta}\{d_{\min}\}$

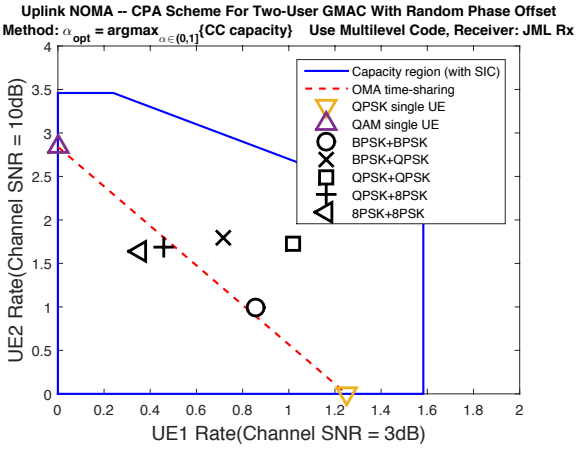

(d) $\alpha_{\text{opt}} = \text{argmax}_{\alpha\in(0,1]}\{\text{CC sum capacity}\}$

Figure 5.25: Capacity region and achievable rate pairs of the CPA scheme under two-user GMAC with random phase offset. Here, JML receiver is employed, UE1 SNR = 3 dB and UE2 SNR = 10 dB.

Table 5.45: Achievable rate pairs of the CPA scheme under two-user GMAC with random phase offset. Here, $(\alpha_{\text{opt}}, \theta_{\text{opt}}) = \text{argmax}_{\alpha\in(0,1)\,\&\,\theta\in\Theta}\{d_{\min}\}$, SIC receiver is employed, UE1 SNR = 3 dB and UE2 SNR = 10 dB. The receiver is also assumed to be able to rotate the two constellations accurately to match θ_{opt}.

Modulation (UE1+UE2)	UE1 Rate	UE2 Rate
BPSK+BPSK	0.853	0.970
BPSK+QPSK	0.828	1.890
QPSK+QPSK	1.185	1.760
QPSK+8PSK	0.695	1.678
8PSK+8PSK	0.630	1.610

Table 5.46: Achievable rate pairs of the CPA scheme under two-user GMAC with random phase offset. Here, $\alpha_{\text{opt}} = \text{argmax}_{\alpha\in(0,1]}\,\text{avg}_{\theta\in\Theta}\{d_{\min}\}$, SIC receiver is employed, UE1 SNR = 3 dB and UE2 SNR = 10 dB.

Modulation (UE1+UE2)	UE1 Rate	UE2 Rate
BPSK+BPSK	0.858	0.990
BPSK+QPSK	0.760	1.800
QPSK+QPSK	1.143	1.730
QPSK+8PSK	0.663	1.665
8PSK+8PSK	0.640	1.615

Table 5.47: Achievable rate pairs of the CPA scheme under two-user GMAC with random phase offset. Here, $\alpha_{\text{opt}} = \text{argmax}_{\alpha\in(0,1]}\,\min_{\theta\in\Theta}\{d_{\min}\}$, SIC receiver is employed, UE1 SNR = 3 dB and UE2 SNR = 10 dB.

Modulation (UE1+UE2)	UE1 Rate	UE2 Rate
BPSK+BPSK	0.858	0.990
BPSK+QPSK	0.760	1.800
QPSK+QPSK	1.143	1.730
QPSK+8PSK	0.663	1.665
8PSK+8PSK	0.560	1.625

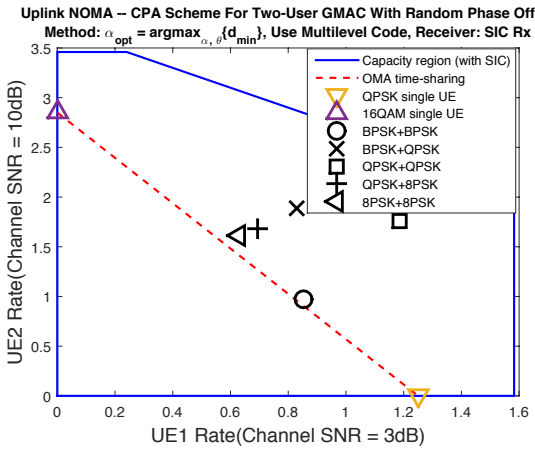

(a) $(\alpha_{\text{opt}}, \theta_{\text{opt}}) = \text{argmax}_{\alpha\in(0,1)\,\&\,\theta\in\Theta}\{d_{\min}\}$

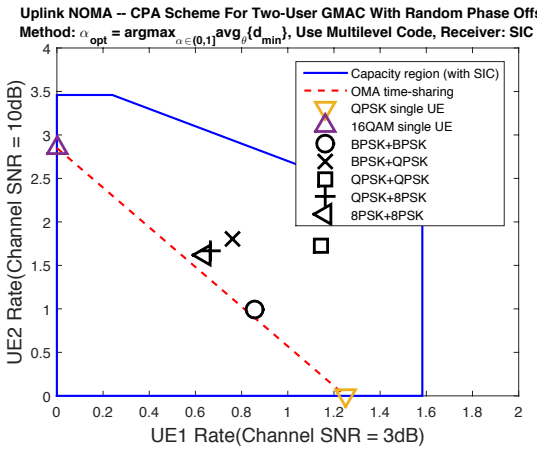

(b) $\alpha_{\text{opt}} = \text{argmax}_{\alpha\in(0,1]}\,\text{avg}_{\theta\in\Theta}\{d_{\min}\}$

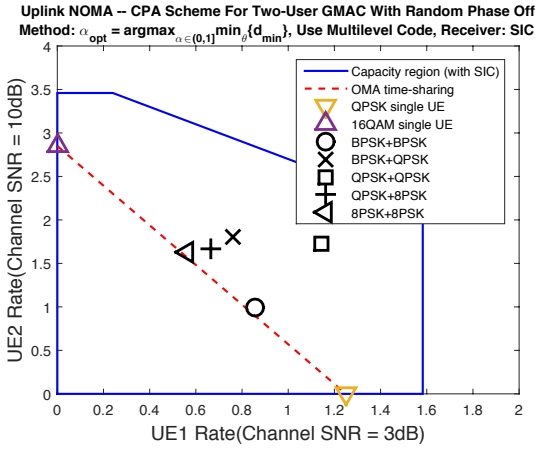

(c) $\alpha_{\text{opt}} = \text{argmax}_{\alpha\in(0,1]}\,\text{min}_{\theta\in\Theta}\{d_{\min}\}$

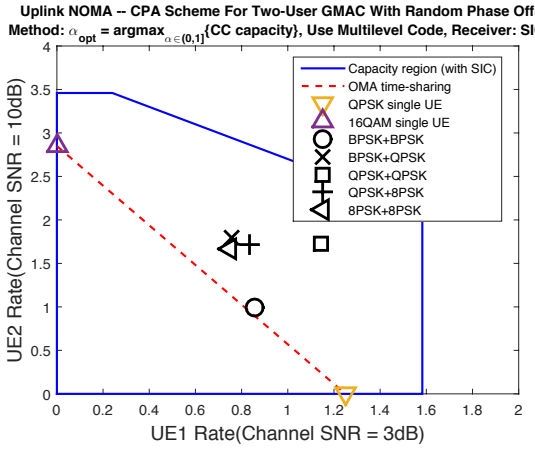

(d) $\alpha_{\text{opt}} = \text{argmax}_{\alpha\in(0,1]}\{\text{CC sum capacity}\}$

Figure 5.26: Capacity region and achievable rate pairs of the CPA scheme under two-user GMAC with random phase offset. Here, SIC receiver is employed, UE1 SNR = 3 dB and UE2 SNR = 10 dB.

Table 5.48: Achievable rate pairs of the CPA scheme under two-user GMAC with random phase offset. Here, $\alpha_{\text{opt}} = \text{argmax}_{\alpha\in(0,1]}\{\text{CC sum capacity of average phases}\}$, SIC receiver is employed, UE1 SNR = 3 dB and UE2 SNR = 10 dB.

Modulation (UE1+UE2)	UE1 Rate	UE2 Rate
BPSK+BPSK	0.858	0.988
BPSK+QPSK	0.758	1.795
QPSK+QPSK	1.143	1.730
QPSK+8PSK	0.835	1.715
8PSK+8PSK	0.75	1.670

In this section, we turn to examine by simulations the performance of the CPA scheme for two-user GMAC with unequal average power constraint and random phase offset.

Tables 5.29 and 5.30 list the values of α_{opt} and θ_{opt} chosen for different modulation combinations and different criterions under UE1 SNR = 3 dB and UE2 SNR = 6 dB. Tables 5.31 and 5.32 perform the same experiment as Tables 5.29 and 5.30 except that UE1 SNR = 3 dB, UE2 SNR = 10 dB.

Subject to BLER ≤ 0.1, Tables 5.33, 5.34, 5.35 and 5.36 list the maximum achievable rates for JML receiver under UE1 SNR = 3 dB and UE2 SNR = 6 dB. These tables are summarized in Figure 5.23, where the capacity region with respect to the SIC receiver is drawn in solid line, and the OMA time-sharing in red dotted line.

Subsequently, the following results are summarized:

(i) Tables 5.37, 5.38, 5.39 and 5.40 and Figure 5.24 for SIC receiver under UE1 SNR = 3 dB and UE2 SNR = 6 dB;

(ii) Table 5.41, 5.42, 5.43 and 5.44 and Figure 5.25 for JML receiver under UE1 SNR = 3 dB and UE2 SNR = 10 dB;

(iii) Table 5.45, 5.46, 5.47 and 5.48 and Figure 5.26 for SIC receiver under UE1 SNR = 3 dB and UE2 SNR = 10 dB.

Several observations can be made from these tables and figures. First, many of the criterion-chosen α_{opt} values in Tables 5.29, 5.30, 5.31 and 5.32 are unity, especially under UE1 SNR = 3 dB and UE2 SNR = 10 dB. This is because under unequal SNRs, the CPA scheme can directly take advantage of the power difference between two UEs; so it is generally unnecessary to adjust the power allocation of the two users. Secondly, the CC sum capacity criterion often results in a larger α_{opt} than the distance-based criterion. For unequal average power constraint, it turns out that the CC sum capacity criterion will provide a better choice of α_{opt}.

5.3 Three-user GMAC with Equal Average Power Constraint and Random Phase Offset

Table 5.49: α_{opt} and $\theta_{\text{opt}} = (\theta_{\text{opt,UE2}}, \theta_{\text{opt,UE3}})$ selected based on different modulation combinations and different distance-based criterions

Modulation (UE1+UE2+UE3)	$\underset{\alpha\in(0,1]\,\&\,\theta\in\Theta}{\text{argmax}}\ \{d_{\min}\}$		$\underset{\alpha\in(0,1]}{\text{argmax}}\ \underset{\theta\in\Theta}{\text{avg}}\{d_{\min}\}$	$\underset{\alpha\in(0,1]}{\text{argmax}}\ \underset{\theta\in\Theta}{\min}\{d_{\min}\}$
	α_{opt}	$(\theta_{\text{opt,UE2}},\theta_{\text{opt,UE3}})$	α_{opt}	α_{opt}
BPSK+	0.60	(130°, 270°)	0.35	0.04
BPSK+		(320°, 230°)		
BPSK		(270°, 320°)		
BPSK+	0.53	(203°, 290°)	0.22	0.04
BPSK+		(95°, 254°)		
QPSK		(288°, 228°)		
BPSK+	1.00	(294°, 163°)	0.09	0.05
QPSK+		(294°, 163°)		
QPSK		(294°, 163°)		
QPSK+	0.93	(289°, 127°)	0.34	0.71
QPSK+		(198°, 341°)		
QPSK		(143°, 342°)		

Table 5.50: α_{opt} based on different modulation combinations and different SNRs

Modulation (UE1+UE2+UE3)	$\alpha_{\text{opt}} = \underset{\alpha\in(0,1]}{\text{argmax}}\{\text{CC sum capacity of average phases}\}$		
SNR of UE1 & UE2 & UE3	3dB	6dB	10dB
BPSK+BPSK+BPSK	0.80	0.52	0.36
BPSK+BPSK+QPSK	0.96	0.66	0.40
BPSK+QPSK+QPSK	0.91	0.52	0.33
QPSK+QPSK+QPSK	0.76	0.41	0.32

Table 5.51: Achievable rate pairs of the CPA scheme for three-user GMAC with random phase offset. Here, $(\alpha_{\text{opt}}, \theta_{\text{opt}}) = \text{argmax}_{\alpha\in(0,1)\,\&\,\theta\in\Theta}\{d_{\min}\}$, JML receiver is employed, and SNR = 3 dB. The receiver is also assumed to be able to rotate the two constellations accurately to match θ_{opt}.

Modulation (UE1+UE2+UE3)	UE1 Rate	UE2 Rate	UE3 Rate
BPSK+BPSK+BPSK	0.665	0.665	0.667
BPSK+BPSK+QPSK	0.470	0.493	0.655
BPSK+QPSK+QPSK	0.295	0.380	0.375
QPSK+QPSK+QPSK	0.280	0.280	0.280

Table 5.52: Achievable rate pairs of the CPA scheme for three-user GMAC with random phase offset. Here, $\alpha_{\text{opt}} = \text{argmax}_{\alpha\in(0,1]}\,\text{avg}_{\theta\in\Theta}\{d_{\min}\}$, JML receiver is employed, and SNR = 3 dB.

Modulation (UE1+UE2+UE3)	UE1 Rate	UE2 Rate	UE3 Rate
BPSK+BPSK+BPSK	0.552	0.552	0.552
BPSK+BPSK+QPSK	0.422	0.477	0.683
BPSK+QPSK+QPSK	0.398	0.633	0.557
QPSK+QPSK+QPSK	0.377	0.377	0.377

Table 5.53: Achievable rate pairs of the CPA scheme for three-user GMAC with random phase offset. Here, $\alpha_{\text{opt}} = \text{argmax}_{\alpha\in(0,1]}\,\min_{\theta\in\Theta}\{d_{\min}\}$, JML receiver is employed, and SNR = 3 dB.

Modulation (UE1+UE2+UE3)	UE1 Rate	UE2 Rate	UE3 Rate
BPSK+BPSK+BPSK	0.532	0.532	0.532
BPSK+BPSK+QPSK	0.433	0.500	0.750
BPSK+QPSK+QPSK	0.405	0.657	0.577
QPSK+QPSK+QPSK	0.293	0.295	0.293

Table 5.54: Achievable rate pairs of the CPA scheme for three-user GMAC with random phase offset. Here, $\alpha_{\text{opt}} = \text{argmax}_{\alpha\in(0,1]}\{\text{CC sum capacity of average phases}\}$, JML receiver is employed, and SNR = 3 dB.

Modulation (UE1+UE2+UE3)	UE1 Rate	UE2 Rate	UE3 Rate
BPSK+BPSK+BPSK	0.520	0.520	0.520
BPSK+BPSK+QPSK	0.393	0.392	0.603
BPSK+QPSK+QPSK	0.307	0.387	0.387
QPSK+QPSK+QPSK	0.287	0.287	0.287

Table 5.55: Achievable rate pairs of the CPA scheme for three-user GMAC with random phase offset. Here, $(\alpha_{\text{opt}}, \theta_{\text{opt}}) = \text{argmax}_{\alpha\in(0,1)\,\&\,\theta\in\Theta}\{d_{\min}\}$, SIC receiver is employed, and SNR = 3 dB.

Modulation (UE1+UE2+UE3)	UE1 Rate	UE2 Rate	UE3 Rate
BPSK+BPSK+BPSK	0.738	0.737	0.738
BPSK+BPSK+QPSK	0.657	0.633	0.890
BPSK+QPSK+QPSK	0.547	0.750	0.870
QPSK+QPSK+QPSK	0.685	0.698	0.688

Table 5.56: Achievable rate pairs of the CPA scheme for three-user GMAC with random phase offset. Here, $\alpha_{\text{opt}} = \text{argmax}_{\alpha\in(0,1]}\,\text{avg}_{\theta\in\Theta}\{d_{\min}\}$, SIC receiver is employed, and SNR = 3 dB.

Modulation (UE1+UE2+UE3)	UE1 Rate	UE2 Rate	UE3 Rate
BPSK+BPSK+BPSK	0.652	0.652	0.652
BPSK+BPSK+QPSK	0.590	0.592	0.815
BPSK+QPSK+QPSK	0.552	0.732	0.723
QPSK+QPSK+QPSK	0.587	0.627	0.650

Table 5.57: Achievable rate pairs of the CPA scheme for three-user GMAC with random phase offset. Here, $\alpha_{\text{opt}} = \text{argmax}_{\alpha\in(0,1]} \min_{\theta\in\Theta}\{d_{\min}\}$, SIC receiver is employed, and SNR = 3 dB.

Modulation (UE1+UE2+UE3)	UE1 Rate	UE2 Rate	UE3 Rate
BPSK+BPSK+BPSK	0.573	0.575	0.575
BPSK+BPSK+QPSK	0.572	0.548	0.833
BPSK+QPSK+QPSK	0.550	0.727	0.732
QPSK+QPSK+QPSK	0.547	0.543	0.538

Table 5.58: Achievable rate pairs of the CPA scheme for three-user GMAC with random phase offset. Here, $\alpha_{\text{opt}} = \text{argmax}_{\alpha\in(0,1]}\{\text{CC sum capacity of average phases}\}$, SIC receiver is employed, and SNR = 3 dB.

Modulation (UE1+UE2+UE3)	UE1 Rate	UE2 Rate	UE3 Rate
BPSK+BPSK+BPSK	0.668	0.672	0.658
BPSK+BPSK+QPSK	0.630	0.578	0.938
BPSK+QPSK+QPSK	0.503	0.730	0.760
QPSK+QPSK+QPSK	0.673	0.672	0.645

Table 5.59: Achievable rate pairs of the CPA scheme for three-user GMAC with random phase offset. Here, $(\alpha_{\text{opt}}, \theta_{\text{opt}}) = \text{argmax}_{\alpha\in(0,1)\,\&\,\theta\in\Theta}\{d_{\min}\}$, JML receiver is employed, and SNR = 6 dB. The receiver is assumed to be able to rotate the two constellations accurately to match θ_{opt}.

Modulation (UE1+UE2+UE3)	UE1 Rate	UE2 Rate	UE3 Rate
BPSK+BPSK+BPSK	0.890	0.890	0.890
BPSK+BPSK+QPSK	0.622	0.667	1.110
BPSK+QPSK+QPSK	0.400	0.615	0.605
QPSK+QPSK+QPSK	0.437	0.437	0.437

Table 5.60: Achievable rate pairs of the CPA scheme for three-user GMAC with random phase offset. Here, $\alpha_{\text{opt}} = \text{argmax}_{\alpha\in(0,1]} \text{avg}_{\theta\in\Theta}\{d_{\min}\}$, JML receiver is employed, and SNR = 6 dB.

Modulation (UE1+UE2+UE3)	UE1 Rate	UE2 Rate	UE3 Rate
BPSK+BPSK+BPSK	0.733	0.733	0.733
BPSK+BPSK+QPSK	0.542	0.635	1.015
BPSK+QPSK+QPSK	0.497	0.903	0.770
QPSK+QPSK+QPSK	0.510	0.510	0.510

Table 5.61: Achievable rate pairs of the CPA scheme for three-user GMAC with random phase offset. Here, $\alpha_{\text{opt}} = \text{argmax}_{\alpha\in(0,1]} \min_{\theta\in\Theta}\{d_{\min}\}$, JML receiver is employed, and SNR = 6 dB.

Modulation (UE1+UE2+UE3)	UE1 Rate	UE2 Rate	UE3 Rate
BPSK+BPSK+BPSK	0.637	0.635	0.635
BPSK+BPSK+QPSK	0.522	0.615	1.023
BPSK+QPSK+QPSK	0.502	0.918	0.785
QPSK+QPSK+QPSK	0.427	0.427	0.427

Table 5.62: Achievable rate pairs of the CPA scheme for three-user GMAC with random phase offset. Here, $\alpha_{\text{opt}} = \text{argmax}_{\alpha\in(0,1]}\{\text{CC sum capacity of average phases}\}$, JML receiver is employed, and SNR = 6 dB.

Modulation (UE1+UE2+UE3)	UE1 Rate	UE2 Rate	UE3 Rate
BPSK+BPSK+BPSK	0.717	0.715	0.717
BPSK+BPSK+QPSK	0.522	0.540	0.985
BPSK+QPSK+QPSK	0.455	0.770	0.683
QPSK+QPSK+QPSK	0.483	0.483	0.483

Table 5.63: Achievable rate pairs of the CPA scheme for three-user GMAC with random phase offset. Here, $(\alpha_{\text{opt}}, \theta_{\text{opt}}) = \text{argmax}_{\alpha\in(0,1)\,\&\,\theta\in\Theta}\{d_{\min}\}$, SIC receiver is employed, and SNR = 6 dB. The receiver is assumed to be able to rotate the two constellations accurately to match θ_{opt}.

Modulation (UE1+UE2+UE3)	UE1 Rate	UE2 Rate	UE3 Rate
BPSK+BPSK+BPSK	0.922	0.918	0.917
BPSK+BPSK+QPSK	0.830	0.773	1.327
BPSK+QPSK+QPSK	0.653	1.115	1.228
QPSK+QPSK+QPSK	1.003	1.003	0.950

Table 5.64: Achievable rate pairs of the CPA scheme for three-user GMAC with random phase offset. Here, $\alpha_{\text{opt}} = \text{argmax}_{\alpha\in(0,1]}\,\text{avg}_{\theta\in\Theta}\{d_{\min}\}$, SIC receiver is employed, and SNR = 6 dB.

Modulation (UE1+UE2+UE3)	UE1 Rate	UE2 Rate	UE3 Rate
BPSK+BPSK+BPSK	0.818	0.815	0.812
BPSK+BPSK+QPSK	0.738	0.743	1.162
BPSK+QPSK+QPSK	0.668	0.970	0.982
QPSK+QPSK+QPSK	0.832	0.853	0.847

Table 5.65: Achievable rate pairs of the CPA scheme for three-user GMAC with random phase offset. Here, $\alpha_{\text{opt}} = \text{argmax}_{\alpha\in(0,1]}\,\min_{\theta\in\Theta}\{d_{\min}\}$, SIC receiver is employed, and SNR = 6 dB.

Modulation (UE1+UE2+UE3)	UE1 Rate	UE2 Rate	UE3 Rate
BPSK+BPSK+BPSK	0.665	0.665	0.665
BPSK+BPSK+QPSK	0.660	0.650	1.090
BPSK+QPSK+QPSK	0.650	0.982	0.978
QPSK+QPSK+QPSK	0.807	0.858	0.878

Table 5.66: Achievable rate pairs of the CPA scheme for three-user GMAC with random phase offset. Here, $\alpha_{\text{opt}} = \text{argmax}_{\alpha\in(0,1]}\{\text{CC sum capacity of average phases}\}$, SIC receiver is employed, and SNR = 6 dB.

Modulation (UE1+UE2+UE3)	UE1 Rate	UE2 Rate	UE3 Rate
BPSK+BPSK+BPSK	0.823	0.823	0.823
BPSK+BPSK+QPSK	0.800	0.732	1.278
BPSK+QPSK+QPSK	0.732	1.027	1.067
QPSK+QPSK+QPSK	0.843	0.823	0.847

Table 5.67: Achievable rate pairs of the CPA scheme for three-user GMAC with random phase offset. Here, $(\alpha_{\text{opt}}, \theta_{\text{opt}}) = \text{argmax}_{\alpha\in(0,1)\,\&\,\theta\in\Theta}\{d_{\min}\}$, JML receiver is employed, and SNR = 10 dB. The receiver is assumed to be able to rotate the two constellations accurately to match θ_{opt}.

Modulation (UE1+UE2+UE3)	UE1 Rate	UE2 Rate	UE3 Rate
BPSK+BPSK+BPSK	0.993	0.993	0.993
BPSK+BPSK+QPSK	0.847	0.913	1.720
BPSK+QPSK+QPSK	0.657	1.163	1.122
QPSK+QPSK+QPSK	0.853	0.853	0.853

Table 5.68: Achievable rate pairs of the CPA scheme for three-user GMAC with random phase offset. Here, $\alpha_{\text{opt}} = \text{argmax}_{\alpha\in(0,1]}\,\text{avg}_{\theta\in\Theta}\{d_{\min}\}$, JML receiver is employed, and SNR = 10 dB.

Modulation (UE1+UE2+UE3)	UE1 Rate	UE2 Rate	UE3 Rate
BPSK+BPSK+BPSK	0.908	0.908	0.908
BPSK+BPSK+QPSK	0.745	0.847	1.473
BPSK+QPSK+QPSK	0.672	1.275	1.130
QPSK+QPSK+QPSK	0.823	0.823	0.823

Table 5.69: Achievable rate pairs of the CPA scheme for three-user GMAC with random phase offset. Here, $\alpha_{\text{opt}} = \text{argmax}_{\alpha\in(0,1]} \min_{\theta\in\Theta}\{d_{\min}\}$, JML receiver is employed, and SNR = 6 dB.

Modulation (UE1+UE2+UE3)	UE1 Rate	UE2 Rate	UE3 Rate
BPSK+BPSK+BPSK	0.750	0.750	0.750
BPSK+BPSK+QPSK	0.665	0.737	1.297
BPSK+QPSK+QPSK	0.645	1.228	1.087
QPSK+QPSK+QPSK	0.743	0.743	0.745

Table 5.70: Achievable rate pairs of the CPA scheme for three-user GMAC with random phase offset. Here, $\alpha_{\text{opt}} = \text{argmax}_{\alpha\in(0,1]}\{\text{CC sum capacity of average phases}\}$, JML receiver is employed, and SNR = 6 dB.

Modulation (UE1+UE2+UE3)	UE1 Rate	UE2 Rate	UE3 Rate
BPSK+BPSK+BPSK	0.908	0.908	0.908
BPSK+BPSK+QPSK	0.720	0.815	1.500
BPSK+QPSK+QPSK	0.620	1.250	1.100
QPSK+QPSK+QPSK	0.833	0.832	0.833

Table 5.71: Achievable rate pairs of the CPA scheme for three-user GMAC with random phase offset. Here, $(\alpha_{\text{opt}}, \theta_{\text{opt}}) = \text{argmax}_{\alpha\in(0,1)\,\&\,\theta\in\Theta}\{d_{\min}\}$, SIC receiver is employed, and SNR = 10 dB. The receiver is assumed to be able to rotate the two constellations accurately to match θ_{opt}.

Modulation (UE1+UE2+UE3)	UE1 Rate	UE2 Rate	UE3 Rate
BPSK+BPSK+BPSK	0.995	0.995	0.993
BPSK+BPSK+QPSK	0.960	0.953	1.797
BPSK+QPSK+QPSK	0.837	1.560	1.685
QPSK+QPSK+QPSK	1.387	1.355	1.382

Table 5.72: Achievable rate pairs of the CPA scheme for three-user GMAC with random phase offset. Here, $\alpha_{\text{opt}} = \text{argmax}_{\alpha\in(0,1]} \text{avg}_{\theta\in\Theta}\{d_{\min}\}$, SIC receiver is employed, and SNR = 10 dB.

Modulation (UE1+UE2+UE3)	UE1 Rate	UE2 Rate	UE3 Rate
BPSK+BPSK+BPSK	0.948	0.948	0.948
BPSK+BPSK+QPSK	0.900	0.912	1.575
BPSK+QPSK+QPSK	0.835	1.338	1.415
QPSK+QPSK+QPSK	1.287	1.328	1.232

Table 5.73: Achievable rate pairs of the CPA scheme for three-user GMAC with random phase offset. Here, $\alpha_{\text{opt}} = \text{argmax}_{\alpha\in(0,1]} \min_{\theta\in\Theta}\{d_{\min}\}$, SIC receiver is employed, and SNR = 10 dB.

Modulation (UE1+UE2+UE3)	UE1 Rate	UE2 Rate	UE3 Rate
BPSK+BPSK+BPSK	0.763	0.763	0.763
BPSK+BPSK+QPSK	0.763	0.760	1.323
BPSK+QPSK+QPSK	0.775	1.265	1.252
QPSK+QPSK+QPSK	1.332	1.337	1.317

Table 5.74: Achievable rate pairs of the CPA scheme for three-user GMAC with random phase offset. Here, $\alpha_{\text{opt}} = \text{argmax}_{\alpha\in(0,1]}\{\text{CC sum capacity of average phases}\}$, SIC receiver is employed, and SNR = 10 dB.

Modulation (UE1+UE2+UE3)	UE1 Rate	UE2 Rate	UE3 Rate
BPSK+BPSK+BPSK	0.950	0.950	0.950
BPSK+BPSK+QPSK	0.928	0.917	1.632
BPSK+QPSK+QPSK	0.825	1.432	1.575
QPSK+QPSK+QPSK	1.365	1.360	1.352

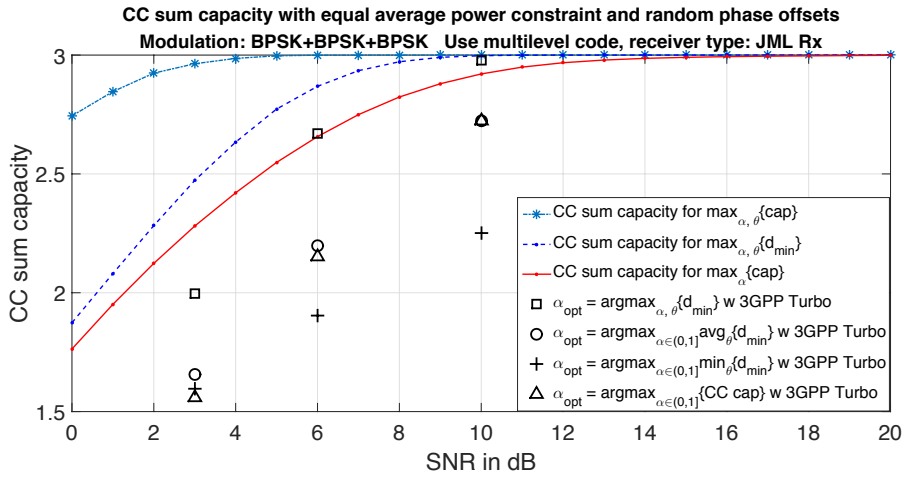

Figure 5.27: CC sum capacity and achievable rates of BPSK+BPSK+BPSK with equal average power constraint and random phase offset. Here, JML receiver is assumed.

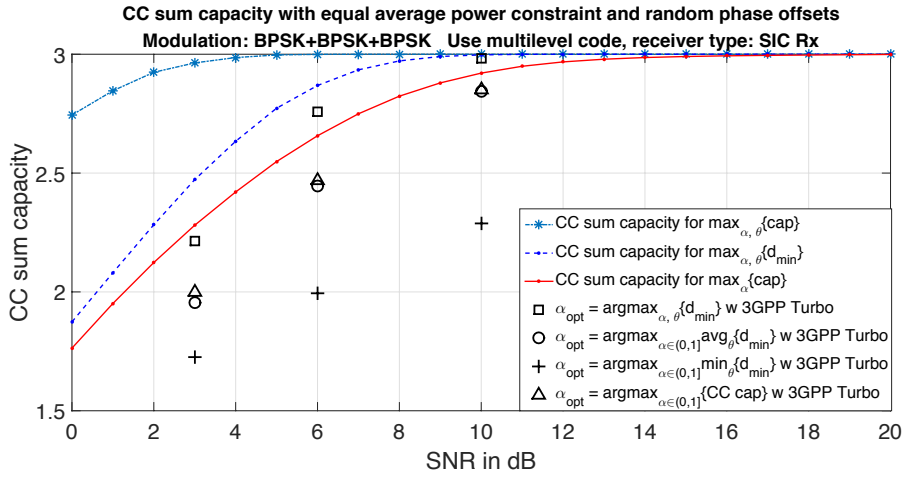

Figure 5.28: CC sum capacity and achievable rates of BPSK+BPSK+BPSK with equal average power constraint and random phase offset. Here, SIC receiver is assumed.

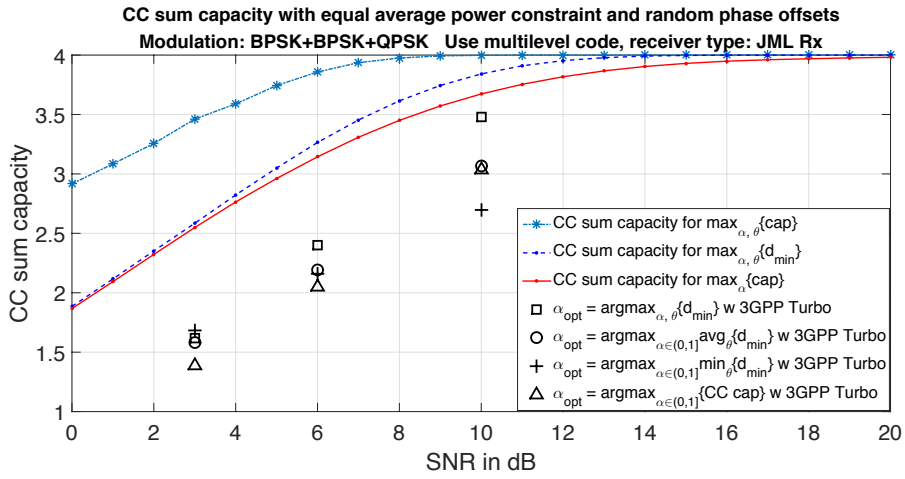

Figure 5.29: CC sum capacity and achievable rates of BPSK+BPSK+QPSK with equal average power constraint and random phase offset. Here, JML receiver is assumed.

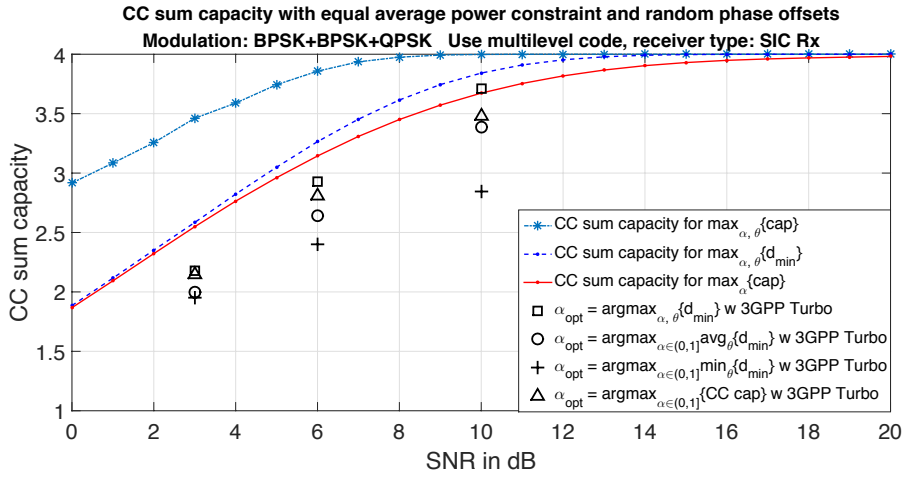

Figure 5.30: CC sum capacity and achievable rates of BPSK+BPSK+QPSK with equal average power constraint and random phase offset. Here, SIC receiver is assumed.

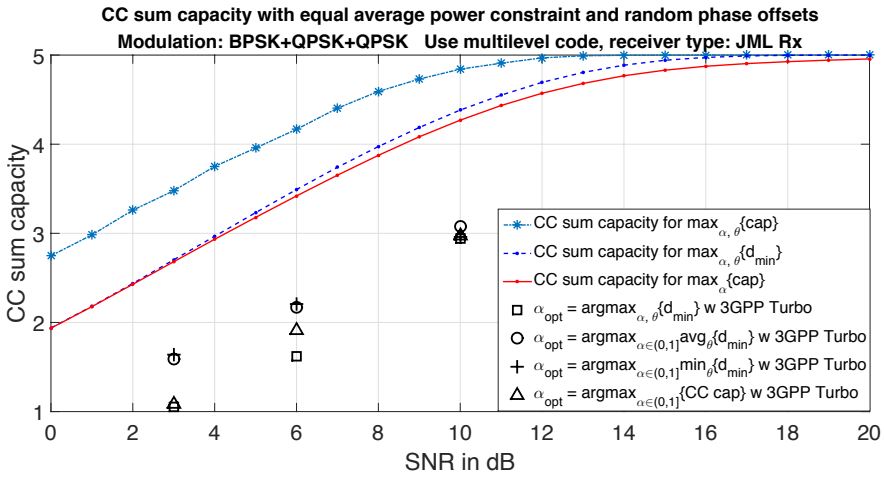

Figure 5.31: CC sum capacity and achievable rates of BPSK+QPSK+QPSK with equal average power constraint and random phase offset. Here, JML receiver is assumed.

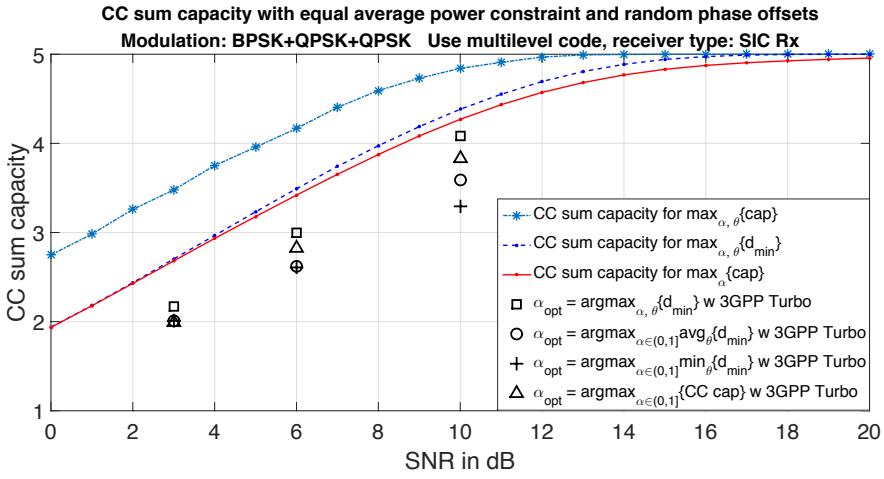

Figure 5.32: CC sum capacity and achievable rates of BPSK+QPSK+QPSK with equal average power constraint and random phase offset. Here, SIC receiver is assumed.

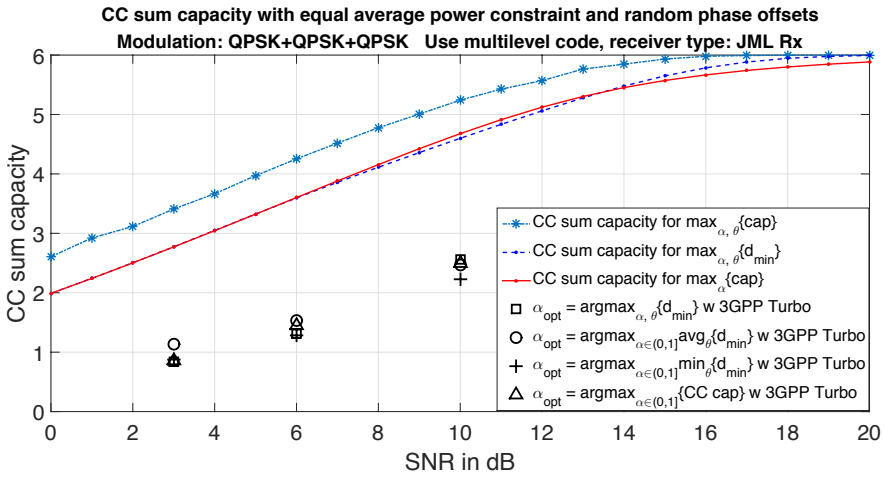

Figure 5.33: CC sum capacity and achievable rates of QPSK+QPSK+QPSK with equal average power constraint and random phase offset. Here, JML receiver is assumed.

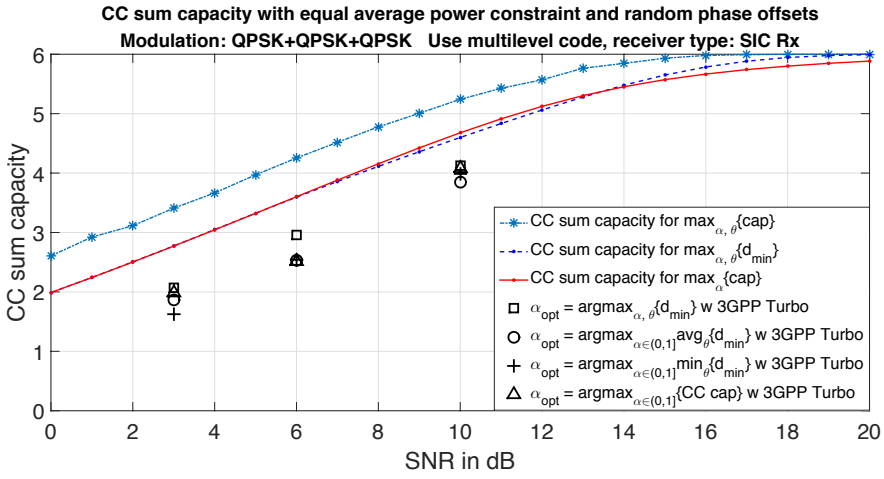

Figure 5.34: CC sum capacity and achievable rates of QPSK+QPSK+QPSK with equal average power constraint and random phase offset. Here, SIC receiver is assumed.

In this section, the performance of the CPA scheme for three-user GMAC with equal average power constraint and random phase offset is examined. Tables 5.49 and 5.50 list the values of α_{opt} and $\theta_{\text{opt}} = (\theta_{\text{opt,UE2}}, \theta_{\text{opt,UE3}})$ corresponding to different modulation combinations for the CPA scheme of three-user GMAC with equal average power constraint and random phase offset. Note that we again fix $\theta_{\text{opt,UE1}} = 0$; hence, we only need to determine the rotation angles of the constellations of UE2 and UE3 relative to that of the constellation of UE1, which are respectively denoted as $\theta_{\text{opt,UE2}}$ and $\theta_{\text{opt,UE3}}$. As such, Θ becomes $[0, 2\pi)^2$.

Subject to BLER ≤ 0.1, the maximum achievable rates are simulated and summarized as follows.

(i) Tables 5.51, 5.52, 5.53 and 5.54 for JML receiver and SNR = 3 dB;

(ii) Tables 5.55, 5.56, 5.57 and 5.58 for SIC receiver and SNR = 3 dB;

(iii) Tables 5.59, 5.60, 5.61 and 5.62 for JML receiver and SNR = 6 dB;

(iv) Tables 5.63, 5.64, 5.65 and 5.66 for SIC receiver and SNR = 6 dB;

(v) Tables 5.67, 5.68, 5.69 and 5.70 for JML receiver and SNR = 10 dB;

(vi) Tables 5.71, 5.72, 5.73 and 5.74 for SIC receiver and SNR = 10 dB.

Similar to the previous sections, we also depict the CC sum capacity for different modulation combinations and different power-allocation optimization criterions under three SNRs, which are SNR = 3 dB, 6 dB and 10 dB. These are summarized below.

(i) Figure 5.27 for BPSK+BPSK+BPSK and JML receiver;

(ii) Figure 5.28 for BPSK+BPSK+BPSK and SIC receiver;

(iii) Figure 5.29 for BPSK+BPSK+QPSK and JML receiver;

(iv) Figure 5.30 for BPSK+BPSK+QPSK and SIC receiver;

(v) Figure 5.31 for BPSK+QPSK+QPSK and JML receiver;

(vi) Figure 5.32 for BPSK+QPSK+QPSK and SIC receiver;

(vii) Figure 5.33 for QPSK+QPSK+QPSK and JML receiver;

(*viii*) Figure 5.34 for QPSK+QPSK+QPSK and SIC receiver.

We make the following observations based on the above tables and figures. First, specifically for JML receiver, we suggest to select the power allocation parameter α by the criterion:

$$\underset{\alpha\in(0,1]}{\operatorname{argmax}} \underset{\theta\in\Theta}{\operatorname{avg}}\{d_{\min}\}$$

since its maximum achievable rate is better than that of the other two distance-based criterions and the CC sum capacity criterion.

Second, for SIC receiver, however, we recommend to use the power allocation parameter α that achieves

$$\max_{\alpha\in(0,1]}\{\text{CC sum capacity of average phases}\}.$$

In fact, our experiments indicate that for SIC receiver, the decoding result of the strongest UE do not have much difference in performance among different criterions. Yet, when decoding the weakest UE, the α-value selected by $\max_{\alpha\in(0,1]}\{\text{CC sum capacity of average phases}\}$ can provide the largest performance gain. This directs to the conclusion that CC sum capacity criterion should be favored when SIC receiver is employed.

Third, we again observe from Tables 5.49 and 5.50 that the α-value selected by $\operatorname{argmax}_{\alpha\in(0,1]}\{\text{CC sum capacity of average phases}\}$ tends to be larger than that those selected by the $d_{\min}$-based criterions.

Chapter 6

Conclusion and Future Work

In this thesis, unlike what have been done in the literature, where the CC sum capacity is used as the objective function for the optimization of the CPA scheme under multi-user GMAC, we proposed three new distance-based objective functions for the same optimization. Depending on whether the BS can compensate for the constellation rotations or not due to the newly introduced random phase offset of the GMAC, our criterions obtained the best power allocation between the two users according to

$$(\alpha_{\text{opt}}, \theta_{\text{opt}}) = \max_{\alpha \in (0,1] \,\&\, \theta \in \Theta} \{d_{min}\}$$

for perfect coordination, and

$$\alpha_{\text{opt}} = \max_{\alpha \in (0,1]} \operatorname{avg}_{\theta \in \Theta} \{d_{min}\} \quad \text{or} \quad \alpha_{\text{opt}} = \max_{\alpha \in (0,1]} \min_{\theta \in \Theta} \{d_{min}\}$$

for uncoordination. Numerical examinations for different modulation combinations under JML and SIC receivers then followed. We also provided a sub-optimal solution for the CPA scheme under three-user GMAC with random phase offset.

This thesis only considered the two-user (and sub-optimally three-user) GMAC with random phase offset. However, in practice, channel fading may seriously impact the system performance. Thus, an interesting future work of practical interest is to examine the proposed distance-based criterions for the GMAC with channel fading. In addition,

how to extend the results in the current work to more than two users is another future work of practical interest.

Bibliography

[1] M. Al-Imari, P. Xiao, M. A. Imran, and R. Tafazolli, "Uplink non-orthogonal multiple access for 5G wireless networks," *The 11th International Symposium on Wireless Communications Systems (ISWCS)*, Barcelona, Spain, pp. 781-785, August 2014.

[2] D. Astely, E. Dahlman, A. Furuskar, Y. Jading, M. Lindstrom, and S. Parkvall, "LTE: the evolution of mobile broadband," *IEEE Communications Magazine*, vol. 47, no. 4, pp. 44-51, April 2009.

[3] A. Benjebbour, Y. Saito, Y. Kishiyama, A. Li, A. Harada, and T. Nakamura, "Concept and practical considerations of non-orthogonal multiple access (NOMA) for future radio access," *International Symposium on Intelligent Signal Processing and Communications Systems (ISPACS)*, pp. 770-774, November 2013.

[4] A. Benjebbour, K. Saito, A. Li, Y. Kishiyama, and T. Nakamura, "Non-orthogonal multiple access (NOMA): Concept, performance evaluation and experimental trials," *WINCOM*, 2015

[5] R. G. Gallager, "A perspective on multiaccess channels," *IEEE Trans. Inform. Theory*, vol. 31, pp. 124-142, March 1985.

[6] J. Harshan and B. S. Rajan, "On two-user Gaussian multiple access channels with finite input constellations," *IEEE Trans. Inform. Theory*, vol. 57, no. 3, pp. 1299-1327, March 2011.

[7] J. Harshan and B. S. Rajan, "A novel power allocation scheme for two-user GMAC with finite input constellation," *IEEE Trans. Wireless Commun.*, vol. 12, no. 2, pp. 818-827, February 2013.

[8] K. Higuchi and Y. Kishiyama, "Non-orthogonal access with successive interference cancellation for future radio access," *APWCS2012*, August 2012.

[9] P. A. Martin and D. P. Taylor, "On multilevel codes and iterative multistage decoding," *IEEE Trans. on Commun.*, vol. 49, no. 11, pp. 1916-1925, November 2001.

[10] J. G. Proakis and M. Salehi, *Digital Communications*, 5th edition, McGraw-Hill International Editions, 2008.

[11] A. Racz, N. Reider, and G. Fodor, "On the impact of inter-cell interference in LTE," *IEEE Global Telecommunications Conference (GLOBECOM'08)*, pp. 5436–5441, November-December 2008.

[12] Y. Saito, Y. Kishiyama, A. Benjebbour, T. Nakamura, A. Li, and K. Higuchi, "Non-orthogonal multiple access (NOMA) for cellular future radio access," *IEEE Vehicular Technology Conference*, Dresden, Germany, June 2013.

[13] S. Timotheou and I. Krikidis, "Fairness for non-orthogonal multiple access in 5G systems," *IEEE Signal Process letters*, vol. 22, no. 10, pp. 1647-1651, October 2015.

[14] U. Wachsmann, R. F. H. Fischer, and J. B. Huber, "Multilevel codes: Theoretical concepts and practical design rules," *IEEE Trans. Inform. Theory*, vol. 45, no. 5, pp. 1361-1391, July 1999.

[15] P. Wang, J. Xiao, and L. Ping, "Comparison of orthogonal and non-orthogonal approaches to future wireless cellular systems," *IEEE Vehicular Technology Magazine*, vol. 1, no. 3, pp. 4-11, September 2006.

[16] S. Zhang, X. Xu, Y. Wu, and L. Lu, "5G: towards energy-efficient, low-latency and high-reliable communications networks," *IEEE International Conference on Communication Systems (ICCS)*, Macau, China, 19-21 November 2014.

[17] M. A. Zheng, Z. Q. Zhang, Z. G. Ding, P. Z. Fan, and H. C. Li, "Key techniques for 5G wireless communications: Network architecture, physical layer, and MAC layer perspectives," *Sci. China Inf. Sci.*, vol. 58, no. 4, pp. 1-20, 2015.